Editor: Gerd Förch

CICD Series Vol.3: Summary of Master Theses from Arba Minch University, Ethiopia

Oktober 2009

CICD Series

Editor

Prof. Dr.-Ing. Gerd Förch,
Universität Siegen,
Centre for International Capacity Development,
Paul-Bonatz-Str. 9-11
57076 Siegen

E-Mail: info@cicd.uni-siegen.de

Printing Printing Office, Universität Siegen, Germany

ISSN: 1868-8578

Preface

The following volume is a result of long term cooperation between University of Siegen and Arba Minch University (AMU), which started in 1992 and which was supported by the German Government through its Ministry of Economic Cooperation and Development (BMZ). The project "Assistance to Arba Minch Water Technology Institute - AWTI" started in 1990 and ended in 2007. University of Siegen, namely the Research Institute for Water and Environment (FWU) were active partners in this long lasting project of technical cooperation with Ethiopia. It needs to be acknowledged that BMZ as well sponsored the printing of this document.

One of the objectives during the last phase of the project was to establish MSc programmes in water related subjects. Three programmes were started initially in water resources, irrigation and hydraulic engineering. Later programmes in meteorology and sanitary engineering were added. The programmes were handled by the School of Graduate Studies which received special support from the German side with sponsoring research projects as basis for the master degrees, establishing some essential infrastructure like hydrological networks and a PC Pool with internet connection.

The following papers are summaries of the first master theses finalised under this scheme of university cooperation. They underline the good standard of post graduate education at this still young Ethiopian University, which was promoted to this status in 2005. Other results like PhD dissertations are as well going to be published in this CICD series. The international conference Lars2007 is as well documented (as Vol.1).
It should be stated that with a considerable German support Arba Minch University (AMU) became one of the leading universities in the water sector in Eastern Africa.

The Editor

November 2009

List of Authors

Ingrid Althoff - Research Institute for Water and Environment, Water Resources Management Group, University of Siegen, P. O. Box: D-57068 Siegen-Germany
Tel.: +49-271-7403178, Fax: +49-271-7402921
Email: ingrid.althoff@uni-siegen.de

Tilahun Derib Asfaw - Arba Minch University, Ethiopia

Fikre Assefa - Arba Minch University, P.O.B. 21.

Samuel Dagalo - Arba Minch University, P.O.B. 21.
Arba Minch, Ethiopia

Yilma Demissie - Arba Minch University, School of Graduate Studies
P.O.B. 21., Arba Minch, Ethiopia

Feleke Gerb - Arba Minch University, Ethiopia

Tadesse Taye Meskele - Arba Minch University, School of Graduate Studies
P.O.Box 21, Arba Minch, Ethiopia.
E-mail: tadesse_taye@yahoo.com, 2 Katholieke Universiteit Leuven
Hydraulic Section, Kasteelpark Arenberg 40, BE-3001

Semu Ayalew Moges - Arba Minch University, School of Graduate Studies
P.O.Box 21, Arba Minch, Ethiopia, Tel: +251-46-8810775
Email: smoges@nilebasin.org, semu_moges_2000@yahoo.com

L.B. Roy - Arba Minch University, Ethiopia

Eyasu Shumbulo - Arba Minch University, P.O.B. 21.

Patrick Willems - Katholieke Universiteit Leuven, Hydraulic Section
Kasteelpark Arenberg 40, BE-3001, Leuven,Belgium.
E-mail: Patrick.Willems@bwk.kuleuven.be

Hayalsew Yilma - Ministry of Water Resources, Addis Ababa, Ethiopia
Email: hayalsew@yahoo.com

Tegenu Zerfu - Arba Minch University, School of Graduate Studies
P.O.B. 21., Arba Minch, Ethiopia, Email: zerfutegenu@yahoo.com

Moltot Zewdie - Tel 022-1112900), Email: tambek72@yahoo.com
Semu Ayalew (PhD), Eline Boelee (PhD) and Fentaw Abegaz(PhD)

Contents

List of Figures

1 Water Balance Modelling in the Southern Ethiopian Rift Valley: The Example of the Bilate River Catchment - Ingrid Althoff, Gerd Förch

Gerd Förch, *Ingrid Althoff*[1]

[1]Research Institute for Water and Environment
Water Resources Management Group
University of Siegen
P. O. Box: D-57068 Siegen-Germany
Tel.: +49-271-7403178
Fax: +49-271-7402921
Email: ingrid.althoff@uni-siegen.de

1.1 Abstract

A variety of standardised hydrological models is available in order to estimate the spatial and temporal distribution of water resources in natural systems. However, the applicability of these hydrological models is generally limited to regions where data availability, temporal and spatial, is sufficient, i.e. to developed countries. For most of the still developing countries, the lack of data currently limits the use of verified hydrological models. The aim of this study is to investigate whether a water balance analysis with a standardised hydrological model is achievable in regions of lower temporal and spatial data availability. The Precipitation-Runoff Model NASIM is used for this study.

The area of investigation, the catchment area of the Bilate River (approximately 5500 km^2), is a part of the Abaya Chamo Basin in the southeast of the Ethiopian Rift Valley. The Bilate River covers a difference in altitude of over 2000 m and has a length of approximately 250 km. The lack of sufficient data for the catchment at an adequate scale, i.e. hydro-meteorological and land use data, makes modelling relatively difficult. For instance, only five gauging stations are available in the catchment, which can be used for model calibration. Three of these stations are located in the upper catchment, while only one gauging station is situated in the lower catchment of the Bilate River. Moreover, the operation of some of these stations is outdated.

The Precipitation-Runoff Model NASIM takes into account the necessary water balance parameters. The modelling utilises spatially distributed data with a temporal resolution of one day. NASIM emulates the precipitation-runoff process relatively well in relation to the background of the available data. Certainly, the simulated discharges should be examined closely as, for the discharge peaks, they do not really represent the reality of the situation. The greatest influence of the results can be seen with regard to the meteorological data. For these it is noted that the strong relief and the great variability of the precipitation as well as the influence of evaporation are not represented adequately by the number of climatic stations. In relation to the gauging stations it is noticed that the calibration of the model could only lead to a good description of the natural conditions in the Precipitation-Runoff Model through the use of qualitatively good discharge measurements at several gauges. Furthermore, in NASIM, the meteorological

data are considered as station data, not as interpolated regional data. This implies the following: NASIM does not work on a raster basis at present. Thus, improvements towards a raster basis are recommended. An additional aspect is the non-satisfactory use of GIS for the visualising of simulation results, which can be traced back to the lack of a raster basis. All in all, it can be stated that modelling with NASIM is possible. However, it demands a very close examination of the input parameters and their emphasis with respect to the model. More field work as well as more research is recommended in order to modify the model.

Keywords: *Bilate River Catchment, Precipitation-Runoff Model NASIM*

1.2 Introduction

According to the World Water Report of the UNO (2003), about two-thirds of humanity will suffer from water shortage or unavailability by the year 2025. This development is on the one hand related to increasing demands, on the other hand to the inhomogeneous global and regional distribution of freshwater. The variability of climatic and geo-morphological conditions leads to differentiated water availability and demand, both temporally and spatially. Particularly in the arid and semi-arid regions of the earth, water is a scarce resource, the shortage of which hinders development and represents a high source of natural conflicts (Online-Magazin der Deutschen UNESCO Kommission, Ausgabe 4-5, April / May 2003 - http://www.unesco-heute.de /0403/wweb.htm).

The immense increase in population causes an increase in the agricultural use of land areas. This results in low production rates in agriculture and the loss of natural resources. Moreover, land degradation is caused by the loss of protective natural vegetation. In this connection, it is most important to note that the influences of human effects of climatic extremes on the ecosystem as well as on the society have changed (BMZ 2006 - http://www.bmz.de/de/laender/partnerlaender/ethiopien/zusammenarbeit.html; ZELEKE/HURNI 2001).

The responsibility of water management is to balance the society's demand for water (usage) and the availability of drinking water, which is naturally limited both quantitatively and qualitatively. The impacts of changes of the input com-

ponents on the total "water balancing" system can be represented and evaluated with the help of models for the description and quantification of the spatial and temporal distribution. Significant components of the water balance such as precipitation, evaporation, infiltration, storage and discharge can be used in this context. The primary target of this study was to ascertain to what extent a water balance analysis can be realised using a standardised hydrological model in a region of low spatial and temporal availability of data. The modelled scenarios of land use will not be described in this paper.

1.3 Landscape Characteristics - Area under Investigation

The Abaya Chamo Basin is situated in the southwest of Addis Ababa, between 5-5.8°'N latitude and 37- 38.5°'E longitude. It forms part of the Main Ethiopian Rift, which in turn is part of an active rift system of the Great Rift Valley. The Bilate River Catchment, which was chosen to be the area of study, forms the northern part of the Abaya Chamo Basin. The Bilate River is the longest river in the Abaya Chamo Basin, with a length of about 255 km. It is also the only river which flows into Lake Abaya from the north. The source of the Weira forms the most northerly point in the Bilate Catchment and also in the Abaya Chamo Basin. Together with the Guder, which has its source on the northwestern border of the catchment, it is one of the two source tributaries of the Bilate River. In the west, the area of investigation is defined by the watershed of the catchment of the Omo River, and in the east it is characterised by the Awasa Basin. The southern border is formed by Lake Abaya, into which the Bilate River flows. The upper catchment area of the Bilate is situated on the graben shoulder of the Main Ethiopian Rift. It is characterised by a dense net of tributaries. According to BEKELE (2001, 8), the complete catchment of the Abaya Chamo Basin has an area of around 18.599 km^2, about 5500 km^2 of which form the part of the area which was to be investigated.

1.4 Geology

In East Africa, the geological foundations are formed from a complex of metamorphic and volcanic rocks, which can be assigned to the era of the Precambrian

and the Palaeozoic. During this era, Africa was dominated by large folded mountain ranges and their erosion. The rising of the Ethiopian dome became visible in the Eocene. The continual uprising of the highlands and the continuous drifting apart of the African, Somalian and Arabic tectonic plates led to the breaking inwards of the central part of the highlands, which sank several kilometres. The Main Ethiopian Rift was formed, with a length of over 5000km. It divides the highlands into an eastern and a western part: the Abyssinian Highland and the Somali Plateau. The Main Ethiopian Rift forms the continental part of an active valley system: the Great Rift Valley. The continuous volcanic activity had its main phase (Trapp Series) during the Eocene and the Oligocene. Building on the flood basalts of the Trapp Series, huge basalt plates formed in large areas of the Abyssinian Highlands and the Somali Plateau. Here, one can observe an increasing thickness from a few hundred metres on the plateaus to more than 2000m on the sunken graben borders. In the upper Pliocene, large crevices and pipe eruptions covered major parts of Southern Ethiopia and filled the valleys with a layer of ignimbrite which is several hundred metres thick. The middle of the Pleistocene was defined by an era with immense (volcanic) activity of calderas, which ranged from Kenya into the Afar region along the eastern graben shoulder. Some of the basalt pipes in the Main Ethiopian Rift appeared just in the last century. Geophysical studies show that the entire Main Ethiopian Rift is situated in a hot zone with a width of around 1000km, which displays low density and thickness (BAKER ET AL 1972, 7ff.; FAIRHEAD 1986, 19ff.; MEYER 1987, 32ff.; MOHR 1971, 449; READING 1986, 3ff.).

The geological map of the FAO (1998) shows that the Oligocene-Miocene basalts dominate in the Bilate River Catchment. These basalts can be found in the central area between Alaba Kulito and Bilate Tena, accompanied by Quaternary rhyolites and trachytes in the north and Holocene lacustrine sequences in the south of the catchment. Furthermore, on the southwest border, many subordinated Oligocene and Miocene volcanics can be found.

1.5 Relief

The relief of today's Ethiopia as well as the one of the Bilate River Catchment is strongly influenced by the geological conditions and therefore structurally

strongly dependent. Above all, tectonic and volcanic processes have created the present relief. The Main Ethiopian Rift, situated between the two plateaus (Abyssinian Highlands and the Somali Plateau), forms a broad, relatively plane surface with a breadth in the middle of 50 to 70 km, which has its peak at an elevation of 1700 m above sea level in the region of Lake Ziway. From this point, the main rift falls into the Afar depression to the north and to the south into the Lake Turkana basin. The central volcanic peaks and calderas in the area of the Main Ethiopian Rift divide a row of basins from one another, with lakes without any outlet (NYAMWERU 1996, 19ff.; MEYER 1987, 33ff.). Lake Abaya is the largest of the Ethiopian Rift Valley lakes. The area of investigation is situated in the northern direction of Lake Abaya. The transition from the plateau to the valleys takes place in a variety of ways. On the western edge of the catchment, the graben shoulder is notably steep with a very mountainous relief character, while on the eastern edge it runs in a rather less pronounced step. All in all, the area of investigation shows high relief energy. The northern point of the catchment area (south of Butarija) is located at an elevation of approximately 3350 m above sea level, whereas the most southerly point, in the estuary area of the Bilate River and Lake Abaya, has an elevation of around 1200 m above sea level. This implies a high significance of the erosion and the deposition processes. Furthermore, anthropogenic influences on the relief can be detected in the areas of the catchment, which are agriculturally used in terms of significant soil erosions.

All in all, the relief is determined by the climate and principally, through the form of the land, by its exposure and elevation since with increasing elevation, the temperature in the mountains and highlands falls and the moisture content of the soil increases. The combination of the influences of climate, relief, land usage and soil conditions leads to a differentiated picture of evapotranspiration (SCHEFFER/SCHACHTSCHNABEL 2002, 443).

1.6 Climate

Due to its geographical position between the equator and the northern tropic, Ethiopia is situated at tropical latitudes. It is thus located in the area where the Passat winds are influential (northeast Passat). The Passat winds flow towards the equator. These winds move within the Inner Tropical Convergence Zone (ITCZ)

in the course of the year. The ITCZ moves with the average zenith position of the sun between approximately 20°S and 15°N. In principle, the climate of the tropics and subtropics can be explained by the ITCZ's change of position and the Passat circulation during the year. The summer (rainy season) is under the influence of the ITCZ, the winter (dry season) is distinguished by dry Passat winds. In this respect, however, the Horn of Africa and thus Ethiopia both occupy a special position. The climate of Ethiopia is on the one hand influenced by the relief and on the other hand by the special factors of four atmospheric action centres. These centres are, amongst others, the subtropical high pressure belt of both hemispheres, the equatorial low pressure region lying in between, and the Indian monsoon depression. The monsoon is a particular form of the Passat circulation. In the course of the year, four seasons can be distinguished as a result of the interaction between these pressure systems: the main rainy season (Krempt) which takes place in the highlands between June and September, the dry season (Bega) from October/November until March, as well as two transitional phases (Gu and Der) which take place in April/May and in September/October to November, respectively (ENDLICHER 2000, 283ff.; WESTPHAL 1975, 18ff.).

The Bilate Catchment is not only situated in several precipitation regions but according to the climatic classification of KÖPPEN/GEIGER (1928), it is also located in two main climatic zones. The catchment is characterised by the savannah climate (Aw) of the Main Ethiopian Rift as well as by the moderately warm, dry winter climate (Cw) of the highlands. The monthly average temperature of the Aw-climate lies above 18°C. The Bilate Catchment area partly lies on the graben shoulder of the Main Ethiopian Rift and thus displays a Cw-climate due to the elevation, the lower temperatures and the higher precipitation. The Cw-climate is characterised by average temperatures of under 18°C and a precipitation between 900 and 1500 mm per year. In addition, the area of investigation ranges within four thermal levels, from the Bercha at the altitude of Lake Abaya (under 1500 m a.s.l) with temperatures of above 30°C on a yearly average and an amount of precipitation which lies significantly under 900 mm per year, to Dega (2600 - 3600 m a.s.l) in the north of the catchment. The annual average temperature in this zone is around 16°C. During the dry periods, frosts may appear (ENDLICHER 2000, 284ff.; GRIFFITHS 1972, 380; WESTPHAL 1975, 22ff.).

1.7 Soil

The significant change between the dry and rainy seasons determines the soil conditions in the tropics, the subtropics as well as in the moderate continental climates. In the course of the year, this variation in moisture leads to a much pronounced texture variation in clay rich soils (e.g. Vertisols) and to peloturbation, while in many silt and loamy soils the bioturbation is very intense and reaches far into the underground. In high mountain regions, erosion is dominant, which is the reason why young and flat surfaces prevail. Their mineral content is very similar to that of the source rocks. In more developed older soils, this only applies to the heavier minerals which are more resistant to weathering. The variability (properties, genesis and formation) of the Ethiopian soils is described in detail in GRUNWALD (2003). The soil typology notation is the same one used in the World Soil Map of the FAO (1998).

Within the varying topography of the country, with its diverse geological strata and varying climatic conditions, various soils could develop. According to the FAO Soil Map (1998), soil types such as Luvisols, Nitisols and Leptosols dominate in the area of investigation. They can be found throughout the catchment. Cambisols are present in the north, Vertisols can be found in the south and the southwest, and Andosols are present in the central area of the catchment between Alaba Kulito and Bilate Tena. Soil types such as Fluvisols and Phaeozem are only found in small amounts on the southeastern and on the eastern catchment borders. According to the FAO Soil Map (1998), the soil depths are between 1.00 and 2.00 m.

1.8 Land Usage

The vegetation is essentially dependent on the topography, the climate and the soil. The relief of Ethiopia has a special importance in this context as it leads to a vertical differentiation of the climatic zones, which consequently influences the vegetation. One must differentiate between the natural vegetation and the anthropogenical influences and therefore also the actually existing vegetation (land use). Climatic changes in the vegetation are usually slow processes; changes in the landscape caused by humans require a comparatively short time. The main

populated areas of Ethiopia are found in the cooler middle elevations and not in the hot lowlands. The natural vegetation in these middle elevations is thus strongly anthropogenically influenced. A growing population pressure and limited available land cause a modification of this landscape, which is difficult to reverse, and the natural vegetation in this zone continues to retreat. Land use is altering, steeper and steeper slopes are ploughed, cattle must be settled in wooded areas. This creates soil erosion and the woods disappear in response to the increased need for fields and pastureland (SCHULTZ 2000, 469ff.; WESTPHAL 1975, 44ff.).

During the rainy season and under normal conditions for rain planting, the precipitation amounts in the wet summer tropics are generally sufficient. The fact that again and again longer dry periods can occur normally leads to the planting of annual species. The agricultural areas are largely used by small farmers (subsistence agriculture). Agricultural use is, as is the natural vegetation, dependent on the climatic conditions of the thermal elevation zones. The Weyna Dega (1800 - 2600 m a.s.l) as well as the lower part of the Dega represent the most fertile zone due to the temperature and precipitation. They are particularly suitable for agriculture. In the area under investigation, a range of field crops such as the Ensete are cultivated at altitudes of 1800 m above sea level. Apart from Ensete, one can find tuber vegetables such as yams, taro or potatoes, but also grains such as barley, wheat and teff. Teff is a cultivated plant bounded to Ethiopia. In the region above 2500 m a.s.l., beside cereals, only a few other plants such as the Ensete or some bean varieties find suitable growing conditions. The cultivation limit for cereals is reached at about 3000 m a.s.l. In higher regions, grazing is the only existing form of food production. Farming is generally carried out with the help of livestock, which includes cattle, goats and donkeys. However, high stock levels are linked with the problem of finding suitable grazing conditions. In the lower regions, commercial agriculture and livestock holdings are carried out in the areas of the rivers and lakes such as the Bilate River and Lake Abaya. The state farms consist of huge complexes. In the Bilate Catchment area, three such farms are present: the farm near Alaba Kulito, the one south of Bilate Tena (Dimtu) and the Bilate State Farm. Apart from the state farms, little farming takes place at this elevation. Livestock is found only in a few areas of the valley (WESTPHAL 1975, 82ff.).

1.9 Basics of the Precipitation-Runoff Model

1.9.1 Model Conception

In order to simulate the equations of the water balance for the Bilate River Catchment (Southern Ethiopian Rift Valley) and to find a solution for these, the lumped Precipitation-Runoff Model NASIM (Hydrotec GmbH, Aachen) was used. NASIM is distinguished by factors such as the methodology of long-term simulation in the hydrological section, the mathematical modelling of surface waters, the representation of all significant physical processes of water storage and water movement as well as by the simulation of urban drainage. Through variable time iteration philosophy the flexibility of the model has increased (DOKUMENTATION NASIM June 2005, P. 1.1-1.4).

NASIM belongs to the lumped models which are simply analogous to physical laws. Using a cascade of storages, the physical parameters of the area of investigation are simulated. Variables and parameters represent average values in these models, which are representative of the whole area. The description of the hydrological processes takes place with the help of semi-empirical formulae with a physical background. If the parameters of the model are based on physics, such a model can also consider characteristic changes in the catchment area (OSTROWSKI 1982; WALTER 1995; HYDROTEC 2005).

NASIM offers the possibility to work through all the significant features of deterministic hydrology with a single model. This is realised by means of the representation of all necessary components of the/a hydrological cycle, along with the appropriate programming controls. NASIM represents a balanced combination of conceptual elements, which are based on physics. The model represents the significant elements of the/a hydrological cycle and hence allows the simulation of a closed water balance. The simulation rests upon the representation of rain loads and/or melting snow as well as on the load distribution calculated from the regional precipitation. Furthermore, it is based on the differentiation of the load into infiltration, the evaporation and the runoff distribution as well as on the runoff concentration, which results from the transport and the delay of the runoff portions. Finally, the simulation is based on the translation of the runoff wave due to retention in the river (DOKUMENTATION NASIM June 2005, Chapter

1).

1.9.2 Data Base

The data necessary for modelling can be distinguished into geometrical (space) data, hydrological data and meteorological data. The primary data include digital terrain models and digital maps of the sub-catchment; land usage and the soil type are also necessary. The secondary data required for the digital maps (themes) is available within the GIS in attribute tables. The tables form an interface to NASIM. The required soil parameters are: the wilting point, the field capacity, the total pore volume, the water permeability and the maximum infiltration rate. The land use parameters are: the rate of impervious area, the land coverage, the content of the interception store as well as the depth of root penetration. Soil and topography data remain constant over time. Land usage data are dependent on the season (DOKUMENTATION NASIM June 2005, 3-120ff.).

Meteorological and hydrological data in the form of time series are also required for modelling. For each time step, meteorological secondary data such as precipitation, air temperature, relative humidity and possible wind speed, global radiation and the relative period of sunshine must be available. That is why the last four parameters are needed for the calculation of the potential evapotranspiration. NASIM does not distinguish between evaporation and transpiration, but these rather are modelled together in the process of evaporation from the soil. Apart from precipitation, evapotranspiration has a high quantitative influence on the total water balance and also influences the actual soil moisture. Thus, balance calculations, especially those in the long run, require the most accurate possible measurement (consideration) of evapotranspiration. The potential evapotranspiration is received exactly like the precipitation and the air temperature as an input time series into the model. In NASIM, regional precipitation, evaporation and temperature are thus used in the form of point measurements, which are individually assigned to system elements. For the present Master's thesis a raster-based assignment in NASIM was not available. Discharge measurements at gauging stations represent the hydrological data. These must be available in the temporal resolution of the chosen time interval. This type of data is not necessary for the modelling process, but the calibration and validation of the model is not possible

without measured drainage values. NASIM expects taking into account the time series minute, hours or daily values (DOKUMENTATION NASIM June 2005, P. 2.8ff., P. 5.59). For the water balance modelling of the Bilate Catchment daily values were used.

1.10 Methodology

1.10.1 Soil Data

The FAO Soil Map (1998) gives information about the varying soil types and the soil depth in the area to be investigated. However, the information which was required for modelling with NASIM, such as the soil grain size and physical parameters like the total pore volume (GPV), the field capacity (FK), the wilting point (WP) or the water permeability (kf value), could not be taken directly from these maps. As soil sampling was not carried out in the course of this study, detailed values for the soil grain sizes and the soil physical parameters are not available in detail. In order to obtain this relevant information, the literature such as Bodenkundliche Kartieranleitung (1995), DVWK Merblatt 238 (1996), SCHEFFER/SCHACHTSCHNABEL (2002), ZECH/HINTERMAIER (2002) was consulted. For defining the soil grain size of the subtler soil, the soil grain sizes were extracted from the soil types with the help of the triangle diagram of SCHEFFER/SCHACHTSCHABEL (2002). The physical parameters were derived from the soil grain size.

1.10.2 Land Use Data

In the area of investigation, the natural vegetation is more or less strongly influenced by the agricultural use. The digitalised map of 1978, which was made available by the Ministry of Agriculture, gives only a very general image of the current distribution pattern of the vegetation, but it was the only available resource for the data required. Thus, on the map, the terms such as “open woodland”, “moderately cultivated”, “dense woodland/perennial”, “crop cultivation” and “state farm” are used without a clearer description of the specific vegetation, or, in mixed cultivation, without giving any details on the percentages of the various types of vegetation. The parameters for the depth of root penetration and

the maximum content of the interception storage were taken from BAUMGARTNER/LIEBSCHER (1990) or estimated on the basis of the latter. The calculation of the interception was carried out in NASIM. However ,an upper limit, the maximum interception, had to be given for every land area and for every type of usage. The degree of vegetation coverage was estimated from photographic material (THIEMANN/FÖRCH Nov. 2004). By means of the input of differently sized interception storages and root depths the annual cycle of the phenology was taken into account in NASIM. This input took place specifically for each month. The impervious land area given in the form of organic and inorganic crusts as well as by the paved road network or covered areas in the populated regions of the Bilate Catchment had to be estimated likewise.

1.10.3 Meteorological Data

For the meteorological data, time series for the last 20 years (from 1984 to 2004) were available as hard copies for total precipitation, minimum and maximum temperature, Piche data (potential evaporation), relative humidity and duration of sunshine. Data for global radiation and wind speeds were not available for the investigation area. Precipitaton data were available for 15 climatic stations, eight of which were located in the area of examination itself, with the others being situated outside the study area. Temperature data were available for eight of the 15 climatic stations. Piche data and data for relative humidity and hours of sunshine were only available for four of the 15 climatic stations. During the quality control of the data, some significant sections of missing data were noticed. For reasons of time, the period between 1997 and 2004 was chosen for the modelling. The availability of the data in the simulation period is given in figure 1.1.

The missing data in these time series were replaced. The method of direct comparison with complete neighbouring stations (RAPP/SCHÖNWIESE 1996), which is also used in the additional NASIM programme TimeView, was considered unsuitable for the investigation area as the relatively large distances between stations made the methodology more complicated. Furthermore, the distinctive relief as well as the relatively large water area of Lake Boyo and the neighbouring wetland in the north of the investigation area led to a strong differentiation of the mesoclimate. The missing data were finally substituted by means of the

long-term (several years) average of the measurement stations in question. From the small spatial representative of the measuring (climatic) stations it followed that the values had to be estimated for potential evapotranspiration for a large region of the catchment.

Station	Precipitation	Max. Temperature	Min. Temperature	Evaporation
Alaba Kulito	Ok	Feb. 1999; Aug.-Dec. 2003	Sept. 1998; Feb. 1999	-
Aleta Wendo	Okt. 2001; 2002	-	-	-
Angacha	Feb., March, June-Sept. 1999; Jan.-June 2000	Feb.-March, June-Sep. 1999; Jan. -June 2000	Nov., Dec. 1998; Jan.-March, June-Sept. 1999; Jan.-June 2000	-
Awassa	Ok	Ok	Ok	Ok
Bedessa	March 1999; January 2000; March 2001; 2002	–	-	-
Bilate State Farm	Ok	April-Dec. 2002; 2003; Jan.-April 2004	Jan.-Nov. 2003	1997-2001; Jan. 2002; July 2003
Bilate Tena	Jan., Feb., April 1997; Feb. -June 1998; June 1999; March 2000; May 2001	-	-	-
Boditi	March 2000	March 2000	March 2000	-
Butajira	Ok	March-Dec. 1998; Jan.- May 1999; 2000	March-Dec. 1998; Jan.-May 1999; Oct. 2000	-
Durame	March 2002; Jan. 2004	-	-	-
Fonko	Ok	-	-	-
Hosaina	Sept. 1998	Sept. 1998; Dec. 2002	Sept. 1998; Jan.- Feb. 2001; June, Aug., Oct. 2004	Ok
Humbo Tebela	May 1999	-	-	-
Shone	Jan. 1997; July 1999; Sept. 2003	-	-	-
Sodo	Ok	May-June 1997; Jan., Feb. 2000	Jan. 2000	Sept. 1999; March-Dec. 2000; 2001-2003; Jan. 2004

Figure 1.1: Missing climatic data in the simulation period

1.10.4 Hydrological Data

In the area of investigation, five stations are available for the measurement of the runoff (discharge). Three of them are situated in the upper reaches of the Bilate River, one in the middle portion and one in the lower reaches of the river. The stations in the upper reaches do not all lie on the Bilate River itself: one is in the middle portion of the Guder, a tributary of the Bilate, and another station is located on the Batena, a tributary of the Guder.

The Guder flows through Lake Boyo with its bordering wetlands before it flows into the Bilate River. According to the MINISTRY of WATER RESOURCES

(Jan. 2006), the discharge in m3/s was calculated from the rating curve and the measured water depth at the station in question. The water depth is measured with a staff gauge. The gauge pressure is either manually documented or automatically registered (analogously or digitally). In relation to the rating curve there is no information available as to whether these values are being checked or from which time period they stem. The water bodies are subject to continuous changes because of the high sediment deposition. The calculation of the discharge is completely dependent on the rating curve, on the gauge pressure and on the water depth, respectively. Furthermore, there is no information about the point in time when, during the day, the manual documentation took place or if the actual flood hydrograph was registered.

During the quality control of the time series, significant missing data were noticed. Figure 1.2 shows the available time series for the chosen simulation period from 1997 to 2004.

Year **Station**	1997	1998	1999	2000	2001	2002	2003	2004
Weira	Ok	Ok	Ok	-	-	-	18.05. – 13.09.	11.01. – 04.09.
Batena	Ok	Ok	01.01. – 30.09.	-	-	-	26.04. – 31.12.	01.01. – 05.06.
Guder	Ok	Ok	Ok	Ok	01.01. – 03.02.	-	01.06. – 31.12.	01.01. – 02.10.
Alaba Kutio	Ok	Ok	Ok	Ok	Ok	Ok	01.01. - 04.10.	30.05. – 31.12.
Bilate Tena	-	04.04. – 31.12.	Ok	Ok	Ok	Ok	01.01. – 19.10.	15.02. – 09.10.

Figure 1.2: Availabiliy of the discharge data in the simulation period

The missing data in the time series could not be coherently replaced since a relevant basis for this was not available and sometimes the missing values covered a period of one to three years.

1.11 Results

1.11.1 Soil Data and Land Use

The soil grain sizes were divided into classes of “Skeletal soil”: sandy loam, loamy sand, silty loam, loamy clay, clayey loam, sandy clayey loam and silty clay. The most common among these are the loamy soil grain sizes, which are to be found throughout the study area. “Skeletal soil” is present in the north and the

south of the Bilate Catchment and where the soil type Leptosol can be found. In the middle region of the investigation area as well as in the north, sandy substrates are to be found, and in the south and southeast silt portions dominate. The usable field capacity demonstrates a range of values between 120 mm/m and 178 mm/m. The lowest value is found in the region of the Lakes Boyo and Abaya as well as in the wetland of Lake Boyo. The highest values spotted in the north, the south and the southeast of the investigation area, where "skeletal soil" (Leptosols) and loamy sand (Cambisols) are present. The evaluated hydraulic permeability of the soil grain sizes or soil types takes values between 0.001 mm/h and 103.4 mm/h. Logically, the lowest value is found in the region of the Kakes Boyo and Abaya (0.001 mm/h). The highest value (103.4 mm/h) is detected where Leptosols are present, followed by the loamy sand (Cambisols) with 38.5 mm/h in the north of the investigation area.

As initially mentioned, the land use in the investigation area can only be represented in a highly generalised manner. Perennial crop cultivation in substance takes place on the western graben shoulder as well as in the northwest of the Bilate River Catchment. Areas which are moderately cultivated are found throughout the catchment. Furthermore, open grassland exists in the region of Lake Boyo and on the eastern flank of the area of investigation. The natural vegetation, for example woods with eucalyptus, various acacia species, juniper trees (Juniperus procera) or yews (Podocarpus gracilior), as well as shrub land is only found in small areas or rather to a small extent. The three State Farms in the investigated area cultivate mainly maize, tobacco and grain. The impervious land area, which is given in the form of organic and inorganic crusts as well as in the form of paved road networks or covered areas in the populated regions of the Bilate Catchment, was estimated between 5% and 10%.

1.11.2 Meteorological Data

For the evaluation of the data, the period from 1997 to 2004 was considered in the first place. However, the period after 1984 was also considered in order to observe potentially significant values.

Precipitation

For the measurement stations a good spatial representation in the investigated area is of great importance. The accuracy of the results desired implies a particular number of registration stations for precipitation measurement, and this is dependent on the size of the area, the form of the land, the altitude, the wind direction and the degree of variation of the precipitation. According to DISSE (2005, 89), in flat land, one station per 40 km^2 is desirable; in mountains, it is one station per 20 km^2. Due to the great variability of the precipitation, stations with a smaller dispersion (10-15 km^2) would have been an advantage for the Bilate River Catchment. Figure 1.3 shows all climatic stations for precipitation in the Bilate Catchment and its surroundings. The circles around the stations have a radius of 11.5 km. The areas of the circles correspond to the spatial representation of the stations. One can see that a complete coverage of the area of investigation is not given.

Comparing the annual averages of precipitation, a decrease in the precipitation from the graben shoulder to the bottom of the rift can be seen (Figure 1.4). Thus, the stations are situated at the thermal altitude level Weyna Dega with a registered precipitation between 1646 mm/a and 1139 mm/a. At this thermal altitude level the stations Angacha, Aleta Wendo, Shone, Fonko, Sodo, Boditi, Hosaina, Durame und Butajira are located.

At the next lower thermal altitude level named Kolla (1500-1800 m a.s.l) the climatic stations Humbo Tebela, Bedessa, Alaba Kulito und Awassa are situated, with annual precipitation values between 1151 mm/a and 927 mm/a. The lowest annual precipitation was found at the station Bilate Tena with 886 mm/a and at the Bilate State Farm with 663 mm/a. The latter can definitely be assigned to the Bercha. The Bilate Tena station, however, lies on the border between the lower Kolla and the upper Bercha. The annual precipitations calculated here give only a rough starting point, not allowing to derive mean values over periods of several years, since the average values were only calculated over a period of 8 years and also because data were missing in the time series at several stations. One should notice that the period from 1984 to 2004 is also not much more expressive be-

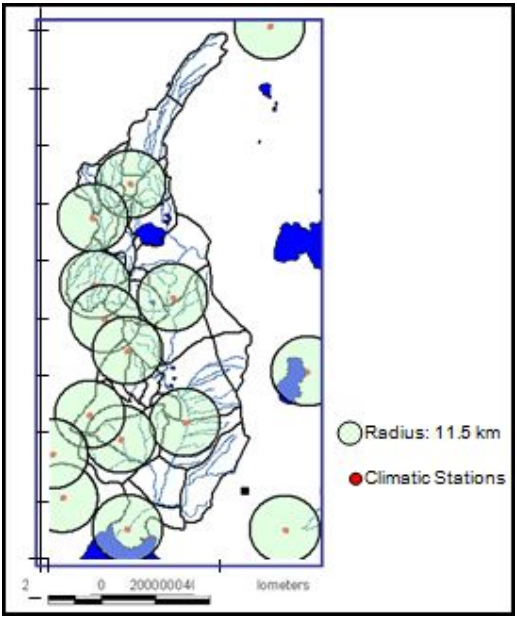

Figure 1.3: Measurement stations in the Bilate Catchment; Source: THIEMANN/FÖRCH Nov 2004; ALTHOFF May 2006

cause missing data in the time series signify that the period of observation is also partly restricted to less than 20 years.

With regard to the average of the annual pattern of the time series, the partly varying distribution is noticeable (figure 1.5). In this connection, the stations Bedessa, Bilate Tena, Humbo Tebela, Boditi and Sodo are clearly distinguishable from the rest. The annual pattern of precipitation demonstrates a division, the maximum of which lies in spring, summer and autumn, and from which no clear second rainy period can be distinguished. The remaining stations are more or less similar in their annual patterns. Relatively high, though not constant amounts of precipitation fall from March to October, usually with an absolute and a relative

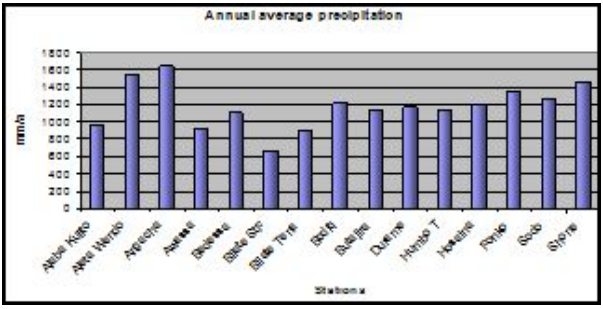

Figure 1.4: Annual average precipitation, middle of 8 years; Source: Own graphic

maximum. The difference between the stations lies in the occurrence of the maxima. For the stations Shone, Fonko, Butajira, Hosaina, Durame and Awassa, the influence of the southwest monsoon can be seen as a significant maximum, which is present in summer, mostly in July/August. The average precipitation amounts are higher than those in spring, in the phase of the "small rains" in April/May. The lowest precipitation months are those from December to February, which are under the influence of the northeast Passat.

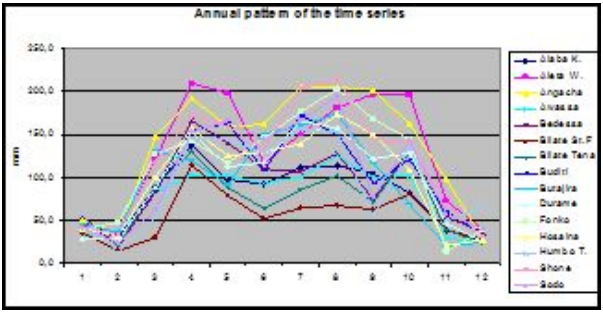

Figure 1.5: Annual pattern of the time series, middle of 8 years; Source: Own graphic

A fact that can nevertheless be derived from the average precipitation is that the Bilate River Catchment is not a homogeneously structured area, but rather an area with different precipitation regimes. This becomes more obvious when one considers the average of the annual patterns of the time series. However, it is evident that apart from the large-scale climatic processes at the stations, micro- and meso-climatic influences also play a role, for example the geographical position within the rift and the windward and leeward positions associated with this at the time of the varying current directions. Furthermore, the orographic precipitation is significant, which appears in southeasterly weather situations in the western highlands.

Temperature and Evaporation

Similar to the precipitation, the temperature time series of the eight stations in the area of investigation shows a certain spatial structure (figure 1.6). It has to be recognised that the stations in the thermal altitude of the Weyna Dega represent a clearly lower annual average value with a maximum temperature of 23.6°C (Hosaina) than they do in the Bercha, with a temperature of 30.3°C (Bilate State Farm). Thus a dependence on the altitude exists. Regarding the minimum temperature, the State Farm has also the highest value with 16.6°C in the middle; and once again Hosaina is last, with 10.8°C in the middle. According to ENDLICHER (2000), the course of the temperature is generally distinguished by the fact that the maximum temperatures fall with the onset of the first rainy season due to the lower irradiation. Likewise, the minimum temperatures rise as a result of the reduced radiation. If one considers the time series of the precipitation and the time series of the temperature (figure 1.6), this can be clearly stated for the majority of the stations.

As for the temperatures, the time series of evaporation of the four stations in the study area shows a certain spatial structure. The highest annual mean values of evaporation are, with regard to the temperature, that of the Bilate State Farm station with 2505 mm/a, followed by the stations Awassa with 1650 mm/a, Sodo with 1608 mm/a, and finally the Hosaina station with a mean annual evaporation of 1321 mm/a.

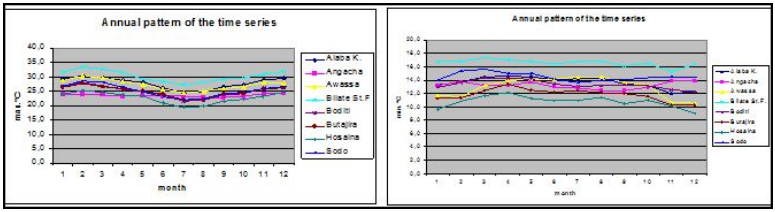

Figure 1.6: Annual pattern of the time series; max. and min. temperature, middle of 8 years; Source: Own graphic

As far as temperature and precipitation are concerned, there is a dependency on the thermal altitude level. The stations in the thermal altitude level of the Weyna Dega show a significantly lower annual amount of evaporation than the station in the Bercha. The annual pattern of the time series for evaporation shows a regular regime for all stations. At the beginning of the first rainy season (February) the curve reaches its peak. However, due to the lower irradiation, it sinks similarly to the maximum temperature. The minimum is reached at the end of the "long rains" in August. After this, the curve slowly rises again.

1.11.3 Results of the Model Calibration and Validation

Regarding the assignment of the climatic stations to the individual sub-catchments, the altitude above see level brought the best results for the precipitation data as well as for the temperature and the evaporation values. The suggestion to use the Thiessen polygon for the assignment was not suitable due to the distinct relief and the variability of the data. The calibration of the simulated discharge wave represents a complex of interactions between precipitation, evaporation and soil functions, and therefore between the runoff formation and the runoff concentration. None of these parts lead to the desired success on their own.
In the following passage, the total result of the calibration process is represented and then briefly described on the basis of the subsequent two examples (figure 1.7 and 1.8). The time period used for the calibration is not identical for every gauging station due to missing data in the discharge values.

In Figure 1.7 the calibrated regional precipitation (above), the measured discharge (below) and the simulated discharge of the gauging station Weira are shown for the period from 20.02.1997 to 15.02.1998. The fast/immediate reaction of the simulated discharge to the events of the precipitation can be clearly seen. Therefore, there is a direct precipitation-runoff dynamic, in which a very fast increase to the peak value of the discharge is present as well as a less steep decrease over an intermediate discharge to the basis-discharge.

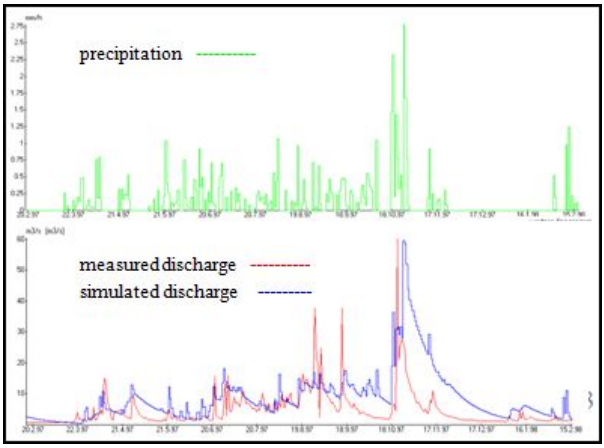

Figure 1.7: Measured and simulated discharge of the gauging station Weira, period 20.02.1997 to 15.02.1998; Source: Own graphic

The measured discharges are in time relatively well in line with the precipitation. In this context, a fast reaction between precipitation and discharge can also be recognised, whereas nevertheless a fast rise to the peak of the discharge is followed by a fast decrease over an intermediate discharge to the basis-discharge. Furthermore, the peaks of the discharge are particularly significantly higher than those that are simulated, and the basis-discharged peaks are lower than those simulated. A good correspondence of measured and simulated discharge levels can be seen for the intense rain of October 1997, whereas in other sections of the

simulated period (Figure 1.7) the conformity has to be assessed as relative.

In Figure 1.8, the calibrated regional precipitation (above), the measured discharge (below) and the simulated discharge of the gauging station Alaba Kulito are shown for the period from 20.02.1997 to 15.02.1998. At this station a direct precipitation discharge dynamic exists as well. A temporal delay between discharge and precipitation can be recognised in the hydrograph including October. In October/November the simulated peak of the discharge lies before the intense rain in November. Furthermore, the peak of the discharge in November is not as high as that in October, despite the significant event. The measured discharge reacts similarly to the simulated one. For the latter, however, a time delay concerning the precipitation can be seen.

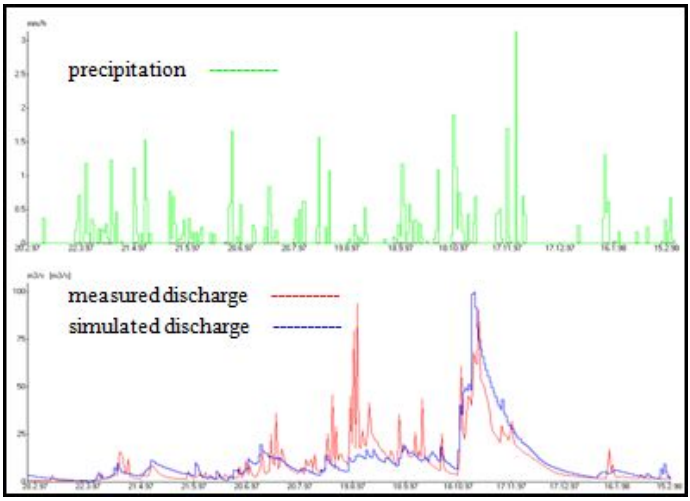

Figure 1.8: Measured and simulated discharge of the gauging station Alaba Kulito, period 20.02.1997 to 15.02.1998; Source: Own graphic

The peak of the discharge measured in November is equally similar. It is not as high as the one in October, despite the intense event. As for the simulated

discharge, the curve rises very fast to the peak and falls, as fast as it rose, to the intermediate and basic discharge. Furthermore, the peaks of the measured discharge are significantly higher than the ones of the simulated discharge, and only in October/November they do lie under the simulated discharge. A relatively good analogy between the measured and simulated discharges is effectively present only in the time between the intense rain in October/November 1997 and at the beginning of the "small rains", from July to October. No correlation can be ascertained. The validation process was carried out for the period after the calibration up to 2004. It should be noted that, with regard to the discharge for some gauging stations, significant sets of data were missing in the time series, so that no continuous validation could be carried out. The parameters specified for the calibration of the Precipitation-Runoff Model were constant during the entire period of validation.

1.12 Discussion

For the calibration of the data, the measured discharge time series from the individual gauging stations were used. The aim of the calibration was to reach the best possible approach for the measured discharge. The calibration of the model between the gauging stations Alaba Kulito and Bilate Tena proved to be most difficult as relatively large catchments had to be calibrated in this connection, with significant inflows from the tributaries. As a result of the lack of gauging stations on the larger tributaries or in the Bilate River, no smaller areas could be calibrated. Another difficulty occurred through the presence of Lake Boyo and the bordering wetland in the catchment of the gauging station Alaba Kulito due to the fact that no measurements for evaporation or for inflow or outflow of Lake Boyo were present here. The lake and the wetlands were finally simulated by a very high evapotranspiration and storage.
The quality of the calibration process must be seen in the context of the fact that many parameters had to be estimated, for example land use, soil and evapotranspiration. Furthermore, the computation was not carried out with regional precipitation and evapotranspiration, but the time series of a particular climatic station were assigned to a certain sub-region, so that only five gauging stations were available for the calibration of the model. Considering this background, the

results of the model calibration can be considered satisfactory. It is important to mention that this was not primarily a question of the exact quantification of precise discharge values, as would for example be the case with the simulation of flood protection. The question was rather whether a simulation of the water balance under the given conditions was sensible and possible anyway. However, the simulated discharges must be regarded very carefully because with regard to the discharge peaks they do not really represent the reality of the situation.

The reasons why the peaks of the measured and simulated discharge-frequency curve differ can be various and will be discussed in the following. One reason is due to the fact that local precipitation in the catchment was not recorded by the climatic stations. Actually, the precipitation captured in the precipitation gauge is only representative of the particular measurement area. If the altitude of precipitation in the measurement areas can be extended to other locations or larger areas, and if so to what extent, is broadly a function of the correct choice of the location (representation) of the individual measuring point. As can be seen in Figure 1, the prevailing part of the Bilate River Catchment demonstrates, according to DISSE (2004), no complete area coverage of the precipitation stations. In respect of this, the situation at the western graben shoulder is better than the one at the valley bottom or at the eastern graben flank of the Bilate Catchment. The orographic disposition of a catchment exerts a relevant impact on the distribution of the precipitation. Due to this impact it is important to realise it when the stations are located windward or leeward, at an open hill top or in deep incised valleys. This can lead to significant differences in the altitude of precipitation, even in a small space. Generally, it can be stated that for a long-term analysis, the orographic and climatologic conditions are important. Due to the special characteristics of the Bilate Catchment a larger spatial density of measuring stations would have been important in order to better record the large spatial and temporal variability of the precipitation. An additional reason for inaccuracies is probably the fact that not interpolated regional precipitation values (raster-based) were used for the calculation, but station values, whereas it is not proven whether the simulation with raster-based regional precipitation would have led to better results. In order to prove this once and for all, a comparative calculation would be necessary. Another aspect is the number of gauging stations. In case of a larger representation of gauging stations in the Bilate River, a calibration in smaller parts would have

been possible, which might have led to better results. One should also mention that the functionality of the stations, up to those in Alaba Kulito, could not be verified because of time shortage. Furthermore, it could not be definitively settled how the recording of the data had been carried out (manually or automatically) and in which way one had measured (with staff gauge or radar). Moreover, it is unknown in which period of time the rating curves were checked and how the discharge had been calculated. Regarding the gauging station Alaba Kulito (figure 1.9) the stones in alignment with the staff gauge are notable. The stones cause a pier accumulation, which falsifies the water level measurement. The same effect can be found under the bridge.

Figure 1.9: Gauging and climatic station Alaba Kulito; Source: Own graphic, January 2006

It cannot be assumed that the hindrances in the rating curve and in the calculation of the discharge have been taken into account. The meteorological and hydrological data were made available in form of hard copies, and errors in the transcription of the data as such cannot be ruled out. But also the discharge parameters (soft copies) can have mistakes because they are manually typed into Excel lists.
In addition, the physical soil parameters and the parameters of the vegetation (root depth, interception storage, etc.) taken from the literature are related to the Central European area and are partly based on subjective assessments. The land coverage was finally estimated.

1.13 Conclusion

The Precipitation-Runoff Model NASIM considers the necessary water balance parameters described above and partly implements them in a physically-based way (soil model). The modelling takes place in a differentiated manner according to the area, and temporally with a daily resolution, although in this connection one can calculate with hour or minute values as well. The choice of a lumped model was necessarily dependent on the available data material. The processes of water balance were relatively well-described and based on the available data (material). The limitations which arose from the missing soil data and land use data could in principle only be corrected through field work, whereas in relation to the results the greatest influence was seen in terms of the meteorological data. With regard to this aspect, it should be noted that the distinct relief and the large variability of the precipitation as well as the influence of the evaporation will in no way be represented by the number of climatic stations. The simulation would probably have led to better results, if a better basis of meteorological data as well as a higher number of gauging stations had been used. As far as the gauging stations are concerned, it should be stated that the calibration of the model can only lead to a good description of the natural conditions in the Precipitation-Runoff Model through the use of qualitatively good discharge measurements at several gauges.

At the time this Master's thesis was written, the NASIM programme did not yet work on a raster basis. Thus, improvements in this very direction make sense, since in this way in relation to meteorological data for example, a calculation with interpolated regional data would be possible instead of a calculation with station data. A supplementary point consists in the non-satisfactory use of the GIS for the visualisation of the simulation results. The GIS is used at present for the administration and pre-processing of the data and only limited to the presentation of results, which are, however, not convincing enough. The relation to the GIS in the form of a raster-based representation would be better in this case. It should be noted in respect of NASIM that the model is prevailingly used for the simulation of flood discharge, which can be seen in the very good representation of the time results by means of TimeView. The simple handling of the programme was an advantage, as was the possibility to directly make changes in

the system plan.

All in all, it can be stated that modelling the water balance with a standardised hydrological model such as NASIM was possible but required a very detailed examination of the results as well as of the input parameters and their emphasis for the model. Both the calibration as well as the validation of the model must be viewed as semi-quantitative since, in addition to the low degree of data availability, the quality of the data could not be sufficiently classified either. In conclusion, the results of the modelling must be seen as satisfactory in the light of the available data material.

1.14 References

BAKER, B.H.; MOHR, P.A.; WILLIAMS, L.A.J. (1972): Geology of the Eastern Rift System of Africa. The Geological Society of America, Special Paper 136, Boulder.

BAUMGARTEN, A.; LIEBSCHER, H.J. (1990): Allgemeine Hydrologie, Quantitative Hydrologie. Lehrbuch der Hydrologie, Bd. 1, Berlin, Stuttgart.

BEHRENS, S. (1971): Physical Environment and its Significance for Economic Development with special reference to Ethiopia. Lund Studies in Geography, Lund.

BEKELE AWULACHEW, S. (2001): Investigation of Water Resources Aimed at Multi-Objective Development with Respect to Limited Data Situation: The Case of Abaya-Chamo Basin, Ethiopia. Dresdner Wasserbauliche Mitteilung, Heft 19, Selbstverlag der TU Dresden.

BOCCALETTI, M., et al. (1998): Quaternary oblique extensional tectonics in the Ethiopian Rift (Horn of Africa). In: Tectophysics, Nr. 287, 97-116.

BODENKUNDLICHE KARTIERANLEITUNG (1995): Arbeitsgruppe Bodenkunde der geologischen Landesämter und der Bundesanstalt f. Geowiss. U. Rohstoffe, 4. Aufl., Hannover.

BROCKWELL, P.J.; DAVIS, R.A. (1987): Time Series: Theory and Methods. Springer-Verlag, New York, Berlin, Heidelberg u.a.

DISSE, M. (2005): Hydrologie und Wasserwirtschaft I. In: Vorlesungsskript, Universität der Bundeswehr München.

DVWK (Hrsg.) (1996): Ermittlung der Verdunstung von Land- und Wasserflächen. DVWK-Merkblätter zur Wasserwirtschaft, H. 238. Bonn: Wirtschafts- und Verl.-Ges. Gas und Wasser.

EBINGER, C. J., et al. (1993): Late Eocene-Recent volcanism and faulting in the southern main Ethiopian Rift. In: Journal of the Geologie Society, Nr. 159, 99- 108.

ENDLICHER, W. (2000): Afrika südlich des Maghreb: Ostafrika. In: WEISCHET, W.; ENDLICHER, W.: Regionale Klimatologie Teil 2: Die Alte Welt Europa, Afrika, Asien. Teubner, Stuttgart, 245- 336.

ETHIOPIAN MAPPING AUTHORITY EMA (1988): National Atlas of Ethiopia, Addis Ababa.

FAIRHEAD, J. D. (1986): Geophysical control on sedimentation within the African Rift System. In: FROSTICK, L.E. (Hrsg.): Sedimentation in the African Rifts, 19-27. Geological Society Special Publication No. 25, Blackwell, Oxford.

GEORGES, R.; ROGERS, N. (1999): The Petrogenesis of Plio-Pleistocene alkaline volcanic Rocks from the Tosa Sucha region, Arba Minch, southern Main Ethiopian Rift. In: Acta Vulcanologica, Nr. 11, 121-130.

GRIFFITHS, J.F. (1972): Climates of Africa. World Survey of Climatology, Vol. 10, Elsevier, Amsterdam, London, New York, 370ff.

HELLDÉN, U,; EKLUNDH, L. (1988): National Drought Impact Monitoring. A NOAA NDVI and precipitation data study of Ethiopia. Lund University Press, Lund.

HURNI, H. (1982): Hochgebirge von Semien - Äthiopien Vol. II: Klima und Dynamik der Höhenstufung von der letzten Kaltzeit bis zur Gegenwart (Teil II gemeinsam mit Peter Stähli). Jahrbuch der Geographischen Gesellschaft von Bern, Beiheft 7, Bern, 40ff.

HURNI, H. (1988): Degradation and Conservation of the Resources in the Ethiopian Highlands. In: MESSERLI, B. (Hsrg.): African mountains and highlands: pro-

ceedings of an international workshop organized by the Comm. On Mountain Geoecology of the Int. Geograph. Union on behalf of the UN University, Addis Ababa, Ethiopia, 18-26 Oct. 1986, Boulder. Mountain Research and Development, 2-8, 123-130.

LILJEQUIST, G.H.; CEHAK, K. (1994): Allgemeine Meteorologie. Vieweg, Braunschweig, Wiesbaden, 294ff .

MENZEL, L. (1997): Modellierung der Evapotranspiration im System Boden-Pflanze-Atmosphäre. In: Züricher Geographische Schriften, ETH Zürich.

MEYER, R. (1987): Äthiopien - Eine geographische Einführung. In: MATTER, H.E.; WESTPHAL, A. (Hrsg.): 20 Jahre Agrarforschung des Tropeninstituts in Äthiopien. Giessener Beiträge zur Entwicklungsforschung, Reihe I, Band 14, 29-39, Selbstverlag Tropeninstitut, GieSSen.

MOHR, P.A. (1971): Outline tectonics of Ethiopia. In: UNESCO (Hrsg.), Tectonics of Africa. Earth Science 6. UNESCO, Paris, 447-458.

NASIM DOCUMENTATION, Hydrotec June 2005.

NYAMWERU, C.K. (1996): The African Rift System. In: ADAMS, W.M.; GOUD, B.A.S.; ORME, A.R. (Hrsg.): The Physical Geography of Africa, 18-33. Oxford University Press, Oxford.

OSTROWSKI, M.W. (1982): Ein Beitrag zur kontinuierlichen Simulation der Wasserbilanz. Mitteilung, Institut für Wasserbau und Wasserwirtschaft, Rheinisch-Westfälische Technische Hochschule Aachen, 42.

RAPP, J.; SCHÖNWIESE, C.D. (1996): Atlas der Niederschlags- und Temperaturtrends in Deutschland 1891-1990. Frankfurter Geowissenschaftliche Arbeiten, Serie B Meterologie und Geophysik, Bd.5, Frankfurt.

READING, H.G. (1986): African Rift tectonics and sedimentation, an introduction. In: FROSTICK, L.E. (Hrsg.): Sedimentation in the African Rifts, 3-7. Geological Society Special Publication No. 25, Blackwell, Oxford.

SCHEFFER, F.; SCHACHTSCHABEL, P. (2002): Lehrbuch der Bodenkunde. 15. Auflage, Spektrum Akademischer Verlag Heidelberg, Berlin, 443ff.

SINGH, V.P.; FREVERT, D.K. (2002): Mathematical Models of Large Watershed Hydrology, Denver, Colorado 80225-0007 USA.

SINGH, V.P.; FREVERT, D.K. (2002): Mathematical Models of Small Watershed Hydrology, Denver, Colorado 80225-0007 USA.

SCHULTZ, J. (2000): Handbuch der Ökozonen. Ulmer, Stuttgart, 468ff.

SCHÜTT, B.; THIEMANN, S. (2005): Modern water level and sediment accumulation changes of Lake Abaya, southern Ethiopia - A case study from Bilate River delta, northern lake area. In: Sustainable Management of Headwater Resources, Research from Africa and India, 137ff.

SELESHI, Y.; DEMARÉE, G.R. (1995): Rainfall variability in the Ethiopian and Eritrean highlands and its links with the Southern Oscillation Index. In: Journal of Biogeography, 4-5, 22, 945-952.

THIEMANN, S.; FÖRCH, G. (2004): Water Resources Assessment in the Bilate River Catchment Precipitation Variability, LARS 2004.

WEISCHET, W. (1995): Einführung in die Allgemeine Klimatologie. 6., überarbeitete Auflage, Teubner, Stuttgart, 15ff.

WESTPHAL, E. (1975): Agricultural systems in Ethiopia. Centre for Agricultural Publishing and Documentation, Wageningen, 15ff.

ZECH, W.; HINTERMAIER-ERHARD, G. (2002): Böden der Welt- Ein Bildatlas.

ZELEKE, G.; HURNI, H. (2001): Implications of Land Use and Land Cover Dynamics for Mountain Resource Degradation in the Northwestern Ethiopian Highlands. In: Mountain Research and Development, 2, 21, 184-191.

Internet Sources

BMZ 2006, http://www.bmt.de/de/laender/partnerlaender/aethiopien/zusammenarbeit.html (06/06/2006)

2 Severity - Duration - Frequency (SDF) Analysis of Drought by using Geographical Information System (GIS) - Tilahun Derib Asfaw, Dr. L.B. Roy

Case of: Abaya and Chamo Lakes basin, South Ethiopia

Tilahun Derib Asfaw, Dr. L.B. Roy[1]

[1] Arba Minch University
Ethiopia

2.1 Abstract

The famous and universally applied drought index known as Palmer Drought Severity Index (PDSI) was used to examine the drought parameters of the basin. This method uses precipitation, evapotranspiration, soil moisture recharge, soil moisture loss and actual and potential values as input data. The drought situation of the basin was studied by using 34 years (1970 - 2003) rainfall and mean temperature data from 18 stations which are located inside the basin. Furthermore, the soil types were utilized in order to determine its available water holding capacity (AWC). The analysis shows that PDSI can be positive (moisture surplus) or it can be negative (moisture stress or drought condition). By using the results of the PDSI values of each station, an SDF graph of the basin was developed. Based on the SDF value of each station, the basin was regionalized by using of Arc View GIS environment.

Key words: *PDSI, SDF, Drought index, GIS, return period, severity, AWC*

2.2 Introduction

A part of the Abaya - Chamo Basin (ACB) is a drought prone area. Through time, the effects are coming into an increasing manner. The expected main reason was the decreasing rate of rainfall amount in the basin. Therefore, the erratic distribution and less amount of rainfall from the long term mean value highly affect the production. As a result, this can cause a problem of food security for the basin. Moreover, in the basin farmers are using a mixed farming system; the problem of drought extends to their cattles as well. Severity, duration and frequency are drought parameters. By determining its magnitude and the return periods of certain durations of drought we can address several of the described elusive drought properties. Obviously, drought is an unavoidable phenomenon, but it can be mitigated through proper mitigation measures by studying the characteristics of its incidences.

The knowledge of regionalized drought maps are important in order to plan and manage the water resources potential of the basin. And also, these maps are important to provide information about the recurring behavior of drought for people that are living inside the basin.

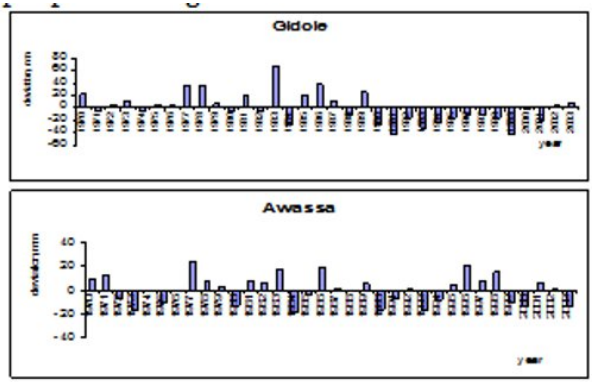

Figure 2.1: Typical rainfall pattern at Gidole and Awassa

2.3 Drought Definition and its Indices

There is no universal definition of drought but some authors tried to produce definitions. These available definitions of drought might be categorized as either *conceptual* or *operational*. With conceptual, it refers to those definitions in general term to identify the boundaries of the concept of drought. For example: "a long period with no rain, especially during the planting season." Conceptual definitions provide little guidance to those who wish to apply them to current (i.e. real time) drought assessments. Drought is frequently defined according to disciplinary perspectives. These definitions of drought are clustered into four types: meteorological, agricultural, hydrologic, and socioeconomic (Donald, 1987). Generally, drought is expressed by using indices. Different indices can interpret drought in different time periods, parameters and concepts. For this paper the Palmer Drought Severity Index (PDSI) is used.

2.3.1 Palmer Drought Severity Index (The Palmer; PDSI)

In 1965, W.C. Palmer developed an index in order to measure the departure of the moisture supply (Palmer, 1965). Palmer based his index on the supply-and-

demand concept of the water balance equation, taking into account more than just the precipitation deficit at specific locations. The objective of the Palmer Drought Severity Index (PDSI), to provide measurements of moisture conditions that were standardized so that comparisons using the index could be made between locations and between months (Palmer 1965). The PDSI is a meteorological drought index, and it responds to weather conditions that have been abnormally dry or abnormally wet. When conditions change from dry to normal or wet, for example, the drought measured by the PDSI ends without taking into account stream flow, lake and reservoir levels and other longer-term hydrologic impacts (Karl and Knight, 1985). The PDSI is calculated based on precipitation and temperature data, as well as the local Available Water Content (AWC) of the soil. From the inputs, all the basic terms of the water balance equation can be determined, including evapotranspiration, soil recharge, runoff, and moisture loss from the surface layer. The analysis is not considering human impacts on the water balance, such as irrigation.

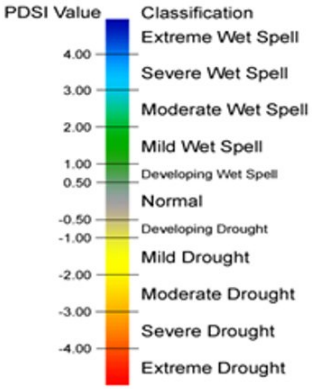

Figure 2.2: PDSI Value Classification

2.4 Analysis Procedure

The PDSI calculation is based on a supply and demand model of the soil moisture at a specific location. The supply is the amount of moisture in the soil plus the amount that is absorbed into the soil from rainfall. The demand, however, is not so as easy to determine, because the amount of water lost from the soil depends on several factors, such as temperature and the amount of moisture in the soil. This method used evapotransiration, runoff, soil moisture recharge and soil moisture loss all in its potential and actual values as input parameters.

2.4.1 Potential Values of Input Data

Potential Evapotranspiration, PET is calculated using Thornthwaite's method. Thornthwaite's method is calculating the PET on a monthly basis.
An Empirical formula to determine Potential Evapotranspiration (PET) developed by Thornthwaite is given by

$$PET = 16 * N_m \left(\frac{10 * T_m}{I} \right)^a \quad \text{---------- (1)}$$

Where

PET = monthly potential Evapotranspiration in mm.
m = 1, 2, 3.....12 (month)
N_m = is a factor to correct for unequal day length between months.
T_m = monthly mean temperature in °C.
I = heat index for the year.

$$I = \sum i_m = \sum \left(\frac{T_m}{5} \right)^{1.5} \quad \text{---------- (2)}$$

i = monthly heat index, and
a = cubic function of I.

$$a = 6.7 * 10^{-7} * I^3 - 7.7 * 10^{-5} * I^2 + 1.8 * 10^{-2} * I + 0.49 \quad \text{---------- (3)}$$

Potential Recharge, PR is the amount of water that could be absorbed by the soil, or the difference between the AWC and current soil moisture, so

PR = AWC - S_{i-1} ———— (4)
Where S_{i-1} is thesoil moisture content at the end of previous month or at the

beginning of current month.

Potential Runoff, PRO is calculated assuming any precipitation that falls is absorbed until the ground is saturated, and then the rest runs off. Thus, PRO is the difference between the potential precipitation and the amount of moisture the soil can absorb. *Palmer decided to set the potential precipitation to AWC*, and the amount of moisture the soil can absorb is then simply PR, so

PR_0 = AWC - PR ———— (5)

Potential Loss, PL is slightly different; it involves the value of PET.

1. S_{i-1} >= PET_i, the moisture in the soil is enough to meet the demand, so the most moisture that can be lost is the amount in the soil.
   PL = PET ————————-(6)

2. S_{i-1} < PET_i, the moisture in the soil is not enough to meet the demand, therefore PL = S_{i-1} ————————(7)

2.4.2 Actual Values of Input Data

Along with these four potential values (PET, PR, PRO, and PL), their corresponding actual values (AET, R, RO, and L) are also calculated depending on the relationship of precipitation P, PET, and the soil moisture model.
The moisture in the soil can be used up, when demand is higher than supply and to be recharged when there is a surplus of precipitation and a deficit of soil moisture. The maximum recharge is up to Available Water Content (AWC), which is the maximum water holding capacity of the corresponding soil type. There are several cases, sub cases, and sub-sub cases to consider in order to determine how much moisture is gained or lost for each soil. The following relation shows the general relationship of a water balance equation:

1. If $P_i >= PET_i$, then
   a. $AET_i = PET_i$
   b. $L_i = 0$

   I. If $(P_i - PET_i) > AWC - S_{i-1}$, then
      a. $R_i = AWC - S_{i-1}$
      b. $Ro_i = P_i - (PET_i + R_i)$
      c. $S_i = S_{i-1} + R_i$

   II. If $(P_i - PET_i) <= AWC - S_{i-1}$, then
      a. $R_i = P_i - PET_i$
      b. $Ro_i = 0$
      c. $S_i = S_{i-1} + R_i$

   2 If $P_i < PET_i$, then
      a. $R_i = 0$
      b. $Ro_i = 0$
      c. $AET_i = P_i + L_i$

      I. If $S_{i-1} > (PET_i - P_i)$, then
         a. $L_i = PET_i - P_i$
         b. $S_i = S_{i-1} - L_i$

      II. If $S_{i-1} <= PET_i - P_i$, then
         a. $L_i = S_{i-1}$
         b. $S_i = 0$

2.5 Water Balance Equation

2.5.1 Moisture Departure, d

The Moisture Departure, d is basically the deficit or surplus of moisture for a given month. It is calculated by using the following formula:

$d = P - \hat{p}$ ——————— (8)

Here, P is the precipitation and $\hat{p}$ is the CAFEC (Climatically Appropriate For Existing Conditions) precipitation. $\hat{P}$ is calculated as follows:

$$\hat{P}_i = \alpha_m . PET_i + \beta_m . PR_i + \gamma_m . PRo_i - \delta_m . PL_i$$

---------- (9)

$\alpha, \beta, \gamma, \delta$ are coefficients, the subscript $_m$ refers to the month of the year any they are determined by the following formulas:

$$\alpha_m = \frac{\sum_{all\ years} AET_m}{\sum_{all\ years} PET_m} \quad \text{----------(10)}$$

$$\beta_m = \frac{\sum_{all\ years} R_m}{\sum_{all\ years} PR_m} \quad \text{----------(11)}$$

$$\gamma_m = \frac{\sum_{all\ years} Ro_m}{\sum_{all\ years} PRo_m} \quad \text{----------(12)}$$

$$\delta_m = \frac{\sum_{all\ years} L_m}{\sum_{all\ years} PL_m} \quad \text{----------(13)}$$

2.5.2 Moisture Anomaly, Z

The moisture departure, d, is the deficit or surplus of moisture, adjusted for the seasonal changes in climate.

$$Z = dK \qquad \text{---------- (14)}$$

Where

d = Moisture Departure
z = Moisture Anomaly
K = Climatic Characteristics

The value of K changes depending on location and time of year, as is evident in the following formulas used to calculate it.

$$K_m = \frac{17.67}{\sum_{m=1}^{12} \overline{D}_m K_m'} K_m' \qquad \text{---------- (15)}$$

Where the value of 17.67 is an empirical value that Palmer derived.

$$K_m' = 1.5 * \log_{10}\left[\frac{\frac{\overline{(PET)}_m + \overline{R}_m + \overline{(Ro)}_m}{\overline{P}_m + \overline{L}_m} + 2.8}{\overline{D}_m}\right] + 0.5 \qquad \text{-- (16)}$$

$$\overline{D}_i = \frac{\sum_{all\ years} |d_i|}{N} \qquad \text{---------- (17)}$$

Where

N - Number of years record

2.5.3 The PDSI

Based on the above moisture departure and moisture anomaly values the drought index i.e. the PDSI is calculated. The PDSI itself can now be calculated using the following formula

$$Z = dK \qquad \text{---------- (14)}$$

Where

d = Moisture Departure
z = Moisture Anomaly
K = Climatic Characteristics

The value of K changes depending on location and time of year, as is evident in the following formulas used to calculate it.

$$K_m = \frac{17.67}{\sum_{m=1}^{12} \overline{D}_m K'_m} K'_m \qquad \text{---------- (15)}$$

Where the value of 17.67 is an empirical value that Palmer derived.

$$K'_m = 1.5 * \log_{10}\left[\frac{\frac{(\overline{PET})_m + \overline{R}_m + (\overline{Ro})_m}{\overline{P}_m + \overline{L}_m} + 2.8}{\overline{D}_m}\right] + 0.5 \qquad \text{-- (16)}$$

$$\overline{D}_i = \frac{\sum_{all\ years} |d_i|}{N} \qquad \text{---------- (17)}$$

Where

N - Number of years record

2.6 Data Analysis & Results

2.6.1 Rainfall, P

In most stations the distribution of rainfall has a bimodal pattern. The first high rainfall was observed from March to May and the next high rainfall was observed from July to November. This shows that there are two cropping seasons per year. Therefore, moisture deficit occurred either one season only or both seasons and it may also extend for the next third consecutive seasons.

From 18 stations the minimum monthly average rainfall was recorded at Mirab Abaya (61.04 mm) and in the contrary the highest average monthly rainfall was recorded at Yirga Chefe (131.30 mm).

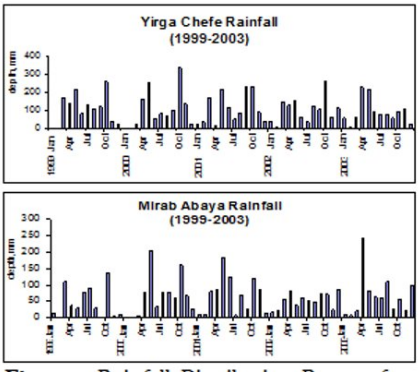

Figure 2.3: Rainfall Distribution Pattern for Mirab Abaya and Yirga Chefe stations for the selected year interval

Analyzing variation from the mean is important to determine the anomalies of rainfall. The highest standard deviation was shown at Yirga Chefe (111.38mm) and the lowest rainfall variation was shown at Awassa (56.72mm). Where the subscript (i) and (i_{-1}) indicate current and previous months respectively, and $PDSI_0 = 0$.

2.6.2 Mean Temperature, T

From 18 stations the highest yearly average temperature occurred at Mirab Abaya (23.35°C) and the lowest yearly average temperature was at Fiseha Genet (17.37°C). But anomalies from mean temperature show that the highest standard deviation was observed at Gidole (3.36°C) and at Yirga Chefe the lowest value was observed i.e. 0.94°C.

2.6.3 Potential Evapotranspiration, PET

For a station, if the difference between potential evapotranspiration and rainfall values for a specific month are small, it can be roughly concluded that the rainfall satisfies the PET demand of that month. A higher gap means that there is an

indication of moisture stress or moisture surplus in the area. A higher negative difference between mean rainfall and mean PET shows a higher moisture stress whereas a higher positive difference shows moisture surplus. Generally, a higher negative value takes place at Mirab Abaya (-39.65mm) and a higher positive value takes place at Yirga Chefe having a value of 63.97mm.

2.6.4 Actual Evapotranspiration, AET

The value of the AET depends on the supply condition of water i.e. the rainfall and the existing soil water content. If the AET is equal to the PET, it shows that there is no moisture stress in the area. The difference between PET & AET gives hints on moisture condition. A higher difference between the two values shows a higher deficit on moisture supply. But the AET itself does not indicate the deficit and surplus of moisture in the soil. A higher variation was observed at Mirab Abaya i.e. its mean monthly PET value was 100.69 mm whereas the mean monthly AET was 55.71 mm.

2.6.5 Relation between Rainfall, Mean Temperature and PDSI Value

The following figure (figure 2.4) shows the condition at Arbaminch in the period from 1999 to 2003. Roughly, it shows that when the rainfall value is increasing, the corresponding mean monthly temperature is relatively at decreasing value. As a result, the PDSI has a positive value i.e. it is a wet spell and the opposite is also true. But the previous month value of rainfall and temperature are influenced by the above remarking statement. For other stations, the relation between rainfall (P), mean temperature (T) and the corresponding PDSI value is similar to the above condition.

2.6.6 Sensitivity Analysis

It is obvious that the variation of input data affects the output (PDSI value). But the degree of influence differs. Such characteristics of input data on output is evaluated with the help of a sensitivity analysis. High sensitive data means that the influence on the result is significant. Therefore, with a sensitivity analysis it can be evaluated which parameter has a great role in influencing the PDSI value.

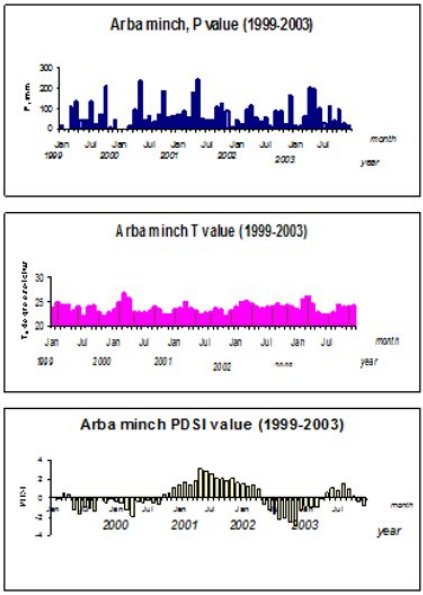

Figure 2.4: Relationship between P, T and PDSI for a typical station (Arba Minch)

The result shows that, if the rainfall amount is reduced by 50% the corresponding average change of deviation of PDSI is 50%. And also if the PET value is reduced by 50%, the corresponding PDSI value is changed by 90%. Therefore, the analysis shows that the PDSI is more sensitive on the change of PET value than rainfall i.e. PDSI highly depends on mean temperature because the PET value is mainly the result of a mean temperature.

2.6.7 Drought Parameter Evaluation

The drought parameters are severity, duration and frequency. Each of these parameters are independent values. But the combination of these three parameters gives a logical meaning for drought monitoring.

2.6.8 Drought Severity

Severity shows the degree of moisture deficit or surplus. It can be expressed based on PDSI values (figure 2.2) and it is calculated by equation 18 above.
For this analysis, drought occurs when PDSI is less than or equal to -1.00 (from mild drought to extreme drought). Mild drought (PDSI between -1.00 & -2.00) means, that the degree of severity is low and the moisture deficit can be recovered by less amount of rainfall compared to moderate drought (PDSI between -2.00 & -3.00).

2.6.9 Drought Duration

The duration of drought is the number of successive months in which the PDSI value is in *mild, moderate, severe or extreme conditions*. A cumulative drought is the sum of all types of drought occurred within a certain return period successively i.e. it considers the worst combination of all forms of drought. Most of the time, one follows the other, but sometimes it occurs randomly.
When counting the length of a drought duration, a single wet month between dry periods does not show the drought was at an end.

2.6.10 Drought Frequency

Drought frequency is the return period (in years) of a specified duration and severity of drought. The frequency is analyzed in a period of 8, and 10 years return periods. The method employed to determine the frequency of drought is by counting the specified drought severity and its duration at a station then by arranging its distribution by a weibull plotting formula. In general, the return period of mild drought is more frequent than moderate drought and so on.

2.6.11 Severity - Duration - Frequency (SDF) values

The SDF value illustrates the severity of certain durations of drought having a specified return period (frequency). For most of the stations, when the degree of severity increases, the corresponding duration for a specific return period are decreases. Based on SDF values, the basin was regionalized. Regionalizing

means delineating areas having similar values of SDF together; it is well suited for decision making procedures.

2.6.12 Predicting Drought Occurrences

Past experience was important in order to forecast future events. So, past occurrence of drought severity, duration and frequency repeats itself in the future. For more simplicity, 8 and 10 years return periods are analyzed for 18 stations. Based on these data the point data were changed into area data by linearly interpolating between stations. This method gives SDF curves of the basin. By doing so, it can regionalize the basin based on drought parameters. Thus, the results are interpreted by the help of Arc View GIS using different colors. Similar colors show areas having equal SDF values.

2.6.13 8 years Return Period Drought

The eight years return period drought expresses that the length of drought in months occurred within eight years. In this case, the frequency of drought is constant i.e. 8 years, but the duration and severity is variable depending on locations.

2.6.14 Mild Drought (MD- 8)

MD - 8 stands for a mild drought 8 years return period. MD - 8 map displayed in figure 2.5, the map shows that 85 percent of the basin areas have a duration of less than 5 months and around Mirab Abaya the duration extends to 6 - 7 months.

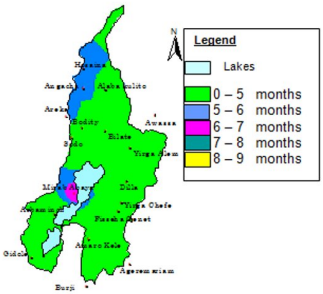

Figure 2.5: MD - 8 maps

2.6.15 Moderate Drought (MoD- 8)

MoD - 8 means a moderate drought having 8 years return period. The MoD - 8 map shown in figure 2.6 shows that most of the eastern part of the basin areas have a drought duration of 3 - 4 months and the western part of the basin areas have a duration of less than 3 months. Around Alaba Kulito, Burji and Ageremariam small areas have 4 to 5 months of moderate drought.

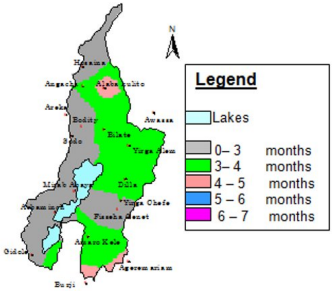

Figure 2.6: MoD - 8 map

2.6.16 Severe Drought (SD- 8)

Severe droughts having 8 years return period is abbreviated by SD - 8. Figure 2.7 shows that most of the areas have less than 2 months of severe drought. Near to Gidole, Fiseha Genet and Yirga Chefe the length of drought extends to 3 - 4 months.

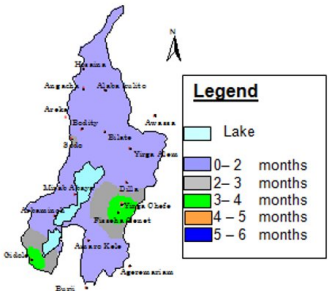

Figure 2.7: SD - 8 map

2.6.17 Cumulative Drought (CUM- 8)

CUM - 8 means a cumulative drought having eight years return period. It shows that the length of drought occurs during this period is greater than six months. Hence, in the basin all areas are affected by drought. A minimum duration will occur around Bodity which has 6 to 7 months of drought. In the vicinity of Gidole, Alaba Kulito, western and eastern border areas of Abaya Lake at least one complete failure of production for both season will happen within eight years, for other areas the condition of drought will be between this two events and it is illustrated by figure 2.8. The duration of drought will increase from north to south of the basin.

2.6.18 10 years Return Period Drought

The ten years return period drought in different severity conditions are shown by the following successive figures. Showing the different trends of drought, it is

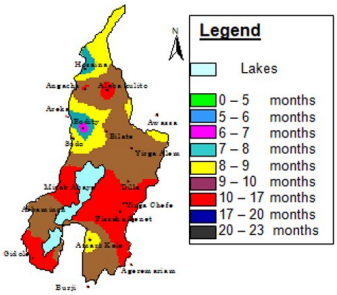

Figure 2.8: CUM - 8 map

important consider it's convalescence opportunity.

2.6.19 Mild Drought (MD- 10)

MD - 10 means mild drought 10 year return period. The MD - 10 maps illustrated in figure 2.9 shows that 58 percent of the basin areas have a duration of less than 5 months of mild drought and close to Mirab Abaya small areas have 7 to 8 months of mild drought.

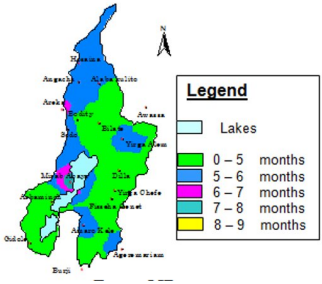

Figure 2.9: MD - 10 map

2.6.20 Moderate Drought (MoD- 10)

Moderate drought having a 10 year return period is abbreviated by MoD - 10 and it is clarified by figure 2.10 below. The map shows that 68 percent of the basin areas have a duration of 3 - 4 months of moderate drought and around Burji and Alaba Kulito small area have 5 to 6 months of moderate drought.

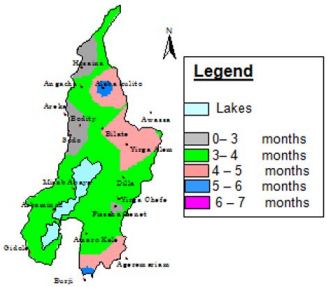

Figure 2.10: MoD - 10 maps

2.6.21 Severe Drought (SD- 10)

Severe drought of 10 years return period is abbreviated by SD - 10 and its distribution is shown in figure 2.11. According to the figure, most of the northern part (it covers 50 percent of the basin) has less than 2 months of severe drought. Hence, the northern part of the basin is less susceptible than the others. But the area around Yirga Chefe the length of drought prolongs to 4 to 5 months.

2.6.22 Cumulative Drought (CUM- 10)

The 10 year return period cumulative drought shows that at least one season will be completely affected by drought i.e. a minimum drought length of 7 to 8 months. But most of the area (92 percent) will be completely lost both season productions. Around Bodity and Hosaina the length of drought moment will be relatively shorter than the others. In this area, the drought length can completely

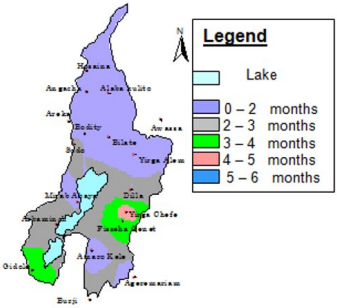

Figure 2.11: SD - 10 mapy

affect the production on one season and slightly on the next season. This is shown by figure 2.12 below.

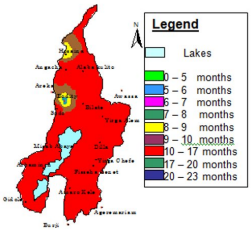

Figure 2.12: CUM - 10 maps

2.7 Summary, Conclusion and Recommendation

Different literature concludes that the PDSI method of drought evaluation is superior to others because its value depends on the demand and supply concept of moisture. But the method does not consider man made adjustments like irrigation practices.

Almost in all the stations the rainfall distribution has a bimodal pattern. This shows that there are two cropping season per year. It is important since, if one season fails the next season covers the problem within a relatively short period of time. High trouble of drought will be expected, when the length of drought extends to both seasons and a more catastrophic drouht can be expected, when it extends to the third consecutive season.

The main input data for the PDSI are rainfall, evapotranspiration, soil moisture recharge and soil moisture loss both its potential and actual values and also available water holding capacity of the soil. But all input data were resulting from either rainfall or mean temperature. Therefore, the sensitivity analysis shows that the PDSI is more sensitive on temperature.
In order to regionalize the basin, the point SDF value at a station should be changed to an area's value by linearly interpolating between stations. For the result it was essential to show several drought maps of a basin. These maps were used to know the coverage of a specific type of drought. For example, from the map of a mild drought having less than 5 months of drought duration occurred within 10 year return periods covers 58% of the basin areas similarly; a moderate drought having less than 3 months of duration occurred within 10 year return periods covers 9% of the total basin area. From this, it can be concluded that the rate of raising drought duration for moderate case is higher than mild.

A successive drought map shows that the most drought prone areas are located at the southern part of the basin comparatively around Gidole, Mirab Abaya and Burji compared to the northern part of the basin. But the result perhaps does not make proportions to the recent available conditions that people are observing, since the study does not consider the existing irrigation practices.

2.8 Recommendations

Rainfed agriculture in areas which are frequently affected by drought is not possible, therefore in such areas irrigation schemes should be constructed in order to reduce the hazards of drought. The construction of irrigation schemes in drought prone areas may be difficult due to lack of enough and good quality of water and also available irrigable land. In that case, less drought prone areas should be se-

lected to resettle the population from high drought prone areas.
Integrated environmental managements, like protection of natural resources from erosion, wild fire etc. must be considered together with drought management strategy.

This investigation is better for preliminary reference for further study about the drought situation of the basin, as well as to extend the studying area.
The study focused only on meteorological drought but for a better analysis this agricultural drought assessment is important,as well.

2.9 References

Asfaw M.T., (2000). Assessment of the 1994 Drought in the southern Ethiopia Meteorological and Hydrological Aspects, Arbaminch, Ethiopia.

Awlachew S.B., (2000). Investigation of Water Resources Aimed at Multi-Objective Development with Respect to Limited Data Situation: The Case of Abaya - Chamo Basin, Ethiopia, Dresden, Germany.

Chow, V.T. Maidmet, D.R. and Mays, L.W. (1988). APPLIED HYDROLOGY, McGraw - Hill, New York, NY.

Cuenca R.H., (1989). Irrigation System Design: An Engineering Approach, Prentice Hall, New Jersey.

Degefu W., (1987). Some aspects of meteorological drought in Ethiopia, Cambridge University press, London, 23 - 26.

Elizabeth M.S. (1994). HYDROLOGY IN PRACTICE, TJ Press, England.

Palmer, W.C. (1965). Meteorological drought. Research paper No. 45, U.S. Department of Commerce Weather Bureau, Washington, D.C.

Palmer, W.C. (1968). Keeping track of crop moisture conditions, nationwide: The new Crop Moisture Index. Weatherwise 21:156-161.

National Meteorological Services Agency (NMSA) of Ethiopia, (1989). Assessment of Drought in Ethiopia, Addis Ababa, Ethiopia.

Smith, D.I., Hutchinson, M.F, McArthur, R.J., (1993). Australian climatic and agricultural drought: Payments and policy. Drought Network News 5(3):11-12.

Subramaniun K. (1984). ENGINEERING HYDROLOGY, Tat. McGraw - Hill publishing co. Ltd, New Delhi, 2nd Edition.

3 Groundwater Condition Assessment in the Arba Minch Area - Samuel Dagalo

Samuel Dagalo[1]

[1]Arba Minch University
P.O.B. 21.
Arba Minch, Ethiopia

3.1 Abstract

When the issue of water supply and demand for certain purposes is raised, the availability of water sources and the assessment of their conditions are inseparable considerations.
The assessment of groundwater (GW) conditions in a certain area may include the water withdrawal rate, the utilisation and management of groundwater, the type of formations from which it is derived, the hydrogeological properties as well as quality conditions of groundwater, the presence of influx (recharge) and other aspects. The type of aquifers out of which the boreholes pump water was determined. The area was highly heterogeneous and anisotropic with the transmission rate of the aquifer varying from 2 to 532.3m^2 per day. The general groundwater flow direction in the area was towards the lake (Abaya), determined by means of water level contour interpolated in the ArcVew GIS.

A natural scene of higher values of groundwater constituents and parameters could be observed near Lake Abaya with a general trend of decreasing upstream to the GW flow direction. The higher levels of Potassium, Nitrate and total dissolved salts in the borehole of the Kola Shara village were indicators for the groundwater recharge from irrigation return in the area.
An approximate soil-water balance approach to determine the groundwater recharge from rainfall after the necessary runoff accounting, evapotranspiration and soil moisture storage requirements indicated almost no recharge from rainfall in the area.

3.2 Introduction

Groundwater is generally the most abundant fresh water source in the world beside glaciers and ice capes. Estimates of global water supply show that GW represents about 0.6% of the world's total water. Since a high amount of GW below a depth of 0.8km is saline or costs too much to develop with the present technology and economic conditions, the total volume of readily available GW is about 4.2x106 km^3, much more than the 0.126x106 km^3 of fresh water stored in lakes and streams (Bouwer,1978).

For the most part, water supply for domestic purposes in the world stems from underground storage systems due to its abundance and potability without excessive treatment. There are also places where GW is used largely for irrigation and industrial consumption (Bouwer, 1978).
Several towns and villages in Ethiopia get their water supply from underground sources due to the greater potential of GW in the country as well as to the unavailability and good inaccessibility, the need of extra treatment and the high investment in the infrastructure set up for surface water sources.
The Arba Minch area is an area characterised by various surface as well as subsurface water bodies. The surface water bodies include the lakes (Abaya and Chamo) and the rivers (Kulfo and Hare). The evidence of existence of subsurface sources consists in the tapping of GW for various purposes at most sites of the area. In this connection, Arba Minch springs also need to be mentioned. These have their eyes at the foot hills of the Bekele Molla Hotel at colluvial deposits, which makes difficult the identification of their actual number (DHV Consultants, 2002).

Geologically, the area belongs to the category of the Rift Valley system. The geological units in the Rift Valley region are mainly the result of volcanic activity during the Tertiary period. The whole Rift Valley is underlain by ancient basement rocks, which are defined as genesis grading in metamorphic granites, ignimbrites (consolidated hot-ash flows) and granodiorites. A more recent layer of volcanic rocks and ignimbrites has been added over the basement (Wayand, 1999).
According to the geological map of Ethiopia (1973, scale 1:2.000.000), basaltic flow and related spatter cones are also the major geologic units from which the well-known 'forty springs' flow.
According to the Ethiopian Institute of Geological Surveys (EIGS, 1973), the area falls into the extensive aquifers with intergranular permeability (unconsolidated sediments: alluvium, eluvium, colluvium, lacustrine sediments and poorly cemented sandstone) of high productivity, which is the result of a high degree of faulting and fracturing of volcanic rocks and the occurrence of relatively permeable and unconsolidated sediments. The evidence of geological well logs of the Arba Minch area consists also in the fact that the area is composed of multilayered aquifer system.

The great advantage of GW is its use for drinking purposes without any treatment. Hence, considerable care should be taken to protect GW aquifers from irreparable damage through the disposal of waste materials. The quality of GW is influenced mainly by the quality of its source. Changes or degradation in the quality of its source waters can seriously affect the quality of GW supply. Unlike organic pollutants, inorganic pollutants can easily get access through the soil, and once introduced they are very difficult to remove. That is why GW possesses a high level of dissolved salts.
Influx of saline lake water into ground water may also partly increase the salinity of the Rift locality. In the southern parts of the Rift, sodium and bicarbonate (high alkalinity) are the dominant dissolved constituents (NERC, 2001). Fluoride has long been recognised with regard to water-related health concerns in Ethiopia. Concentrations greater than 10 mg/l are often found in waters from the Rift. However, unusually low fluoride concentrations have been reported in ground waters from wells and springs in the Rift Valley town of Arba Minch and the nearby escarpments in southern Ethiopia. This is apparently due to inputs of low-fluoride runoff from the highlands or from nearby rivers or lakes (NERC, 2001).

The sources of groundwater could be rain through deep percolation, seepage from streams, lakes and subsurface underflow, artificial recharge and sometimes incidental recharge (Bouwer, 1978).
Because of the lowering of the water level and consequently increased energy costs for pumping, it is recognised that GW extraction should balance GW recharge in areas with scarce fresh water supplies. This is achieved either by restricting the GW use to the water volume which becomes available through the process of natural recharge or by artificial recharge. Both options require knowledge of GW recharge processes through the unsaturated zone from the land surface to the regional water table. Recharge estimation can be based on a wide variety of models which are designed to represent the actual processes. Methods which are currently in use include (i) the soil water balance method (soil moisture budget); (ii) the zero flux method; (iii) the one-dimensional soil water flow model; (iv) inverse modelling for estimation of recharge (the two-dimensional GW flow model); (v) the saturated volume fluctuation method (GW balance); and (vi) isotope techniques and solute profile techniques (Kumar, 2003).

Study Objectives

The objectives of this study were:

Assessing GW conditions

- Determining hydrogeological conditions of the area
- Determining the general direction of GW flow in the area
- Analysing GW quality conditions of the area
- Indicating the source of GW recharge and estimating recharge

Laying the foundation (data-base organisation) for further and more detailed studies of GW in the area

3.3 Data Collection and Organisation

As far as subsurface data are concerned, most of the time they are not available and it is costly to collect primary data of the subsurface. In this study, data concerning the location of boreholes in the area, water levels in the boreholes, pumping test data, water quality indicators (chemical and physical characteristics and parameters) from the respective locations of boreholes, soil characteristics and land use patterns as well as representative temporal rainfall quantity data of the area were collected and organised.

The topographic map of the area (scale 1:50.000) was one of the important pieces of data collected which was scanned and saved in TIFF format. The map was then transferred from the raster map to its vector equivalent in the ArcView GIS environment. In other words, the map was geo-referenced to the real world coordinate system. All other important spatial features useful for the study were incorporated in the final vector map.
The locations of the boreholes were determined using the Global Positioning System (GPS). This was the most important information for the spatial analysis of groundwater conditions in the area since no other underground information could be obtained by using other methods.

3.4 Geological Well Logs and Interpretations

There were 16 boreholes dug in the area in the past years besides several hand-dug wells. Seven of these are at AMU, four at ATF, one at an adult school, three at a crocodile ranch and one in the Kola Shara village. Among these boreholes, only eight currently function according to the intended purpose: two at AMU, three at ATF, one at an adult school, one at a crocodile ranch and one in the Kola Shara village. Other boreholes are non-operational and abandoned due to reasons beyond the scope of this study.
Data of well logs were available for only ten of the boreholes: four at AMU, four at ATF and two at a crocodile farm. There were no field data on pumping test as well as no other necessary data except for the eight boreholes at AMU, the crocodile ranch and ATF.
Depths to the bottom of the boreholes (basaltic in many cases) ranged from 60m at ATF to 100m at AMU. As far as the geological well logs were concerned, there was no significant relation between aquifer materials at the same depth. Variations of formation material with respect to depth at a given borehole site were quite significant. Hence it could be said that the formation was highly heterogeneous and anisotropic.
The dominant formation materials composed mostly of sands, gravels, pebbles and cobbles of basaltic nature were understood as good water-bearing formations. Hence, considering the availability of water in the strata, an abundant amount of GW existed in the area. As the data pertaining to formation materials were scanty, it was difficult to delineate the groundwater basin of the area.

3.5 Borehole Locations and Designations

In past days, the boreholes were not located in their respective positions of real world coordinates. While this study was in progress, the existing boreholes were superimposed on their respective location on the map - a scanned, geo-referenced and digitised map of the Arba Minch area.
The process of locating boreholes on the map required the use of a Global Positioning System in the field as well as bringing these data to a GIS environment. Then, with X & Y coordinates available, a point on the geo-coded map could be

located easily. After ArcView GIS was activated, a project window of the existing file with the map was opened. In the view window of the view menu scroll bar, a new theme was selected and a point was chosen. After the name of the new theme had been specified, the addition of fields and records became possible in the attribute table of the new theme dialog box. In the dialog box, the X & Y coordinates of a point were included as a field and finally the values of a point were entered as a record in the attribute table. When editing had been completed and after the new theme check box had been selected, the points were located on the map (figure 3.2). Figure 3.1 shows the location of boreholes at their respective positions with respect to the UTM (Universal Transverse Mercator) projection of grid zone 37.

S.N	Borehole designation	X - coordinate	Y – coordinate	Relative ground Elevation (a.m .s.l.)
1	AMU 1	340788	670583	1223
2	AMU 2	340846	670796	1217
3	AMU 3	340953	670999	1215
4	AMU 4	340706	670002	1214
5	AMU 5	340605	670126	1216
6	AMU 6	340682	669964	1214
7	AMU 7	340525	669768	1228
8	ATF 1	340948	668336	1216
9	ATF 3	340785	668141	1220
10	ATF 4	341161	668139	1214
11	ATF 5	340906	667869	1215
12	Adult school	341971	667554	1202
13	ACR 1	344951	666104	1180
14	ACR 2	344965	666147	1180
15	ACR 3	343999	666514	1182
16	Kola shara	341419	673206	1230

AMU = Arba Minch University, ATF = Arba Minch Textile Factory, ACR = Arba Minch Crocodile Ranch

Figure 3.1: Locations of boreholes in real world coordinate system

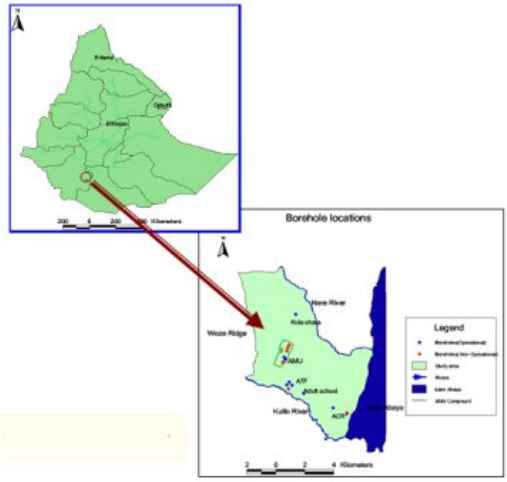

Figure 3.2: Study area and borehole locations

3.6 Aquifer Types and Parameters

The types of aquifers were determined following two approaches: 1) depending on the respective positions of SWL, confining layers and water bearing formations; and 2) depending on the pumping test data analysis (Kruseman & de Ridder, 1994). After the types of aquifers had been determined, aquifer parameters were established using the available models.

The most important parameters of an aquifer system are the permeability (hydraulic conductivity), transmissivity and the storage coefficient or specific yield. Among the variety of techniques to determine hydraulic parameters of aquifers, the most reliable one consists in pumping tests of wells. There were about eight stations (borehole sites) available with such a data in the area. With regard to such a test, a number of models to evaluate the aquifer parameters for different specific conditions have been developed. In this study, the Theis curve matching method, the Cooper-Jacob approximation as well as the Theis recovery method

approach were used for the most part.
The Theis curve matching approach is a graphical method to determine the aquifer transmissivity (T) and the storage coefficient (S). The method is applied for confined aquifers and makes use of the following equations:

$$s(r,t) = \left[\frac{Q}{4\pi T}\right] W(u) \quad \text{and}$$

$$\left[\frac{t}{r^2}\right] = \left[\frac{S}{4T}\right](1/u)$$

having a similar nature of arrangement, where
Q = test pumping rate(L^3/T) - available data for a well; s = drawdown (DD) (L) at a distance r from the pumping well - available data for a well at r = r_w; T = transmissivity (L^2 /T); S = storage coefficient; t = time (T) - time of test pumping; W(u) = Theis well function; u (dummy variable) = r^2 S/4Tt.
By plotting (log-log plot) the field data points (s vs. t/r_w^2) on the transparent paper and by superimposing it on the type of curve (W(u) vs. u) developed by Theis, values of W(u), u, s and t/r_w^2 are obtained (Todd, 1980). The value of aquifer transmissivity is then computed from the above-mentioned equation. Since the values of S obtained by this method go highly beyond the reasonable limit, they are deleted. This is mainly due to S being a highly dependent parameter on the radial distance from a well.
The Cooper-Jacob approximation is an extension of the Theis formula and has the following form (Todd, 1980):

$$s = \frac{2.303Q}{4\pi T} \log_{10}\left[\frac{2.25Tt}{r^2 S}\right]$$

For constant values of r, the derivative turns out to be

$$\Delta s = \frac{2.303Q}{4\pi T} \Delta \log_{10}(t)$$

For a per log cycle of $\Delta \log_{10}(t)$ in s-t of the semi-log plot:

$$T = \frac{2.303Q}{4\pi\Delta s}$$

From the aforementioned equations and derivatives, S can be evaluated as follows:

$$S = \frac{2.25Tt_o}{r_w^2} \quad \text{(Batu, 1998),}$$

where r = r_w and t_o = the time at which s = 0.

The semi-log plot was drawn for the data points (s vs. t) and the best fit line was drawn from which the
Δ s value could be obtained (figure 3.3) for the per log cycle of t in the excel spreadsheet. From the equation of the fitted line, the value of t_o was computed for the drawdown value of zero. Thus, the values of T and S for the known values of Q and r_w were computed from the equations mentioned above.

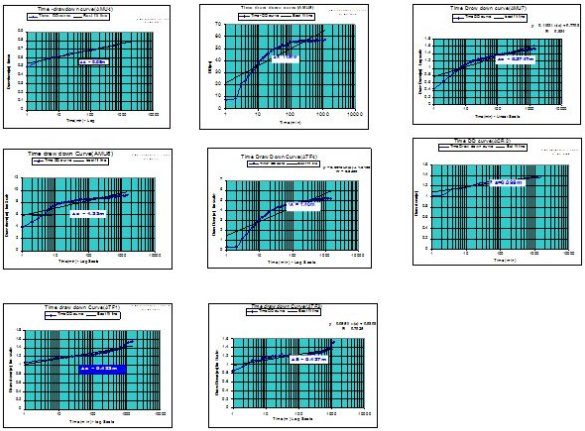

Figure 3.3: Time-DD curve for the estimation of transmissivity according to Cooper and Jacob

The Theis recovery approach, also a useful tool in verifying pumping test data validity, has the following formula for a sufficiently small u (dummy variable):

$$s' = \frac{2.303Q}{4\pi T} \log_{10}(t/t') \ ,$$

where s' is the residual drawdown, t' is the time since pumping has stopped and t is the time since pumping has started with constant discharge (Q).
Consequently, field data of recovery tests were conformed to the above-mentioned equation and the per log cycle of (t/t') was taken for a straight line portion of the s'- t/t' curve (figure 3.4) to determine the value of Δ s' as well as the aquifer transmissivity (T). This method did not support the determination of the value of the aquifer storage coefficient (S). Figure 3.5 summarizes the values of aquifer parameters obtained using the aforementioned methods.

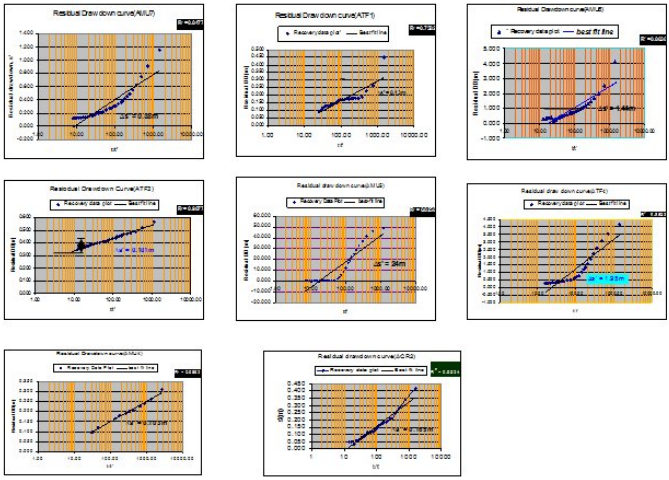

Figure 3.4: Residual drawdown curves to determine aquifer transmissivity (Theis recovery method)

S/N	Well designation	Theis method	Cooper &Jacob		Theis recovery
		T	T	S	T
1	AMU 4	233.35	657.52	$5.17x10^{-6}$	494.55
2	AMU 5	0.874	3.36	0.0105	2.00
3	AMU 6	3.90	34.73	$6.2x10^{-6}$	29.60
4	AMU 7	91.67	207.35	$3.4x10^{-4}$	149.90
5	ATF 1	152.80	479.44	$2x10^{-7}$	486.820
6	ATF 3	150.82	425.56	$5.5x10^{-7}$	535.23
7	ATF 4	7.40	39.55	0.281	28.40
8	ACR 2	103.87	540.21	$2.99x10^{-10}$	316.96

Figure 3.5: Values of T (m^2/day) and S according to various methods

3.7 Water Level Measurements and Groundwater Flow Direction

Water level measurements belong to the subsurface investigation of GW studies. The significance of such measurements lies in the determination of the GW flow direction, the management of aquifer pumping, the determination of contaminant transport and storage coefficients etc.
To get an overview of the regional/general direction of the GW flow in the area, water level measurements were conducted for accessible existing wells in the area. Depths to water level were measured at the respective positions of boreholes indicated in figure 3.6. The measurements were just started at the end of the dry season (March). This work was done using a "hydrometer" with a graduated plastic ring which dipped into a well. When an open-ended stainless rod at the end of the plastic ring dipped into the water, the circuit was completed and the lighter on the body of the instrument gave light. In this way, one could easily read the depth at which the water level was located from the ground.
Having determined the water level elevations at the respective locations of boreholes, the values of water level contours were interpolated and drawn using GIS software (ArcView 3.1). The work was performed in an ArcView GIS environment from the attribute table of well points, which showed the water levels as

S/N	Well designation	X Coordinate	Y Coordinate	Ground elevation	Tape measurement from GL	Water level
1	AMU1	340788	670583	1216	25	1191
2	AMU2	340846	670796	1217	25	1192
3	AMU3	340953	670999	1213	17	1196
4	AMU4	340706	670002	1214	25	1189
5	AMU5	340605	670126	1216	33.20	1182.8
6	AMU6	340682	669964	1214	38	1176
7	Adult Sch.	341971	667554	1202	19.30	1182.7
8	ACR 1	344951	666104	1180	3.60	1176.4
9	ACR 3	343999	666514	1182	9.6	1172.4
10	ATF 3	340785	668141	1218	19	1199
11	ATF 1	340948	668336	1216	19	1197
12	ATF 4	341161	668139	1214	21	1195

Figure 3.6: Measurement values of water level elevations of the wells (typical date)

a field. From the surface menu bar of the view window, the creating contours option was chosen and then with the input of water level values, ArcView automatically computed the water level contours. From the values of the GW level contours, the general direction of GW flow was determined (figure 3.7).

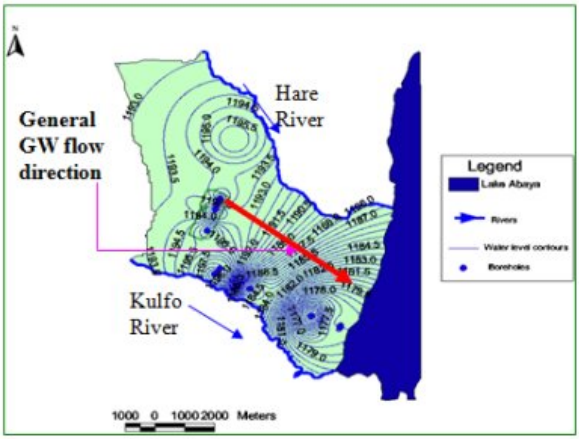

Figure 3.7: Water level contours and GW flow direction

3.8 Groundwater Quality Conditions

The quality of groundwater is determined by its physical, chemical and biological/bacteriological characteristics (Tomar, 1999).
Some important physical and chemical analyses of groundwater in the area were conducted in the field and in the water quality laboratory at AMU. Then the variations of some chemical characteristics were spatially analysed. The measurement values and further information on the data are depicted in figure 3.8 and 3.9.
The results of the chemical analysis of important constituents of GW showed that higher values of chemical constituents could be found near the lake. This effect usually decreased towards the west (study area) (see figure 3.10).

Sampling Point	1	2	3	4	5	6	7
Name of Sampling point	A.M. textile	Crocodile	Crocodile - black	Adult school	AMU Student café.	AMU Student dormitory	Kola shara
X-Coordinate	341161	344951	344965	341971	340823	340810	341419
Y-Coordinate	668139	666104	666147	667554	670594	670773	673206
Date of Sampling	1st Jun/05	1st Jun/05	1st Jun/05	1st Jun/05	1st Jun/05	1st Jun/05	1st Jun/05
Time of Sampling	4.00-12.45	4.00-12.45	4.00-12.45	4.00-12.45	4.00-12.45	4.00-12.45	4.00-12.45
Date of Analysis	1st-18th June/05	1st-18th June/05	1st-18th June/05	1st-18th June/05	1st-18th June/05	1st-18th June/05	1st-18th June/05

Figure 3.8: Sampling point details

Parameter	Unit	Sampling Points						
		1	2	3	4	5	6	7
Odor		Free	Free	Free	Free	Free	Free	Free
Color		Free	Free	Black	Free	Free	Free	Free
Water Temperature	°C	23.5	27.1	25.7	24.7	30.02	29.1	25.8
pH		7.02	6.98	9.24	7.49	7.47	7.47	7.22
Conductivity	mS/cm	303	3400	843	370	657	667	1336
Turbidity	NTU	0.8	1.9	0.4	0.4	0.1	0.1	0.2
Fluoride	mg/lit	0.58	1.62	7.1	0.65	0.71	0.73	0.68
Sulfate	mg/lit	1	188	10	1.1	2	1.8	34
Nitrite	mg/lit	0.005	0.009	0.03	0.007	0.005	0.005	0.004
Nitrate	mg/lit	1	0.2	3	0.4	2.2	2.2	4.8
N-ammonia	mg/lit	0.01	1.14	1.7	0.05	0	0	0
Chloride	mg/lit	11.27	378.7	10.14	33.8	117.21	117.21	112.71
Total Hardness as Caco3	mg/lit	50	950	350	160	220	245	226
Calcium	mg/lit	100	344	120	60	78	92	82
Magnesium	mg/lit	36.45	147.3	55.89	24.3	34.506	37.18	34.99
Sodium	mg/lit	3.13	72.95	37.78	3.68	9.07	9.67	13.76
Potassium	mg/lit	1.544	8.729	2.341	1.065	1.0644	1.064	3.366
Total Alkalinity as $Caco_3$	mg/lit	25	112.5	175	32	35	40	45
Carbonate CO_3^{-2}	mg/lit	3	22.5	4.5	6	7.5	7.5	9
Bio Carbonate HCO_3^{-1}	mg/lit	34.4	91.5	122	27.45	27.47	27.45	39.65
TDS	mg/lit	203.0	2278	564.8	278	440.2	447	895.1

Figure 3.9: Results of the chemical and physical analysis of GW in the area

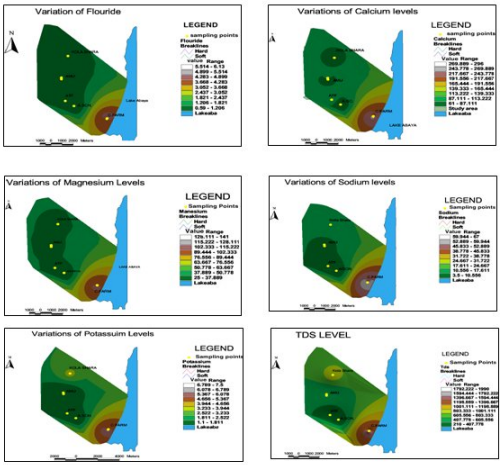

Figure 3.10: Spatial characteristics of some groundwater components

3.9 Groundwater Recharge Estimation from Rainfall

Groundwater recharge refers to the replenishment of aquifer systems from various sources such as rainfall, irrigation return flow, inflow from natural streams, subsurface inflow and artificial recharge (Singh, 1992).
The general soil water balance equation can be represented by:

G_r=[P+I]-E_a+Δ S-R_o,

where
G_r = GW recharge
P = total precipitation
E_a = actual evapotranspiration
Δ S = change in soil water storage
R_o = runoff
I = irrigation return flow

Many components of the soil water balance equation (such as recharge from

canals, reservoirs, injection wells, GW inflow to and outflow from the area, influent and effluent seepage, artificial extraction and leakage from the bottom of semi-confining layers) were ignored in the aforementioned equation since some of them were not necessary for the report. Moreover, some of the components were difficult to obtain and beyond the scope of this paper.

The area experienced surface irrigation since the past decades, but there were no adequate data on the amount of inflow/diversion of irrigation water and the history of water loss due to deep percolation. Therefore, the estimation of GW recharge due to this parameter was left out. Thus, the amount of recharge was to be estimated from total daily rainfall.

Using the above-mentioned soil water accounting model, GW recharge was estimated as follows: The rainfall data for 10 years (1989-1998) were arranged according to their temporal sequence; by means of this procedure, the conditional antecedent moisture condition was determined. Runoff was estimated using the SCS method for known land use and hydrologic soil groups. The average PET value according to Penman-Montheith was one of the inputs to the evaluation of recharge. Soil water storage was computed as follows:

$S_t = P_{eff(t)} + S_{(t-1)} - PET_{(t)}$,

where
t = the day under consideration
(t-1) = the previous day
$P_{eff(t)}$ = effective rainfall (P-R_o)
$S_{(t-1)}$ = storage considered from the previous day
$PET_{(t)}$ = potential evapotranspiration expected at that particular date

Hence, storage was considered to be zero when $P_{eff(t)} + S_{(t-1)}$ - PET was less than zero and there was no recharge. When the net amount of the algorithm (value of typical day soil moisture storage) was positive and beyond 120mm on a particular day, the offset was taken to be the recharge. The whole algorithm was caught using the Excel spreadsheet.

3.10 Results and Discussion

The boreholes in the area were mainly installed for domestic and industrial water supply (ATF) purposes. Only eight (50%) of the developed wells were in operation at the time of the study.
The dominant type of aquifers from which the wells pump water was determined. The potential aquifers near AMU were mostly confined types; in the vicinity of the textile factory, both semi-confined and unconfined aquifers prevailed. This showed that, in combination with the variation of formation material at borehole sites, the aquifers were strictly heterogeneous and anisotropic, composed of multiple aquifer systems.

Representative values of aquifer parameters were determined using various approaches. The value of transmissivity according to the Theis recovery approach varied from $2m^2$/day (AMU5) to 535.23.5m^2/day (ATF3). The storage coefficient according to Cooper & Jacob, though rough, fell in the range from 2.99x10-10 (ACR2) to 0.281 (ATF4).
The static water level measurements at the boreholes indicated that the water level elevation in the boreholes varied from 1199m (at ATF3) to 1172m a.m.s.l. near Lake Abaya.
The general direction of the GW flow of the area, determined by means of the water table contour map, was from north-west (from the north-west high escarpments) towards the south-east to Lake Abaya.

The chemical analysis of the GW revealed that the values of constituent elements and water quality parameters (conductivity, hardness, TDS, etc.) near Lake Abaya were generally higher than in other parts of the area. The values of the constituent components generally decreased when proceeding from Lake Abaya towards the west (AMU area). This also indirectly confirmed that the direction of GW was from AMU towards Lake Abaya. Relatively high values of Potassium, Nitrate and TDS occurred in the borehole of Kola Shara.
An approximate soil water balance approach on daily bases for the estimation of recharge from rainfall showed that there was no recharge from rainfall in the area for the analysis period. The basic assumption of the analysis was that the volume of water beyond the field capacity of the particular soil satisfying the maximum evaporative demand percolated and joined the GW reserve.

3.11 Conclusion

Aquifer types in the area are dominantly confined, with unconfined and semi-confined types also existing in some parts. The high values of transmissivity in the area indicate that one can carry a good yield from the formation in the area. The flow of GW from the area of AMU towards Lake Abaya indicates that the GW gradient also follows the surface gradient in the area.

The area most probably gets main recharge from the upstream highlands (most probably through an extensive fault line running north to south along the ridges west of the area). Additional recharge is obtained from the two accompanying perennial rivers. The area also gets appreciable recharge from irrigation water loss.
The overall condition of the GW quality for drinking purposes is fair and suitable except for the case of the crocodile farm.

3.12 References

Batu, V. (1998). Aquifer Hydraulics. A Comprehensive Guide to Hydrogeologic Data Analysis. John Wiley & Sons, New York.

Bouwer, H. (1978). Ground Water Hydrology. McGraw Hill, New York.

DHV Consultants, BV (2002). Feasibility Studies and Detailed Designs for Ten Towns, Arba Minch Town Water Supply and Sanitation. Environment support project, Component 3, 1, 6/3-8/3.

EIGS (1973) Hydro geological Map of Ethiopia. 1:2000000 scale Ethiopian Institute of Geological Surveys, Addis Ababa.

Ethiopian Mapping Authority (EMA) (1979). Map of Arba Minch. 1:50000 Scale, Series ETH (DOS 450), Sheet 0637 D3, Ethiopian Mapping Agency, Addis Ababa.

Kruseman, G.P., & de Ridder, N.A. (1994). Analysis and Evaluation of Pumping Test Data. 2nd Edition. ILRI, Netherlands.

Kumar, C.P. (2003). Estimation of Ground Water Recharge Using Soil Water Bal-

ance Approach. http://www.angelfire.com/nh/cpkumar/publication/Smbp.pdf.

NERC (2001). Ground Water Quality: Ethiopia. http://www.wateraid.org

Singh, P.V. (1992). Elementary Hydrology. Prentice Hall of India, New Delhi.

Todd, D.K. (1980). Ground Water Hydrology. 2nd Edition. John Wiley & Sons, California.

Tomar, M. (1999). Quality Assessment of Water and West Water. Lewis Publishers, London.

Wayand, A. (1999). Description of Kulfo and Hare River Watershed Characteristics in the Abaya Chamo Basin in South Ethiopia with Support of GIS. Siegen, Germany.

4 Assessment of the Impact of Limited Irrigation Development in the Blue Nile River Basin - Yilma Demissie, Semu Ayalew Moges

Yilma Demissie, *Semu Ayalew Moges*[1]

[1] Arba Minch University
School of Graduate Studies
P.O.B. 21.
Arba Minch, Ethiopia
Email: smoges@nilebasin.org
semu$_m$*oges*$_2$000@*yahoo.com*

4.1 Abstract

This study was carried out to evaluate the impacts of limited irrigation development in the Blue Nile River Basin, Ethiopia, with regard to the spatial availability of water resources for downstream countries, using the WEAP water resources planning model. 17 irrigation projects covering an area of 220.416 ha of land were considered from the gauged tributaries of the basin. Accordingly, the total water requirement of these irrigation projects was estimated to be 3 bcm annually. This is equivalent to less than a 6% reduction of the total mean annual volume of an approximately 52.9 bcm flow at the border to Sudan (Tesfahun, 2006).

Key words: *Limited Irrigation Development, Blue Nile River Basin, WEAP Model*

4.2 Introduction

The development of transboundary rivers like that of the Nile River Basin primarily requires a forum for communication, understanding and building trust among riparian countries through implementing various confidence building measures as well as through the upstream and downstream riparian countries building collaborative efforts for the common good of all and by means of deriving sustainable benefit from the waters of such basins. It is a fundamental requirement to guarantee a sustainable allocation of the available water resources based on scientifically proven approaches and internationally accepted rules.

Due to growing food insecurity coupled with the population explosion and the degradation of the environment, it becomes more and more clear that riparian countries have to utilise their water resources sustainably and without causing harm to each other (particularly to downstream users). This shared responsibility is the binding tie for the cooperation of both upstream and downstream riparian counties. Despite recent opportunities and an enabling environment created by the NBI programme, there is neither a clearly articulated statement of agreement acceptable for all riparian countries nor a consensus of any kind that may dictate the sustainable development and sharing of the resources of the Nile River system.

In this regard, due to unreliable climatic conditions and the high demographic pressure, Ethiopia is embarking to develop its land and water resources potential. High emphasis has been put on using the available irrigation potential for alleviating the prevalent food insecurity and the dependency syndrome on food aid. In this respect, the study was carried out to evaluate the impact of limited irrigation development in the Abbay Basin.
Ethiopia may be one of only few countries in Africa with abundant water resources but is still frequently hit by recurrent drought and famine associated with health problems and other extended social crises. The majority of the country's rivers are transboundary in nature, transporting multitudes of water and fertile soil abroad, leaving their country of origin degraded and abandoned. The utilisation of these rivers is limited to the development of minor small-scale irrigation projects and to the purpose of drinking at some of the uppermost tributaries of the rivers.
On the basis of the necessity to develop the resources and to formulate a solution for the proper utilisation and management, a number of master plan studies have been conducted. For most of the main basins of the country master plan study documents have been prepared by foreign contractors. The involvement of local professionals in the study is either limited or non-existent. This restricts the exposure of the master plans on the indigenous professionals' awareness and discussions. Moreover, the habit of evaluating the development plans using updated models for an alternative resources allocation is not common in the country.

On the one hand, the need to see previously developed proposals with advanced and recent models will facilitate the formulation of other alternatives and optimal domestic resource allocations. On the other hand, for the case of transboundary rivers, a proper allocation of the precious asset using such models will minimise the apprehension of riparian nations. Besides, with the advancement of models, additional outputs are also expected which have not been parts of the previous models applied to the development of master plans.
The model selected for this purpose was the Water Evaluation and Planning System (WEAP) which evaluates a full range of water development and management options and takes into account multiple and competing uses of water systems.

The main objectives of the study were 1) to examine the flow of the main and

tributary river flows before and after the implementation of the irrigation projects under consideration and 2) to investigate the repercussions on the downstream water availability.

4.3 The Blue Nile River Basin

The Blue Nile River Basin is located in the western part of Ethiopia between 7°45'N - 12°46'N latitude and 34°05'E - 39°45' E longitude. The basin has an estimated area of 199.812 km^2. About 46% of the basin area falls into the Amhara State, 32% falls into Oromia and the rest of about 22% into the Binishangul-Gumuz State. The basin covers about 17.5% of Ethiopia's land area (BCEOM phase3, part1, 1998). The location of the basin with respect to the other major basins of the country is shown in figure 4.1.

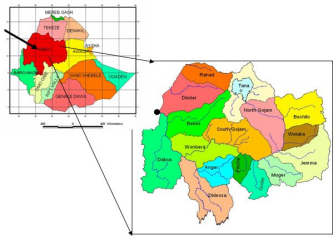

Figure 4.1: Location map of the study area with respect to other basins

The basin accounts for the major share of the country's irrigation and hydropower potential. However, the current utilisation is very low. Irrigation development is very limited except for the operational Finchaa project phase one of 6.205 ha and other small-scale farms constructed along tributaries.
According to the 1994 census (figure 4.2), the total population of the Abbay Basin alone is estimated to be around 14.231.429 which represents 25% of the country's population. The region-wise population distribution shows that 64% of the population inhabits the Amhara Region. The corresponding figures for Oromia and Benishangul-Gumuz are 33% and 3%, respectively.

Region	Area with in the basin (km^2)	Population with in the Basin			
		Rural	Urban	Total	percentage
Amhara	92639	8356311	792452	9148763	64
Oromia	62474	4232725	428768	4661493	33
Benishangul	44699	385468	35705	421173	3
Total	199812	12974504	1256925	14231429	100

Figure 4.2: Population of the basin according to the 1994 census; Source: BCEOM (1998, phase 2, section II, volume XVIII, page 44)

The rain-fed agriculture could provide about 18.5 tons of this requirement. The balance of 11.5 million tons has to be produced under irrigated conditions or to be imported into the country. Similarly, the sugar requirement will reach over 2.7 million tons and about 1.13 tons of cotton should be produced for clothing. To meet the aforementioned demands, about 2.9 million ha should be brought under irrigation in the sub-basins.

The need to produce more food to meet the demands of the rapidly increasing population throughout the basin and in the country is unquestionable. In the last two to three decades, however, the recurrence of droughts and famines as well as the inconsistency and variability of rainfall has often refused the people of Ethiopia the access to the basic human right of getting food. Therefore, rain-fed agriculture can no longer provide the people with sufficient food and relying on irrigation development can be considered the only viable alternative to cope with the severity of the problem. This study was an attempt to investigate the limited irrigation development option in the tributaries of the Blue Nile Basin, using the WEAP model. The study focused on answering the following questions: 1) What amount of water will be consumed by projects proposed on the tributaries of the river distributed over the basin? 2) What will be the impact of the consumption on the flow of the tributaries in particular and on the main course in general? 3) Are there any environmental and transboundary impacts of such limited irrigation development on the downstream countries?

4.4 Overview of the Nile Basin and its Irrigation Development

Various studies conducted on the Nile basin have revealed the geomorphology of the river as well as the extent of its irrigation potential and hydro-politics conditions. Regarding the Ethiopian part, the Nile emanates from the highlands of three major tributaries (Tefera, 1997). The contribution of these main tributaries to the Nile from the Ethiopian highlands is between 70-90%, mostly (86%) of the flow at the Aswan High Dam. The three tributaries Blue Nile (Abbay), Baro-Akobo and Tekeze contribute 59%, 14% and 13%, respectively, to the total low and peak flows of the Nile.

Appelgren (2000) on his part states that in 1990, the human population in the Nile Basin was estimated to be 160 million and projected to increase to 300 million people by 2010. Some of these countries fall below the poverty line (GDP $\leq$ $ US 300 per head) with the exception of Egypt, Uganda and to some extent Kenya. The Nile economies are expected to continue being dependent upon low productivity. Subsistence agriculture contributes more than 50% to their GDP. The basin comprises on average % of the labour force that represents only 22% of the cumulated economy in the Nile Basin countries. Except Egypt, most of the countries in the basin are classified as food insecure. Food security is threatened either by demographic growth or by shortage of land and/or water or both as well as by a limited capacity to absorb shocks such as droughts, floods and civil conflicts. To provide the minimum acceptable level of food security, the food availability in the basin needs to increase by 35%-50%.

4.4.1 Irrigation Potential and Utilised Extent of the Basin

The majority of irrigation potential studies conducted in the country so far have revealed that the Abbay Basin accounts for the principal proportion. The overall irrigation potential of the country was estimated to be 2.716.600ha, with the Abbay Basin constituting an area of 760.000ha equivalent to 28%.
Based on pre-feasibility and other reconnaissance studies conducted in the basin, its maximum irrigable area was estimated 72.829 km2 of which 525.957ha were identified as maximum irrigable land. As shown in figure 4.3, the unrestricted potential scenario evaluates the upper limit for the development of irrigation within

the Abbay River Basin. The scenario considers that 100% of the average water resources (after deducting the ecological requirement) can actuall bey delivered to any potential irrigation areas. On the basis of this analysis, excluding the potential of the Beshelo, Welka, Jema and Northwest Sub-basins of Rahad and Dendir, the total identified irrigable land amountedto 411.377ha (BCEOM, phase 3, main report, 1998).

Regarding the potential of the basin brought under utilisation, BCEOM (phase 3, main report, 1998) considered the first phase 6.205ha of Finchaa as the only large-scale development site. The total command area of small-scale irrigation sites under operation was not given except specified as entirely traditional. As a result, no clear-cut extent of the total irrigation area brought under development was given. On the other hand, according to HALCROW (1989) the percentage of the area utilised did not exceed 4%. This shows that the potential of the basin is yet untouched.

Sub basin name	Sub Basin area (km^2)	Agriculture Suitable land (Km^2)	Maximum irrigable land (Km^2)	Identified irrigable area (ha)
Lake Tana	15054	10497	4639	113669
North Gojjam	14389	10330	4245	11716
Beshelo	13242	8538	3474	-
Weleka	6415	3903	1973	-
Jimma	15782	6819	6408	11687
South Gojjam	16762	11414	5459	19789
Mugar	8188	5885	3384	-
Guder	7011	3990	3990	8040
Fincha	4089	3048	1165	17358
Didessa	19630	18235	14809	52617
Angar	7901	6684	4177	26563
Wombera	12957	9222	3916	2357
Dabus	21032	18978	8513	8861
Beles	14200	11358	2908	138720
Dinder		14016	1975	59555
Galegu/Rahad	23160	4655	1794	54995
Total	**199812**	**147572**	**72829**	**525,957**

Figure 4.3: Overall unrestricted full development potential of each sub-basin of the Abbay Basin; Source: BCEOM (1998, phase 3, main report, Appendix 10.8, p. 66)

The requirement of water for the development of irrigation has been estimated by some studies. The estimates lack consistency as presented by Ethiopia's technical experts' paper on the 1993 Nile conference. This paper states that according to the United States Bureau of Reclamation (USBR) study of the Blue Nile Catchment in Ethiopia, conducted between 1958 and 1963, 6 billion m^3 of water were

estimated as the optimal requirement to irrigate 430.000ha of land. The paper adds that a recent water resource study conducted in 1990 offered an estimate of 12 billion m^3 of water to irrigate 300.000 ha of land within the Blue Nile Basin alone (Nile 2002 Conference, 1993). The amount of water estimated by both studies for one ha of land is thus contradictory. In other words, the first study proposes a relatively small amount of water for a large area whereas the second study allocates a huge amount of water for a relatively small irrigable area. This shows that a lot of work needs to be done to estimate the actual water requirement of the basin.

BCEOM on its part states that if all the currently identified projects were to be built at some time in the future including the four large hydropower schemes on the main stream, the average annual flow at the border gauging station would be reduced by about 11 to 12%, which would allow Ethiopia to irrigate 370.000 to 440.000 ha within the basin and to produce 26.000 to 28.000 GWh/year of hydro-electric power (BCEOM, part 1, main report, 1998).

4.5 Sources of Data and Data Availability

4.5.1 Selected Irrigation Development Coverage

On the basis of gauged tributaries the following 17 sites were selected from the master plan document for the analysis:

serial No	project name	Irrigable area(ha)
1	Lower Dabus	5,100
2	Arjo Didessa	14,280
3	Angar	14,450
4	Dabana	16,388
5	Negesso	22,815
6	Finchaa	6,205
7	Nekemte	11,220
8	Upper Guder	4,698
9	Megech	7,311
10	Rib	19,625
11	Gumera	13,976
12	Jema	7,786
13	Gilgel Abbay	11,508
14	Nesh A	7,217
15	Middle Birr	10,000
16	Tis Abbay	41,837
17	Koga	6,000
	total irrigable area	***220,416***

Figure 4.4: Demand sites selected for the analysis

4.5.2 Crops and Cropping Patterns for the Projects

25 types of crops were considered for the development within the basin, depending on the ecological requirements of the crops and their economic advantage. The document considered the wet season covering the period from May to October, the months of November and April as dry season. The maximum cropping intensity amounted to 100% during the rainy season and to 80% during the dry season. The spatial distribution and the types of crops proposed for irrigation were presented as follows:

Cropping pattern 1 assumed to be representative for the Lake Tana Basin with maize, wheat, barley and sugarcane as the major irrigated crops.
Cropping pattern 2 represented the future patterns in the Northwest Basin and the Lower Beles Basin with cotton and maize dominating during the wet season and maize, sunflowers, sugarcane and soybeans during the dry season.
Cropping pattern 3 was representative of projects in the Upper Beles, Fincha and Amerti-Nesh Basins with sugarcane as the dominant crop.

Cropping pattern 4 included projects in the Didessa, Angar and Dabus Basins with cereals and oil crops dominating in the wet season.
Cropping pattern 5 was representative of the Guder project with major crops being maize, wheat, barley, groundnut fruits and grapes during the wet and dry season.
Cropping pattern 6 assumed to be representative of rice projects in the Lake Tana area comprising 60% of the irrigable area during wet and dry seasons.
Cropping pattern 7 represented projects in the Debre Markos Basin with cereals during the wet season, vegetables during the dry season and fruits as perennial crops.

4.5.3 Stream Flow Data

The stream flow data provided in the master plan document were updated by including recent years' records obtained from the Ministry of Water Resources. Except the data of currently non-functional and abandoned stream gages, most of the stations' recent data were included in the analysis. For some of the stations short-duration missing data filling was carried out by simply averaging backwards and forwards the recorded monthly historical values.

4.5.4 Precipitation and Potential Evapotranspiration Data

The WEAP model required the data of precipitation and evaporation to compute the net evaporation from the reservoirs of the project sites. It also needed the annual irrigation water requirement to compute the monthly consumption of the crops to fulfil their evapotranspiration need.
The data provided in the master plan document were effective precipitation and potential evapotranspiration, which were computed for each sub-basin.

The net evaporation of the reservoirs was computed as the difference between the potential evapotranspiration and the effective precipitation. It became apparent that the effective rainfall was less than the actual precipitation. Effective rainfall is that portion of the total rainfall that satisfies the evapotranspiration requirements. Rainfall lost by runoff from the soil surface and by drainage through the soil is not considered effective (Acres, 1995).

No	Project/ reservoir Site Name	project Catchment area (km^2)(a)	Gauge catchment area (km2) (b)	Location of reservoir from the gauge	Area Ratio(a/ b)	gauge site location at
1	Angar	1962	4674	U/S	0.42	Nekemte
2	Dabana	2554	2881	U/S	0.89	Aba sena
3	Gl. AbbayB	1980	1664	D/S	1.19	Merawi
4	Gumara A	379	1394	U/S	0.27	Bahirdar
5	Jema	218				
6	Koga	164.8	244	U/S	0.67	Merawi
7	Lower Dabus	10088	10139	U/S	1	Assosa
8	Fincha	1391	1391	U/S	1	Shambu
9	Tis Abbay	15042	15042	D/S	1	Dahir dar
10	Middle Bir	714	978	U/S	0.73	
11	Megech	416	462	U/S	0.90	Azezo
12	Negeso	402	844	U/S	0.48	
13	Nekemte	4623	4674	U/S	0.99	
14	Nesh A	339	1391	U/S	0.24	
15	Rib	677	1592	U/S	0.43	Addis Zemen
16	Upper Didessa	4001	9981	U/S	0.40	Arjo
17	Upper Guder	239	524	U/S	0.46	Chan-Cho

Figure 4.5: Relative location of project sites with stream gages and discharge estimation methods used

Besides, utilising the potential evapotranspiration maximises the actual evaporation rate. According to Linesly and Franzini (1984) evapotranspiration is sometimes called consumptive use or total evaporation, describing the total water removed from one area by transpiration and by evaporation from soil, snow and water surfaces. Allen et al. (1998) regard climatic parameters as the only factors affecting potential evapotranspiration (ETo). ETo expresses the evaporating power of the atmosphere at a specific location and time of the year and does not consider the crop characteristics and soil factors.

Hence, taking the difference of these two values obviously maximises the net evaporation. This implies that the water lost as a result of evaporation in Ethiopia gets maximised. This in turn maximises the reduction of flow at the border.
On the other hand, it was attempted to estimate the actual precipitation and evaporation data using a FAO-developed software known as local climate estimator (LocClim). LocClim is a computer programme that estimates the climate for any

location on the earth. It uses the database of FAO agrometeorology for both domestic and neighbouring countries' station data. Moreover, the programme uses the altitude, latitudinal and longitudinal location of the area of interest. It utilises at least 10 neighbouring stations for full performance to compute various values of temperature, rainfall, potential evaporation, wind speed and relative humidity. LocCLim computes these values based on the equation of the Inverse Distance Weighted Average Method (Grieser, 2002).

The data of net evaporation computed from LocClim and those values derived from the master plan data were compared. It could be concluded from their overall annual net evaporation value that the results obtained from LocClim were underestimated as compared to those of the master plan. While investigating the monthly values, the results of LocClim estimated more for the dry months than the wet season, contrary to the master plan except for some cases. The effect of this variation in the overall water consumption of the projects was seen as insignificant.

4.5.5 Reservoir Capacity and Physical Data

The sources of the reservoirs' geographic location, capacity and elevation vs. the volume relation of the storage area and dead storage data were taken from phase 2, section III, volume 2 of the master plan document. Due to the absence of a clearly stated optimal storage capacity, the highest value from the volume-elevation curve data was taken as the storage capacity. This might be a drawback from an economic as well as from a volume of stored water point of view.

4.5.6 WEAP Model Configuration of Irrigation Projects

Before proceeding directly to the methodology of the data analysis section of the study, it is worth mentioning and looking at the overall versatility and operation of the WEAP model from a bird's eye view (Figure 4.6).

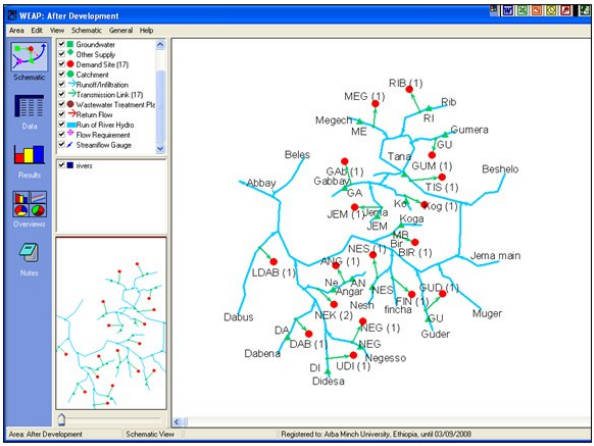

Figure 4.6: Programme structure of the WEAP model

4.5.7 Data Organisation for the WEAP Model

Stream Flow Data

As stated before the stream flow data at each project site were of different nature. There were rivers having stream flow historical data recorded at the spot where development projects were proposed or the project sites were close enough to the stream gages, which resulted in insignificant water resource variation between the two sites.

Some of the project sites were situated either upstream or downstream of the stream gages. In this case, the stream flow data of the sites were estimated to show considerable differences in comparison with the recorded data. There were also some project sites which had neither upstream nor downstream flow data. The only option for such kinds of sites was to use the basin-specific discharge provided in the master plan document.
Hence, based on the above-mentioned conditions the selection of sources and data analysis performed can be summarised as follows:

1. Direct data from the master plan: Depending on the similarity of area between the proposed reservoir site and the stream flow gage location, direct mean monthly stream flow data were computed from the available years' mean monthly data of the master plan updated to the recent record.

2. Simple area ratio method: The area ratio method was used to determine the flows at the required sites from the main or tributary rivers' mean stream gauge values. This method used the drainage areas to interpolate flow values between or near gauged sites on the same stream. Flow values were transferred from a gauged site, either upstream or downstream to the ungauged site (Rumenik, 1996).

The area ratio method formula and the preconditions for utilising the formula were set as follows:

$Q_{s_{ite}} = (\frac{A_{s_{ite}}}{A_{g_{auge}}})^n * \mathrm{Q}_{g_{auge}}$

where
$Q_{s_{ite}}$ is the discharge required at the reservoir site
$Q_{g_{auge}}$ is the discharge at the nearby gauge site
$A_{s_{ite}}$ and $A_{g_{auge}}$ are the drainage areas at the reservoir and the gauge, respectively
n is a coefficient that varies between 0.6 and 1.2

If $A_{s_{ite}}$ is 20% of the $A_{g_{auge}}$ value or lies within the range of $0.8 \leq A_{s_{ite}}/A_{g_{auge}} \leq 1.2$, then n=1

According to Dereje (2005) quoting Awulachew (2000) the obtained estimated discharge at site was estimated to be within 10% of the actual discharge.
The steps followed during applying the simple area ratio method were given by Rumenik (1996):

1) Locating the nearest gauge sites.
2) Determining the drainage area for the ungauged site between the gauged sites.
3) Multiplying the mean flow at the gauged site by the drainage area of the ungauged site and dividing it by the drainage area of the gauged sites.

The area ratio method was employed for those areas where Asite was 20% of the $A_{g_{auge}}$ or the ratio $A_{s_{ite}}/A_{g_{auge}}$ lay within the range of 0.8-1.2.

3. Weighted area ratio method: This method was employed for computing the mean flow of a given dam site situated in between two flow gages. It considered the weighted area ratio of the catchment area of upstream and downstream gages. When Asite was within 50% of Agauge, two stations' data were taken for data transfer. A relation can be developed to estimate a weighted average flow at a site lying between upstream and downstream gauges (Gulliver & Rogger, 1991).

The governing formula employed for the computation is given as follows:

$$Q_{site} = \frac{(A_{guage1} - A_{site}) * Q_{gauge1} + (A_{site} - A_{gauge2}) * Q_{gauge2}}{A_{guage1} - A_{gauge2}}$$

where the suffixes 1 and 2 represent downstream and upstream discharge and areas, respectively. The method incorporates the discharges of upstream and downstream catchment properties. This technique was mainly applied for those sites where there were upstream and downstream flow gages and a A_{site}/A_{gauge} ratio beyond the limit given for the simple area ratio method.

4. Specific discharge: BCEOM provided specific discharge values expressed in terms of litre per second per km^2 for each month for some basins.
The results of these estimates were used for a number of sites that did not have closer stream flow gages and where the area ratio value was highly variable. For the purpose of dependability the discharge values computed from these specific discharges were compared with the recorded values of known sites like Didessa and Guder. The results obtained showed significant similarity.

Border Flow Estimation Using Main Stream Gages

The stream flow data of four main river course flows were utilised for the computation of the border flow volume. The mean monthly flows obtained from the historical records of Bahir Dar, Kesse, Shegole and Border were utilised. Based on these data the overall stream flow volume at each gage site on the mainstream was computed by WEAP. As indicated in Figure 4.7 and 4.8 the mean annual flow of Abbay was found to be 49.7bcm at the border and 3.8bcm at Bahir Dar below the outlet of Lake Tana. The value of border flow obtained from this analysis was highly compatible with the estimate provided in the master plan, which was 50bcm.

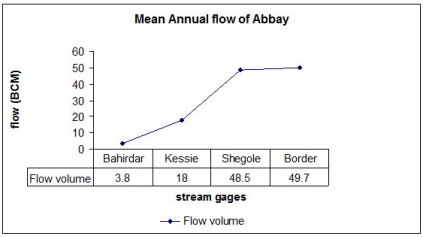

Figure 4.7: : Mean annual flow volume at the main stream flow gages

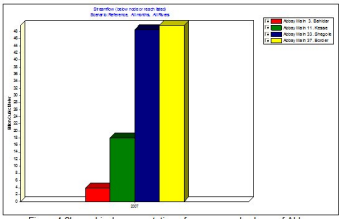

Figure 4.8: Graphical representation of the mean annual volume of Abbay

Figure 4.9 and 4.10 reveal that with regard to the discharge of the river in October, November and December the volume of water at Shegole exceeded that of the Border, which requires further investigation.

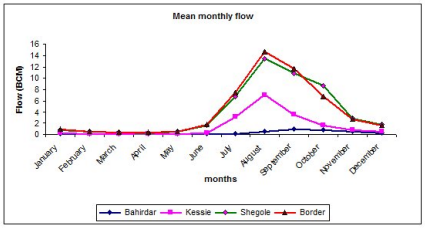

Figure 4.9: Mean monthly flow volume of Abbay at each gage

	Jan	Feb	Mar	Apr	May	Jun	Jul	Aug	Sep	Oct	Nov	Dec	Sum	
Bahidar	0.2	0.1	0.1	0.1	0.1	0.1	0.1	0.5	0.9	0.8	0.5	0.3	**3.8**	
Kesse	0.3	0.2	0.2	0.2	0.2	0.3	3.1	7.1	3.5	1.6	0.8	0.5	**18.0**	
Shegole	0.8	0.5	0.4	0.3	0.6	1.6	6.8	13.4	10.8	8.7	2.9	1.7		**48.5**
Border	0.9	0.6	0.4	0.4	0.6	1.8	7.5	14.7	11.7	6.8	2.7	1.6		**49.7**

Figure 4.10: Mean monthly volume of Abbay at the main stream gages (bcm)

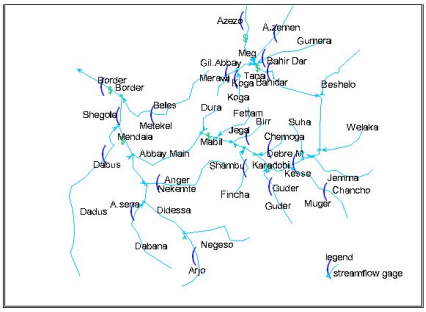

Figure 4.11: Schematic overview of stream gage locations on the main stream and on tributaries

In order to ease the analysis, the last tributary river with record data, Besles, was taken as a point of downstream reference. The total mean annual volume of water obtained from the gauged tributaries was analysed. The monthly and annual flow conditions for the projected 20 years assumed as a cut-off year for the impact analysis are indicated in the graphs of figure 4.12.

Figure 4.12 shows that the mean monthly discharge volumes of all the projected years indicate a rapid peaking in August and a subsequent decline. The mean monthly flow amounted up to 4.915bcm in August.

Figure 4.14 on the other hand shows the projected flow conditions for the coming 20 years. It indicates the flow trend if the existing condition tends to continue. While developing the graph, the software took the trend of the historical data into consideration.

As shown in figure 4.13, the mean annual flow volume obtained from the gauged tributaries was found to be 18.111bcm at the downstream of Beles. Compared

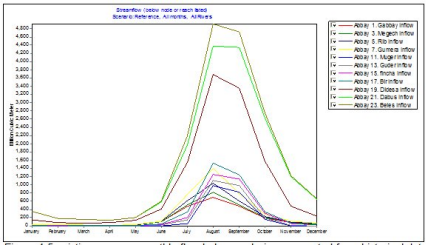

Figure 4.12: Existing average monthly flow below each river computed from historical data of gauged tributaries

Proj.	Jan	Feb	Mar	Apr	May	Jun	Jul	AugSep	OctNov	Dec	Sum	
Gabbay	28.6	18.9	16.6	13.2	23.2	100.2	482.5	693.1	480.8	198.7	83.3	47.4 2,186.4
Megech	29.4	19.4	17.1	13.9	24.4	105.1	513.9	816.5	515.1	205.1	86.0	49.0 2,395.0
Rib	30.9	20.4	17.9	14.7	25.6	112.5	615.7	1,036.8	604.9	226.0	94.2	52.5 2,852.1
Gumera	36.8	24.1	21.2	16.9	28.6	119.7	763.7	1,398.4	788.4	283.4	114.9	62.8 3,659.0
Muger	0.8	0.7	0.8	0.9	0.9	1.8	58.3	978.4	824.8	161.4	2.9	1.4 2,033.1
Guder	2.8	2.5	3.6	3.0	4.5	20.9	146.4	1,106.6	976.8	195.2	8.3	3.9 2,474.4
Fincha	8.9	4.6	6.0	5.7	11.2	33.2	208.9	1,249.9	1,138.4	309.0	59.3	20.2 3,055.2
Bir	12.0	6.3	7.5	6.9	13.2	41.2	339.6	1,523.7	1,246.6	343.6	70.5	26.7 3,637.9
Didessa	146.5	3.8	73.1	74.3	135.5	411.2	1,555.9	3,683.1	3,357.1	1,577.5	474.1	240.9 11,813.0
Dabus	350.8	183.2	154.0	136.4	204.1	582.7	1,977.0	4,375.9	4,349.1	2,618.4	1,194.2	651.6 16,777.5
Beles	355.7	185.8	156.0	137.8	207.7	608.2	2,202.8	4,915.0	4,721.6	2,744.7	1,216.0	659.8 **18,111.2**

Figure 4.13: Mean monthly discharge (MCM) of the main tributaries before the implementation of the projects

to the previously computed mean annual volume of flow (49.7bcm), the contribution of the gauged rivers was 36%. This shows that the contribution of the sub-basins excluded from the analysis was considerably high and the stream flow gages on the mentioned tributaries did not represent the exact confluence point input.

4.5.8 Computation of Irrigation Water Requirements

On the basis of the availability of complete data for the model, 17 irrigation sites indicated in figure 4.15 and 4.16 were selected and analysed to their full potential. Thus, the impact assessment of this study considered the development

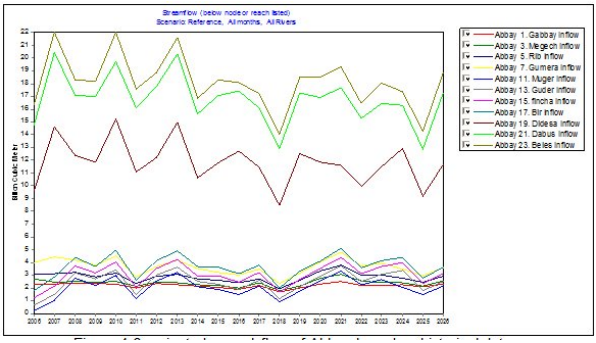

Figure 4.14: Projected annual flow of Abbay based on historical data

of 220.416ha of irrigable land. Two techniques were implemented to compute the water requirement of the project sites as given in the subsequent sections.

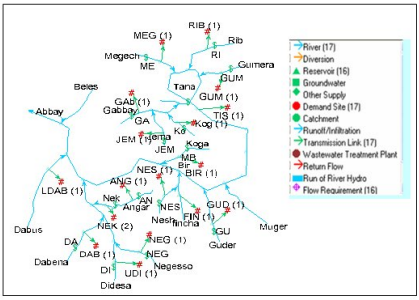

Figure 4.15: Schematic overview of irrigation project sites and reservoir locations

Demand sites	Longitude	Latitude	River bed elev. (m)	Catchment area (km^2)	Irrigable area (ha)
Angar	36.744	9.69	1320	1962	14450
Dabana	36.013	8.92	1230	2554	16388
Gilgel Abbay B	37.009	11.46	1840	1980	11508
Gumara B	37.794	11.74	1910	401	13976
Jema	37.182	11.20	2060	218	7786
Koga			1875	164.8	6000
Finchaa	37.733	9.55		1391	6205
lower Didessa	35.975	9.48	885	17770	5167
Middle Bir			2003	714	10000
Megech	37.467	12.52	1870	416	7311
Negesso	36.564	8.86	1945	402	22815
Nekemte	36.5	9.43	1267	4623	11220
Nesh A	37.256	9.75	2205	339	7217
Rib	37.996	12.04	1867	677	19625
Upper Didessa	36.806	8.21	1335	4001	14280
Upper Guder	37.667	8.86	2400	239	4896
Tis Abbay				1505	41837
				Total	***220,416 ha***

Figure 4.16: Description of irrigation projects included in the analysis

Direct Water Demand Computation Method

The total water demand excluding losses at each site was computed with WEAP after filling the required data. The water demand of all projects summed up to 1.53bcm. Reviewing the consumption of each project, it could be revealed that the peak water requirement belonged to the Tis Abbay project associated with its high command area size, whereas the water demand to area ratio was found to be high for the Finchaa project (close to 8.735m^3/ha); the minimum of 5.535 m^3/ha was found for the Upper Guder project which is situated in the high land area.

Figure 4.17 shows that the irrigation requirement of the projects culminates during the months of January to March and November to December. On the other hand, during the months of June to September the analysis revealed that there was almost no need of irrigation. However, there could be supplementary irrigation during these months to prevent crop failure that could happen as a result of rainfall, delayed setoff or early cut-off.

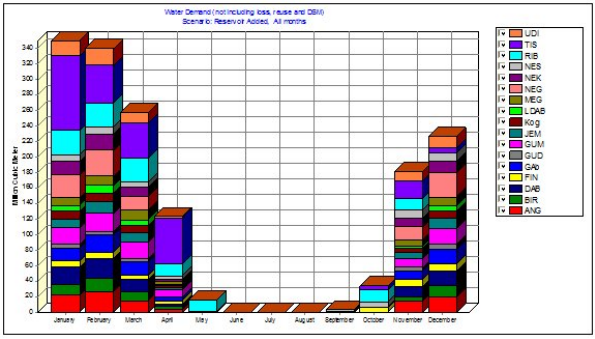

Figure 4.17: Mean monthly water demand of all the demand sites

Figure 4.18 indicates the total water requirement for fulfilling the irrigation requirement without including the losses that could happen with regard to conveyance, distribution and application to the plant. The results of the computation revealed that, disregarding the losses, the annual water requirement to irrigate the proposed 220.416 ha of land was 1.532 billion m^3. Assuming that the irrigation system was of a surface irrigation type and had an overall efficiency range of 40% to 70%, the annual gross volume of water consumed in Ethiopia would amount to 2.2-3.83bcm.

Indirect Total Water Demand Computation Method

This method was implemented in relation to the computation of the border flow which was carried out using the historical data of the gauged tributaries. As previously determined the border flow of the river was found to be 18.11bcm before the implementation of the irrigation projects under consideration. Using the same historical data and projection year, the condition of flow volume after full potential implementation of the irrigation projects was investigated. The same projection year was considered so that the differences that could arise due to external factors related to periodical variation were deleted.
Having run the model for this condition, the results obtained from the analysis

Proj.	Jan	Feb	Mar	Apr	May	Jun	Jul	Aug	Sep	Oct	Nov	Dec	Sum
ANG	22.0	27.1	15.0	3.0	0.0	0.0	0.0	0.0	0.0	0.0	14.0	19.0	100.2
BIR	13.9	17.3	11.8	5.5	0.0	0.0	0.0	0.0	0.0	0.0	5.5	15.3	69.3
DAB	22.0	24.9	15.3	1.9	0.0	0.0	0.0	0.0	0.0	0.0	13.4	18.2	95.7
FIN	8.1	8.1	6.0	4.3	0.5	0.0	0.0	0.0	1.1	6.0	9.8	10.3	54.2
Gab	16.9	22.2	16.9	5.3	0.0	0.0	0.0	0.0	0.0	0.0	9.8	17.8	88.9
GUD	4.5	4.6	4.5	0.0	0.0	0.0	0.0	0.0	0.5	0.8	5.4	6.8	27.1
GUM	21.6	23.7	21.6	8.6	0.0	0.0	0.0	0.0	0.0	0.0	11.9	20.5	107.9
JEM	11.4	14.4	11.4	3.0	0.0	0.0	0.0	0.0	0.0	0.0	7.2	12.6	60.1
Kog	9.3	11.1	8.8	2.3	0.0	0.0	0.0	0.0	0.0	0.0	5.6	9.3	46.3
LDAB	7.5	9.8	8.3	1.1	0.0	0.0	0.0	0.0	0.0	0.0	3.4	7.5	37.7
MEG	10.2	11.9	11.9	4.5	0.0	0.0	0.0	0.0	0.0	0.0	6.8	11.3	56.5
NEG	30.0	33.9	18.2	0.0	0.0	0.0	0.0	0.0	0.0	0.0	16.9	31.3	130.3
NEK	17.1	21.0	11.7	2.3	0.0	0.0	0.0	0.0	0.0	0.0	10.9	14.8	77.8
NES	9.0	9.0	6.6	4.8	0.6	0.0	0.0	0.0	1.8	6.6	10.8	10.8	60.0
RIB	30.3	30.3	30.3	15.2	15.2	0.0	0.0	0.0	0.0	15.2	15.2	0.0	151.6
TIS	97.0	48.5	45.6	59.9	0.0	0.0	0.0	0.0	0.0	5.7	22.8	5.7	285.3
UDI	19.2	21.7	13.3	1.7	0.0	0.0	0.0	0.0	0.0	0.0	11.7	15.8	83.4
Sum	350.0	339.5	257.2	123.6	16.3	0.0	0.0	0.0	3.4	34.2	181.0	226.9	***1,532.2***

Figure 4.18: Average monthly water demand excluding losses (MCM) for the case of reservoir added

are presented in figure 4.19 and 4.20.

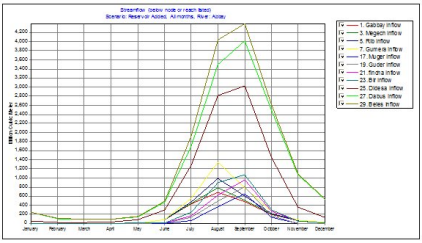

Figure 4.19: Average monthly stream flow hydrograph of Abbay after the operationalisation of the irrigation projects

The graph of figure 4.19 reveals that the shape and volume of the peak changed in comparison to the previous figures. The graph showed an attenuation and gradual rise nature which could be considered the result of the reservoirs' regulation on the tributaries. The peak month shifted from August to September.

The mean annual flow volume of the river after the implementation of all the projects under consideration was reduced to 15.78 billion m^3 and the peak monthly

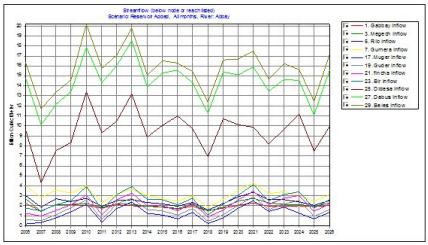

Figure 4.20: Projected stream flow of Abbay after the implementation of the projects

flow became 4.4MCM in September.
From the two analyses mentioned before and according to the project condition, the difference in the magnitude (2.33bcm) was the water consumed for the development of 220.416 ha of land.

4.5.9 Unmet Demands

Without Reservoir Scenario

In this case, the amount of water delivered to each project by a simple diversion of the stream flow was considered. The analysis showed there were projects that did not require a reservoir to meet their water demand for the specified command area. Among such projects the Lower Dabus project capable of irrigating 5.100 ha needed no reservoir. This was also confirmed by the master plan. On the other hand, with regard to the Fincha project at its initial phase of irrigating 6.205 ha, the need for a reservoir was not compulsory. But for the generation of hydropower and further intensification of the farm the presence of the dam as it exists now is crucial.

In the absence of reservoirs the model predicted the probable annual unmet demand based on the historical data of the rivers. Figure 4.21 shows the variability of the unmet demand in the coming twenty years that emanate from the nature of the historical data utilised and the procedure followed by the software to predict future flows. The graph indicates the need of reservoirs to meet the demands of

the projects.

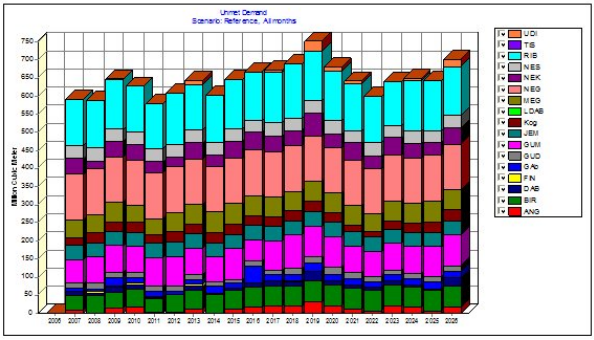

Figure 4.21: Without reservoir scenario, projected annual unmet demand

With Reservoir Scenario

Having discovered the necessity of reservoirs and taken the master plan's recommendation into consideration, the proposed reservoirs for each project were analysed. The amount of water supplied to the projects and the demands met were evaluated.

In this scenario those projects found to be at low coverage of their water requirement in the "without reservoir" case became operational to their full potential. This was mainly due to the fact that the water stored in the reservoir had augmented the existing flow deficit.

The water delivered to each project in the "with reservoir" case, which amounted to 1.351bcm annually, is shown in figure 4.22. Compared to the total water demand (1.532bcm) the annual supply was less (by 0.181bcm) for all the projects under consideration. The project-wise and mean monthly distribution of the unmet demand is shown in figure 4.23.

As indicated in figure 4.23, even in the presence of the proposed reservoirs there were still projects in shortage of water to satisfy their monthly demand. The degree of shortage varied among the projects and months as shown in figure

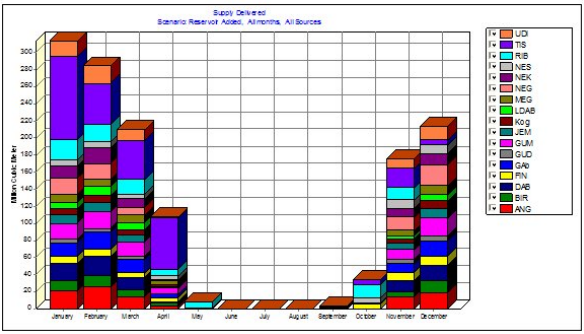

Figure 4.22: Supply delivered for each project on a monthly basis

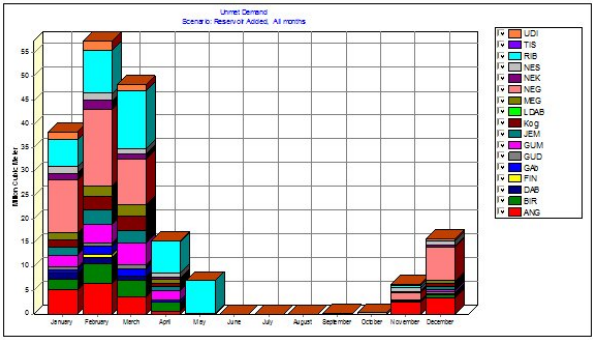

Figure 4.23: Mean monthly unmet demand of demand sites over the whole years

4.25. The probable unmet demand for the coming twenty years projected from the historical data is shown in figure 4.24.

Both the monthly and annual unmet water demand showed that the shortage of Rib and Negesso was considerably high and extended the whole projected period. As indicated in figure 4.26, the monthly coverage or the percentage of water demand fulfilled at a particular month of these projects lowered up to 49.6% for

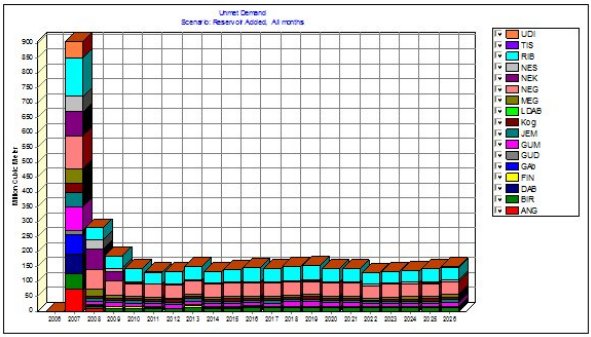

Figure 4.24: Projected annual unmet demand for reservoir-added scenario computed from historical data

Negesso in March and 56.7% for Rib during April. Unless this deficit is deleted by supply from other sources or the command area is reduced, the deficit will have a considerable impact on productivity.

Proj	Jan	Feb	Mar	Apr	May	Jun	Jul	Aug	Sep	Oct	Nov	Dec	Sum
ANG	1.2	1.6	0.9	0.2	0.0	0.0	0.0	0.0	0.0	0.0	0.1	0.1	4.1
BIR	2.3	4.2	3.4	1.7	0.0	0.0	0.0	0.0	0.0	0.0	0.0	0.9	12.5
DAB	1.1	1.4	0.9	0.1	0.0	0.0	0.0	0.0	0.0	0.0	0.0	0.0	3.4
FIN	0.0	0.9	0.4	0.2	0.0	0.0	0.0	0.0	0.0	0.0	0.0	0.0	1.6
Gab	0.8	1.6	1.4	0.4	0.0	0.0	0.0	0.0	0.0	0.0	0.0	0.0	4.2
GUD	0.5	0.6	0.7	0.0	0.0	0.0	0.0	0.0	0.0	0.0	0.1	0.3	2.2
GUM	2.7	4.3	4.9	2.1	0.0	0.0	0.0	0.0	0.0	0.0	0.0	0.7	14.7
JEM	1.7	3.0	2.8	0.8	0.0	0.0	0.0	0.0	0.0	0.0	0.1	0.7	9.1
KOG	1.6	2.9	2.8	0.8	0.0	0.0	0.0	0.0	0.0	0.0	0.0	0.6	8.8
LDAB	0.0	0.0	0.0	0.0	0.0	0.0	0.0	0.0	0.0	0.0	0.0	0.0	0.0
MEG	1.7	2.4	2.8	1.1	0.0	0.0	0.0	0.0	0.0	0.0	0.3	0.9	9.3
NEG	11.2	16.2	9.7	0.0	0.0	0.0	0.0	0.0	0.0	0.0	1.6	7.1	45.8
NEK	2.3	3.1	1.8	0.4	0.0	0.0	0.0	0.0	0.0	0.0	0.8	1.2	9.6
NES	1.4	1.5	1.2	0.9	0.1	0.0	0.0	0.0	0.1	0.3	0.7	0.9	7.2
RIB	6.6	9.9	12.8	7.1	7.6	0.0	0.0	0.0	0.0	0.2	0.9	0.0	45.0
TIS	0.0	0.0	0.0	0.0	0.0	0.0	0.0	0.0	0.0	0.0	0.0	0.0	0.0
UDI	0.4	2.9	1.1	0.0	0.0	0.0	0.0	0.0	0.0	0.0	0.0	0.0	4.4
Sum	35.5	56.3	47.7	15.8	7.7	0.0	0.0	0.0	0.1	0.5	4.7	13.5	181.8

Figure 4.25: Average monthly unmet demand of each demand site (MCM) for reservoir-added scenario

Proj	Jan	Feb	Mar	Apr	May	Jun	Jul	Aug	Sep	Oct	Nov	Dec	Min	Max
ANG	77.8	77.2	76.9	76.8	100.0	100.0	100.0	100.0	100.0	100.0	83.0	82.9	76.8	100.0
BIR	85.0	77.5	72.7	70.6	100.0	100.0	100.0	100.0	100.0	100.0	100.0	95.2	70.6	100.0
DAB	95.0	94.5	94.3	94.9	100.0	100.0	100.0	100.0	100.0	100.0	99.5	99.6	94.3	100.0
FIN	100.0	93.5	100.0	100.0	100.0	100.0	100.0	100.0	100.0	100.0	100.0	100.0	93.5	100.0
GAb	94.8	92.5	91.0	91.1	100.0	100.0	100.0	100.0	100.0	100.0	100.0	100.0	91.0	100.0
GUD	87.7	85.6	83.7	100.0	100.0	100.0	100.0	100.0	98.8	99.2	97.3	94.3	83.7	100.0
GUM	89.3	84.3	80.1	78.7	100.0	100.0	100.0	100.0	100.0	100.0	100.0	97.9	78.7	100.0
JEM	85.8	80.2	76.2	75.9	100.0	100.0	100.0	100.0	100.0	100.0	98.8	94.4	75.9	100.0
KOG	83.2	74.8	69.1	68.9	100.0	100.0	100.0	100.0	100.0	100.0	100.0	94.3	68.9	100.0
MEG	87.3	83.6	80.1	78.9	100.0	100.0	100.0	100.0	100.0	100.0	98.6	95.0	78.9	100.0
NEG	64.4	54.3	49.6	100.0	100.0	100.0	100.0	100.0	100.0	100.0	90.9	78.3	49.6	100.0
NEK	92.7	92.1	91.7	91.4	100.0	100.0	100.0	100.0	100.0	100.0	97.5	97.5	91.4	100.0
NES	85.7	83.8	82.5	81.4	81.5	100.0	100.0	100.0	94.8	95.3	93.9	92.0	81.4	100.0
RIB	82.1	71.3	62.0	58.0	56.7	100.0	100.0	100.0	100.0	100.0	97.0	100.0	56.7	100.0
UDI	92.1	91.5	91.1	91.1	100.0	100.0	100.0	100.0	100.0	100.0	97.1	97.2	91.1	100.0
Min	64.4	54.3	49.6	58.0	56.7	100.0	100.0	100.0	94.8	95.3	83.0	78.3		
Max	100.0	94.5	100.0	100.0	100.0	100.0	100.0	100.0	100.0	100.0	100.0	100.0		

Figure 4.26: Demand requirement coverage (in %) of the demand sites for the reservoir-added scenario

Assuming the two cases of 80% and 75% monthly coverage as the minimum reliable values, the projects not fulfilling these conditions and the number of failure months derived from figure 4.26 are shown in figure 4.27.

reliability	Angar	Bir	Gumera	Jema	Koga	Megch	Negeso	Rib
80%	4	3	1	2	3	1	4	4
75%	-	-	-	-	3	-	3	4

Figure 4.27: Percentage of reliability and number of months below the threshold

From figure 4.27 it can be concluded that due consideration should be given to implementing the Rib, Negesso and Koga irrigation projects. Figure 4.28 shows the probable overall condition for the water allocation of each project.

4.5.10 Discharge before and after the Project Condition

The overall flow condition of the tributaries utilised for irrigation development and that of the main stream was computed for the conditions of the pre- and post-project case.
On the basis of the above-mentioned procedure, WEAP computed the whole tributaries' flow and the main stream flow before and after the implementation of the projects. In order to convert the monthly flow volume into discharge (m^3/sec), the volume given was divided by the number of days in the month multiplied by

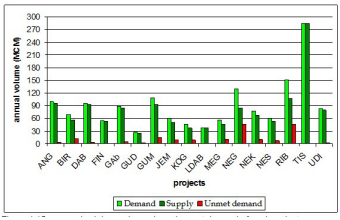

Figure 4.28: Summarised demand, supply and unmet demand of each project

86.400 seconds/day.

Based on these computational methods, the following fundamental issues can be highlighted:

- The flow in the natural stream became zero for a month or consecutive months. This conditions needed due consideration for the Tis-Abbay, Rib, Negesso, Bir and Megech projects. However, the flow lowered up to 40 litres per second for the Koga, Jema and Gumera projects.
- Unless other downstream tributaries of the above-mentioned rivers with zero stream flows augment the ecological and downstream water users' demand, it will be difficult to implement the proposed irrigation potential.
- The overall reduction of flow of the main river Abbay before and after the projects is shown in figure 4.29 and 4.30. The figures reveal the monthly and projected annual flow of the river below its confluence with the mentioned rivers selected for comparison. The projected flow indicates that the volume of water to be abstracted annually after the year 2010 will remain constant.

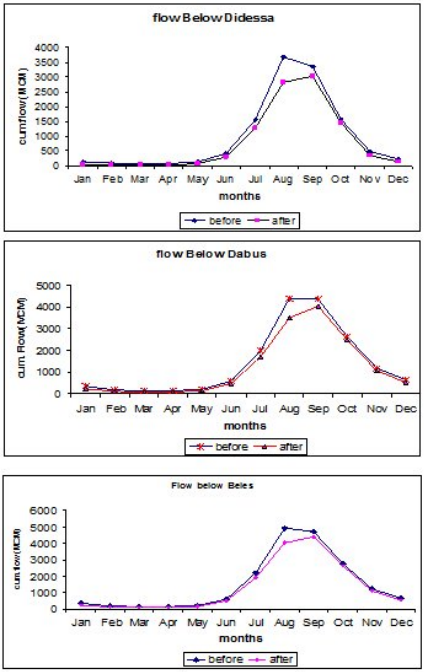

Figure 4.29: Mean monthly flow of Abbay before and after the projectsŠ conditions

4.6 Conclusion

From the analysis performed in this study it can be concluded that the total irrigation water requirement to irrigate 220.416 ha of land was found to be 3bcm. The overall mean annual flow from the mean monthly data of the main stream gauges was estimated to be 49.7bcm at the Sudan border. The water required to irrigate the mentioned command area accounts for 6% of the Abbay mean annual flow at the border to Sudan. Compared to the results of scenario 1 of the master plan, the border flow reduction amounted to 7%, which was compatible with the results of the master plan. However, the mean annual flow of 50bcm given in the

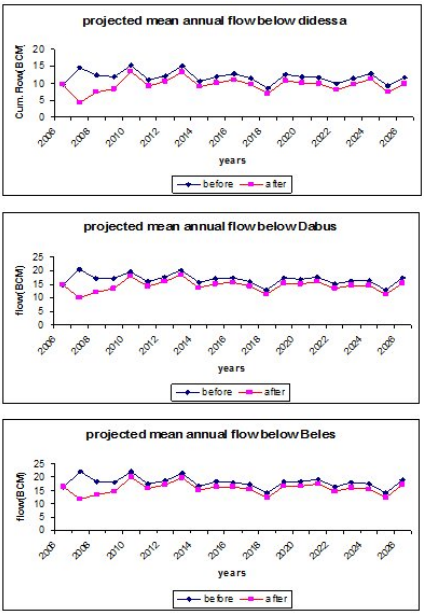

Figure 4.30: Projected mean annual flow of Abbay before and after the projects

master plan was almost equal to the study result of 49.7bcm.

4.7 References

ACRES International and Shawel Consultant (1995). Feasibility Study of the Bir and Koga Irrigation Project, Bir Catchment and Irrigation Studies, p. 75, Addis Ababa, Ethiopia

Allen, R.G., et al. (1998). Crop Evapotranspiration Guidelines for Computing Crop Water Requirements, FAO Irrigation and Drainage 56, p. 13, Rome, Italy.

Appelgren, B., Klohm, I., & Undala, A. (2000). Water and Agriculture in the

Nile Basin, Nile Basin Initiative Report to ICCON, background paper prepared by FAO of the United Nations, Land and Water Development Division, Rome, Italy.

BCEOM (1998). ARBIDMP Land Resource Development Reconnaissance Soils Survey Project, phase 2, section II, volume VIII, Addis Ababa, Ethiopia.

BCEOM (1998). ARBIDMP Project Land Resource Development Land Cover/ Land Use, phase 2 section II, volume X, Addis Ababa, Ethiopia.

BCEOM (1998). ARBIDMP Project Infrastructure, phase 2, section II, Volume XVIII, part 4 and 5, p 4-44, Addis Ababa, Ethiopia.

BCEOM (1998). ARBIDMP Project Data Collection and Site Investigation Survey and Analysis, section III, annexes volume II, Dams project profile; and section I, volume 6, Dams and Reservoirs, Addis Ababa, Ethiopia.

BCEOM (1998). ARBIDMP Project Water Resources Development Irrigation and Drainage, phase 2, appendix B, section 4, table 2, 3 and 4, pp 40-42, Addis Ababa, Ethiopia.

BCEOM (1998). ARBIDMP Project Data Collection and Site Investigation Survey and Analysis, section II, sectoral studies volume VI, Water Resource Development, part I, Large Dams and Hydropower Schemes, part 3, Dams and Reservoir Sites, Addis Ababa, Ethiopia.

BCEOM (1998). ARBIDMP Project Water Resource Studies, part 1, main report, phase 3, Addis Ababa, Ethiopia.

Bricheri-Colombi, J.S.A. (1997). Nile Basin Irrigation Development and its Impact, Vth Nile Conference Proceedings: Comprehensive Water Resources Development of the Nile Basin, p.103, Addis Ababa, Ethiopia.

Grieser, J. (2002). LocClim, Local Climate estimator, FAO of the United Nations Environmental and Natural Resource Service, grieser@meteor.uni-frankfurt.de.

HALCROW (1989). Master Plan for the Development of Surface Water Resources in the Awash Basin, final report, volume 2, main report, Sir William Halcrow and Partners Comp. Addis Ababa, Ethiopia.

Linsley, R.K, & Franzini, J.B. (1984). Water Resources Engineering, 3rd edition, p.33, MCGRAW-Hill International Book Company, London.

Nile 2002 Conference. Compressive Water Resources Development of the Nile Basin: getting started proceedings, volume 2, special issue Aswan, Egypt, February 1-6, 1993.

Rumenuk, R.P, & Grubbs, J.W. (1996). Methods of Estimating Low Flow Characteristics of Ungauged Stream in Selected Areas, US Geological Survey Water Resource Investigations Report 96-4124, Tallahassee, Florida.

Sieber, J., Charis, S., & Huber-Lee, A. (2005). User Guide for WEAP 21, Stockholm Environmental Institute, Tellus Institute Boston, USA.

Tadesse, D. (2005). Evaluation of Selected Hydropower Potential Sites: A Case Study of Abbay River Basin - Ethiopia, thesis submitted in partial fulfilment of the requirements for the degree Master of Science of Arba Minch University, p.33, Arba Minch University, Ethiopia.

Tulore, A. (2005). Assessment of cause of Lake Tana water level change and its impact on Tiss Abbay hydropower production and Tiss Issat fall Arba Minch, a thesis submitted in partial fulfilment of the requirements for the degree Master of Science of Arba Minch University, Ethiopia.

Wolf, A.T. (1999). Transboundary Water Allocations, Natural Resource Forum 23.1, 3-30, wolfa@geo.oregonstate.edu.

Woudneh, T. (1997). Vth Nile Conference Proceedings: Comprehensive Water Resources Development of the Nile Basin, Basis for Cooperation, ECA printing department, Addis Ababa, Ethiopia.

Woulers, K.P., et al. (2005). An Integrated Assessment of Equitable Entitlement, Legal Assessment Model, Technical Documents in Hydrology No. 74, UNESCO, Paris.

Zhu, Z., & Hansen, E. (1993). Potential Application of the WEAP to the Nile Basin, Nile Conference 2002, p.III-1, Aswan, Egypt.

5 Development of Intensity-Duration-Frequency Relationships for gauged and un-gauged location of Southern Nations, Nationalities Peoples Region (SNNPR) - Feleke Gerb, Semu Aylew Moges

Feleke Gerb, *Semu Aylew Moges*[1]

[1] Arba Minch University
School of Graduate Studies
P.O. Box 21
Arbaminch, Ethiopia
telephone: +251-46-8810775
Email:semu_moges_2000@yahoo.com

5.1 Abstract

The Intensity-Duration-Frequency (IDF) relationship of rainfall amount is one of the most commonly used tools in water resources engineering for planning, designing and operation of water resources projects. The reason for the objective of this research, is to develop operational IDF relationships for the SNNPR State based on nineteen first class stations. Three different forms of IDF curves have been developed considering application to both gauged and un-gauged areas and presented in the form of general mathematical equations, curves relating to the Intensity-Duration-Frequency of rainfall and the IDF regionalized maps.
The IDF curve and the general mathematical form are intended to estimate the magnitude of the rainfall intensity of a given return period within 25 km radius of the principal station. For areas that are further away than 25 km from the principal station (un-gauged area), regional IDF parameters have been developed and can be used to estimate the magnitude of intensity values.

Therefore, planners and designers in the country, as well as the regional state can effectively utilize one or all of the procedures to derive the IDF value in any part of the region. The objective is the planning and designing of reasonable water use and road infrastructures. We also recommend that the projects that are operating in the state may revisit their planning and design guidelines on the basis of the new findings.

Key: *IDF curve, Regional IDF curves, distributions, parameters, Standard Error of Estimates (SEE)*

5.2 Introduction

Rainfall Intensity-Duration-Frequency curves (IDF curves) are a graphical representation of the precipitation within a given period of time. The Intensity of Rainfall (I) is the rate at which it is falling, Duration (D) is the time during which it is falling with that given intensity and frequency (F) is the average recurrence time of that magnitude of rainfall (DuPont & Allen, 2000).
The development of intensity duration frequency IDF curves for precipitation remains a powerful tool in the risk analysis of natural hazards. Indeed, the IDF

curves allow for the estimation of the return period of an observed rainfall event or, conversely, of the rainfall amount corresponding to a given return period for different aggregation times. The purpose of this study is mainly to produce IDF relationships for the precipitation at nineteen different first order recording climate stations in the South Nations Nationalities and Peoples Regional State.

This study can be considered as a essential work to fill the gap of design parameters as a result of limited data. Furthermore, the study was intended to develop regional IDF curves for the Southern Nations Nationalities and Peoples Regional State (SNNPR) which can be found in the south western part of Ethiopia (figure 5.1).
According to the Central Statistics Authority (CSA, 2005), (an annual statistical report cited in www.ethiopar.net, 2005), the state has an estimated area of about 112.323 km^2 and accounts for some 10% of Ethiopia's total area. Regarding the size of its population, the regional state has an estimated population of about 14.9 million, or 20 percent of the total population. About 56% of the state's total area is located below 1.500 metres mean sea level, which is categorized largely as the hottest low land ("Kolla"). The other 44% is situated in the temperate climatic zone. The state's mean annual rainfall ranges from 500 - 2.200 mm. Its intensity, duration and amount increases from South to Northeast and Northwest. The mean annual temperature of the state in general ranges form 15°C to 300°C (www.ethiopar.net, 2005).

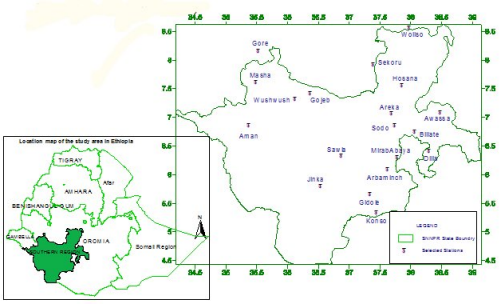

Figure 5.1: Location maps of the selected rainfall stations with in the study area

5.3 The Data

Rainfall recording stations with automatic recorders have been identified in and around the state to extract different data concerning the rainfall duration and intensity. A total of 19 stations and their data have been identified and were collected by the NMSA. Those stations are located inside the state, except for Gore, Woliso and Sekoru. These stations were added from the neighboring region, Oromia, to develop more refined regional curves that will be more applicable. Figure 5.2 lists the basic information and length of observed data for the selected stations.

No.	Station Name	Sample size (years)	Location			Period of record	Mean annual temp. °C	Mean annual rainfall (mm)
			Long. (degree)	Lat. (degree)	Elevation (masl)			
1	Arbaminch	32	37.66	6.06	1219	1969-2005	20.83	833
2	Sekoru	17	37.4	7.92	2100	1987-2004		
3	Konso	17	37.58	5.25	1460	1986-2005	21.93	398
4	Sawla	11	36.88	6.32	1500	1987-2002		
5	Aman	10	35.38	6.85	1360	1988-2005		
6	Gore	22	35.53	8.15	2002	1968-1991	18.16	1897.8
7	Gidole	13	37.48	5.61	2550	1989-2001	16.66	1191
8	Masha	16	35.5	7.6	2310	1988-2005		2062.6
9	M/Abaya	13	37.83	6.33	1290	1990-2002	24.17	690
10	Jinka	28	36.63	5.83	1430	1972-2005	21.15	1345
11	Billate	31	37.96	6.65	1200	1971-2005	22.48	902
12	Sodo	28	37.71	6.83	2020	1972-2005	19.98	1333
13	Dilla	13	38.3	6.41	1670	1988-2005	20.12	1360
14	Areka	15	37.7	7.06	1750	1988-2003		1336
15	Awassa	30	38.5	7.06	1652	1975-2005	19.2	952.8
16	Hosaina	22*	37.83	7.58	2290	1979-2005	16.54	1194
17	Woliso	13	37.98	8.51	1960	1988-2005	17.99	1208
18	Wushwush	5	36.13	7.32	1950	1988-1993	18.33	1892
19	Gojeb	6	36.38	7.42	1250	1980-1985		

Figure 5.2: Basic information of the rainfall stations

For most of the stations, charts of continuous data recorder are available and the rainfall intensity of different durations has been extracted. Table 2 shows the sample intensity values for durations of 30-minute, 1-hour, 2-hour, 3-hour, 5-hour, 6-hour, 12-hour and 24-hour which occurred in different months of the year 1974 E.C at Arbaminch station.

For an individual duration the maximum rainfall depth is extracted as the annual maximum D-hour intensity (for e.g. 1974 the maximum intensity is shown at the bottom of figure 5.3). This procedure has been done for the whole period of time

.Year	Date of record	Observed Rainfall (mm) for the indicated duration(hr)							
		0.5	1	2	3	5	6	12	24
1974	6-7/10/1974	3.7	4.5	4.5	5.9	6.5	6.5	6.5	6.5
1974	28-29/9/1974	1	0.4	5.2	7.4	7.4	7.4	7.4	7.4
1974	20-21/9/1974	13.5	15.9	17.8	18.5	18.9	18.9	18.9	18.9
1974	7-8/9/1974	0.9	10	27	29.1	30.1	30.1	30.1	30.1
1974	21-22/7/1974	4.3	4.5	5.5	8.4	10.5	10.6	10.6	10.6
1974	3-4/7/1974	6.4	11.5	13.2	13.2	13.2	13.2	13.2	13.2
1974	31/6-1/7/1974	8.7	10.2	11.5	15.8	21.6	21.6	21.6	21.6
1974	25-26/5/1974	1.7	6.3	10.1	12.3	20.5	21.9	25	25
1974	19-20/5/1974	6.7	7.5	9.6	10.2	10.4	10.4	10.4	10.4
1974	10-11/5/1974	31.8	45.5	46.9	50.4	52.4	52.4	53	53
1974	6-7/5/1974	8.3	10.3	13.3	14.8	19.5	19.5	19.5	19.5
1974	4-5/5/1974	14.8	14.8	14.8	14.8	14.9	14.9	14.9	14.9
1974	11-12/4/1974	19.5	20	20	20	20	20.1	20.1	20.1
1974	**Max**	**31.8**	**45.5**	**46.9**	**50.4**	**52.4**	**52.4**	**53**	**53**

Figure 5.3: Samples of data collected from rainfall charts for 1994 E.C

in which the data is available and to all the 19 station.

In order to validate the quality and nature of the data, various tests have been carried out, such as the outlier test (Maidment, 1993), independence and stationarity tests. All in all, the outlier tests proved that there is no data out off the outlier test threshold and the data series from all station have been found to be random.

5.4 Procedure and Development of IDF-Curves

5.4.1 Selection and Evaluation of Parent Distributions for the Rainfall Data

The abstracted annual maximum series of different durations of rainfall depths have been treated by using a frequency analysis procedure in order to select the best applicable probability distribution and parameter estimates to each station (Rao and Hamed, 2000). 15 probability distribution methods have been tested, both graphically and numerically. Some of the graphical methods include Moment Ratio Diagrams (Cunnane, 1989), L-Moment Ratio Diagrams Hosking (1990) and probability plots. Finally, the standard error of estimate

(SEE) has been used as a final distribution and parameter selection method. The most efficient method is the one which gives the smallest SEE (Rao and Hamed, 2000). Figure 5.4 presents the type of distribution and estimation method for Arba Minch station.

Distributions	SEE for the indicated return periods in years					
	T=2	T=2	T=2	T=2	T=2	T=2
EV1/ML	2.13	3.16	3.94	4.97	5.76	6.54
EV1/PWM	2.14	3.4	4.39	5.71	6.71	7.71
LN/MOM	2.11	3.28	4.3	5.78	6.96	8.24
P3/MOM	2.36	3.47	4.57	6.36	7.88	9.57
P3/PWM	2.12	3.28	4.55	6.56	8.22	10.04
LP3/MOM	2.2	3.26	4.44	6.56	8.57	11.02
G2/MOM	2.17	3.46	4.52	5.89	6.9	7.92
G2/ML	2.17	3.48	4.51	5.83	6.79	7.76
G2/PWM	2.16	3.44	4.43	5.73	6.68	7.64
GEV/PWM	2.12	3.18	4.36	6.63	8.97	11.89

Figure 5.4: SEES of the Candidate distributions for1-h rainfall at Arbaminch station

Distributions	SEE for the indicated return periods in years					
	T=2	T=5	T=10	T=25	T=50	T=100
EV1/MOM	2.43	3.51	4.47	5.79	6.81	7.84
EV1/ML	2.43	3.39	4.27	5.49	6.44	7.4
EV1/PWM	2.43	3.52	4.49	5.82	6.85	7.9
LN/MOM	2.48	3.48	4.54	6.14	7.44	8.85
P3/MOM	2.54	3.59	4.71	6.47	7.92	9.49
P3/PWM	2.35	3.25	4.16	5.58	6.77	8.09
LP3/MOM	2.54	3.54	4.66	6.58	8.3	10.31
G2/MOM	2.49	3.59	4.53	5.78	6.69	7.62
G2/ML	2.49	3.6	4.53	5.75	6.64	7.55
G2/PWM	2.49	3.57	4.51	5.75	6.66	7.59
GEV/PWM	2.43	3.44	4.61	6.81	8.95	11.48
GEV/MOM	2.47	3.55	4.68	6.56	8.22	10.05
LLG/PWM	2.43	3.34	4.44	6.57	8.81	11.69
EXP/MOM	2.34	3.34	4.46	6.11	7.41	8.74

Figure 5.5: SEE of the candidate distributions for 6-h rainfall at Arbaminch station

Based on the smallest standard error of estimate, the best fitted candidate distributions of different rainfall durations for all stations are shown in figure 5.6.
On the basis of distribution and parameter estimation methods shown in the above

No	Station Name	0.5	1	2	3	5	6	12	24
1	Aman	P3/MOM	GEV/MOM	P3/MOM	P3/MOM	G2/ML	G2/PWM	P3/PWM	P3/MOM
2	Arbaminch	PII/PWM	EV1/ML	EV1/ML	EV1/ML	EV1/ML	EV1/ML	EV1/ML	EV1/ML
3	Areka	G2/ML	G2/ML	P3/MOM	P3/MOM	P3/MOM	G2/PWM	EV1/PWM	EV1/PWM
4	Awassa	EV1/ML	G2/ML	EV1/ML	EV1/ML	EV1/ML	EV1/ML	EV1/ML	P3/MOM
5	Billate	P3/MOM	G2/ML	EV1/MOM	LLG/PWM	P3/PWM	G2/MOM	G2/MOM	P3/PWM
6	Dilla	P3/PWM	P3/PWM	P3/PWM	P3/PWM	P3/PWM	P3/PWM	G2/PWM	G2/ML
7	Gidole	P3/PWM	P3/MOM	P3/MOM	P3/MOM	P3/MOM	G2/ML	P3/MOM	P3/MOM
8	Gore	G2/ML	G2/ML	G2/PWM	G2/PWM	G2/ML	G2/ML	EV1/ML	EV1/ML
9	Jinka	P3/MOM	G2/ML	G2/ML	G2/ML	EV1/ML	EV1/ML	EV1/ML	EV1/ML
10	Konso	P3/MOM	P3/MOM	P3/PWM	LN/MOM	G2/MOM	G2/MOM	WAKEBY-4	P3/MOM
11	M/Abaya	G2/ML	P3/MOM	P3/MOM	P3/MOM	P3/MOM	P3/PWM	P3/MOM	P3/MOM
12	Masha	GEV/MOM	G2/ML	EV1/ML	EV1/PWM	EV1/PWM	EV1/PWM	EV1/ML	EV1/ML
13	Sawla	P3/PWM	P3/PWM	P3/PWM	P3/MOM	P3/PWM	P3/PWM	P3/PWM	EV1/ML
14	Sekoru	P3/MOM	EV1/ML	G2/ML	G2/ML	G2/MOM	G2/ML	P3/PWM	G2/ML
15	Sodo	EV1/ML	EV1/ML	EV1/ML	EV1/MOM	P3/PWM	P3/PWM	P3/PWM	G2/MOM
16	Gojeb	GEV/MOM	G2/ML	G2/PWM	G2/PWM	EV1/MOM	GEV/PWM	GEV/MOM	GEV/MOM
17	Hosaina	P3/MOM	P3/MOM	P3/MOM	P3/MOM	P3/MOM	G2/PWM	P3/PWM	EV1/ML
18	Woliso	P3/PWM	P3/PWM	G2/MOM	P3/PWM	P3/PWM	LP3/MOM	GEV/MOM	P3/PWM
19	Wushwush	GEV/MOM	GEV/MOM	LP3/MOM	P3/PWM	GEV/PWM	G2/PWM	EV1/PWM	WAK-4

Figure 5.6: Best Fitted Distributions for the indicated durations

table, estimated quantiles of the return period, starting from 2 to 100 years, have been derived for each station. This quantiles are used to derive the IDF curves. Figure 5.7 shows typical quantiles for the Arba Minch station.

Return Period (years)	Estimated Quantiles for the indicated durations of rainfall, mm Arbaminch static							
	0.5hr	1hr	2hr	3hr	5hr	6hr	12hr	24hr
2	24.4	30.9	35.1	37.1	39.7	40.3	42.0	45.1
5	29.2	40.6	45.8	48.6	52.0	52.8	55.5	60.4
10	31.8	47.1	52.9	56.2	60.1	61.0	64.5	70.6
25	34.6	55.3	61.9	65.9	70.3	71.4	75.7	83.4
50	36.4	61.3	68.5	73.0	77.9	79.1	84.1	92.9
100	38.1	67.4	75.1	80.1	85.4	86.8	92.4	102.3

Figure 5.7: Estimated Quantiles for Arba Minch station

5.4.2 Estimation of the IDF Parameters

The general mathematical form of the IDF equation (Eqn.1) has been used to meet each return period quantile estimates of different durations. Parameter estimations of 'A', 'B' and 'C' have been done using minimum standard error of estimate (SEE) criteria. For instance, for Arbaminch station each I_2, I_5, I_{10}, I_{25}, I_{50},, I_{100}, IDF equation can be derived for each duration. This procedure has been applied to all 19 stations and derived IDF equation given.

$I = \frac{A}{(D+B)^C}$ ——————————(1)

Where: I= rainfall intensity (mm/hr)

D= duration of rainfall (minutes)

A= coefficient with units of mm/hr

B= time constant in minutes

C= an exponent usually less than one

The derived parameter of 'A', 'B', and 'C' for all 19 stations and selected durations (2, 5, 10, 25, 50 and 100 hour) have been given in figure 5.8.

In general, the value of the "A" coefficient increases with an increase in return period for most of the stations considered. However, there are some cases where this coefficient decreases with an increase in the return period. This decrease in the "A" coefficient is obtained mainly for larger return periods (50 and 100 years). The "B" constant depends on the relative increase or decrease of the "A" coefficient. For most of the stations with a different frequency, these two parameters increase or decrease with an increase or decrease of the "A" coefficient. Similar to the cases for the "A" coefficient, there are some cases where these parameters decrease for an increase in the "A" coefficient.

After determining the numerical value of the IDF parameters, the rainfall intensity for any duration and recurrence interval can be determined. Based on the estimated parameters of the IDF relationships a general equation of the form shown below (Equ. 2) has been derived for all durations and each station.

$i = exp[(ln(A) - Cln(B+D))]$ ——————————-(2)

The resulting six equations for each station can be used for intensity calculations

in the area represented by that station. Listed below, are the six equations for the IDF relationships for Arbaminch station.

$$2\ \text{Year return period},\ i = \exp[7.53 - 0.95 * \ln(16.33 + D)] \text{---------- (3)}$$
$$5\ \text{Year return period},\ i = \exp[7.9 - 0.96 * \ln(22.96 + D)] \text{---------- (4)}$$
$$10\ \text{Year return period},\ i = \exp[8.06 - 0.96 * \ln(25.8 + D)] \text{---------- (5)}$$
$$25\ \text{Year return period},\ i = \exp[8.39 - 0.98 * \ln(34.27 + D)] \text{--------- (6)}$$
$$50\ \text{year return period},\ i = \exp[8.5 - 0.98 * \ln(36.88 + D)] \text{---------- (7)}$$
$$100\ \text{Year return period},\ i = \exp[8.68 - 0.997 * \ln(42.13 + D)] \text{------- (8)}$$

Similar mathematical equations have been developed for each station located in the Regional State of SNNRP. Such equations can be used to plan and design water and related infrastructures such as bridges, culverts, dams, etc. for locations within 25km radius from each stations.

Station Name	T=2 Years			T=5 Years			T=10 Years			T=25 Years			T=50 Years			T=100 Years		
	A	B	C	A	B	C	A	B	C	A	B	C	A	B	C	A	B	C
Aman	2470.83	20.55	0.95	3117.48	25.79	0.94	3259.40	27.80	0.92	3222.23	29.00	0.90	3092.32	29.03	0.88	3032.42	30.01	0.86
Arbaminch	1862.35	16.33	0.95	2703.13	22.96	0.96	3165.89	25.80	0.96	4388.28	34.27	0.98	4914.46	36.88	0.98	5903.33	42.13	1.00
Areka	1387.59	2.80	0.90	3117.48	4.62	0.90	1927.23	4.62	0.90	1992.46	3.97	0.89	1964.22	2.91	0.87	1988.51	2.58	0.86
Awassa	1238.34	0.10	0.87	3226.63	12.72	0.98	3653.69	13.48	0.98	4174.17	14.35	0.97	4582.97	15.09	0.97	5071.28	16.33	0.97
Billate	1393.18	4.09	0.91	1616.06	2.58	0.89	1856.77	3.20	0.89	2314.50	5.60	0.90	2702.43	7.47	0.92	3114.50	9.24	0.93
Dilla	1540.04	2.76	0.91	2167.66	6.00	0.92	2493.53	7.47	0.92	2807.34	8.70	0.92	2978.77	9.23	0.91	3175.53	10.09	0.91
Gidole	1753.47	9.23	0.92	2253.04	10.65	0.92	2667.47	12.70	0.92	3007.71	13.48	0.92	3361.77	15.03	0.93	3647.97	15.95	0.93
Gore	1722.91	5.37	0.94	2037.28	4.47	0.94	2170.17	3.97	0.93	2154.34	2.09	0.91	2091.12	0.53	0.90	2164.44	0.53	0.89
Jinka	1082.55	1.35	0.86	1175.23	0.99	0.83	1255.04	2.00	0.82	1271.90	2.10	0.80	1288.91	2.53	0.79	1286.48	2.58	0.77
Konso	1357.97	4.47	0.92	1719.28	4.63	0.93	2026.57	5.62	0.94	2500.73	7.47	0.96	2869.26	8.69	0.98	3306.14	10.10	0.99
M/Abaya	960.35	2.58	0.85	1631.72	8.76	0.89	2038.97	11.15	0.91	2527.86	13.42	0.92	2904.89	15.09	0.93	3255.91	16.33	0.93
Masha	1275.01	0.04	0.89	1528.14	2.09	0.86	1921.10	7.47	0.87	2617.62	16.33	0.88	3185.68	23.30	0.89	4045.19	32.27	0.91
Sawla	1987.81	14.47	0.97	2136.07	13.76	0.93	1940.82	11.12	0.89	1656.52	7.47	0.85	1445.53	4.47	0.81	1314.43	2.60	0.79
Sekoru	1615.40	10.09	0.93	2028.28	9.22	0.94	2297.00	8.76	0.94	2676.53	8.71	0.95	2948.03	8.60	0.96	3088.25	7.47	0.96
Sodo	1889.95	12.70	0.92	2428.47	10.95	0.92	2933.14	10.91	0.93	3540.04	10.09	0.94	4113.34	10.09	0.95	4711.54	10.09	0.96
Wushwush	1570.95	0.03	0.91	1969.86	0.53	0.93	2338.01	3.44	0.94	2015.58	0.53	0.91	2088.62	2.58	0.90	1742.19	0.04	0.87
Woliso	3109.40	42.42	1.02	3365.95	32.27	1.02	3605.08	29.00	1.02	3646.82	25.80	1.02	3700.04	23.27	1.02	3603.10	20.56	1.01
Hosana	546.34	0.53	0.77	828.81	0.53	0.82	987.28	0.16	0.83	1173.46	0.04	0.85	1301.85	0.04	0.86	1427.72	0.01	0.87
Gojeb	840.72	34.03	0.82	1768.13	55.42	0.92	2967.40	71.99	0.99	4978.40	88.05	1.06	7986.20	104.67	1.12	11664.43	117.38	1.17

Figure 5.8: Summary of the Estimated IDF parameters

5.4.3 Construction of the IDF Curve

The IDF curves were plotted on a double logarithmic scale, the duration D as abscissa and the intensity I as ordinate, thereby making use of the IDF curve fit tool. Figures 5.9 and 5.10 show the IDF curves plotted on double logarithmic scales and normal scales respectively for the Arbaminch station.

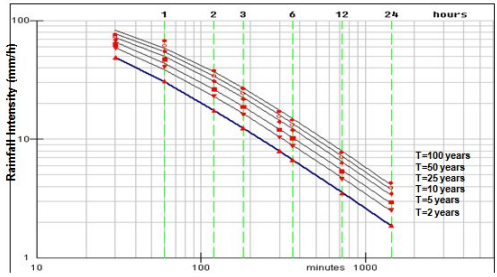

Figure 5.9: IDF curves plotted on double logarithmic scale for Arbaminch Station

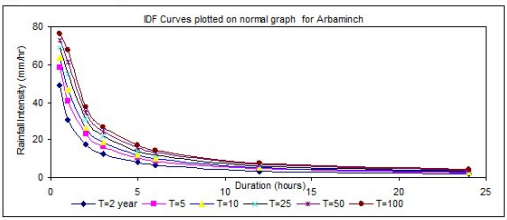

Figure 5.10: IDF curves plotted on a normal scale for Arbaminch station

5.5 Regional IDF Maps

Regionalization refers to the identification of a homogenous region that contains stations having similar climatic characteristics. This can be achieved by using information that is obtained from geographic proximity, physiographic and climatic characteristics. Statistically, a homogenous region is a region which consists of sites having the same standardized frequency distributional form and parameters. Such a region must be geographically continuous and it forms a basic unit for carrying out regional frequency analysis.

In the case of estimating rainfall quantiles, the regional analysis is based on the concept of regional homogeneity. This assumes that annual maximum event populations at several sites in a region are similar in statistical characteristics and are

not dependent on a certain catchment size (Cunnane, 1989).
Regionalization serves two purposes: for sites where data are not available, the analysis is based on regional data (Cunnane, 1989). For sites with available data, the joint use of data measured at a site, called at-site data, and regional data from a number of stations in a region provides sufficient information to enable a probability distribution which then can be used with greater reliability.

5.5.1 Homogenous IDF Regions

Homogenous regions have been developed for the annual maximum rainfall depth of all durations on the basis of L-MRD. It is assumed that (LCs, LCk) values of one station varies linearly with (LCs, LCk) values of the neighboring station. These parameters have been used to delineate homogeneous regions. Two boundaries are fixed, one from the LCs and the other from the LCk values. The final boundary between regions is fixed between the mid ways of the two boundaries.

Two statistical tests have been utilized to test the homogeneity of each region (Hosking et. al., 1991; cited in Rao & Hamed, 2000). The first statistic is a discordance measure, intended to identify those sites that are grossly discordant with the group as a whole.
The second statistic is a heterogeneity measure intended to estimate the degree of heterogeneity in a group of sites and to asses whether they might reasonably be treated as homogenous. Figure 5.11 shows the L-MRD.

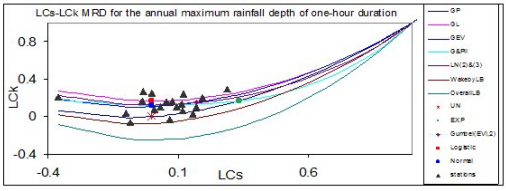

Figure 5.11: L-MRD used to identifying stations of similar nature

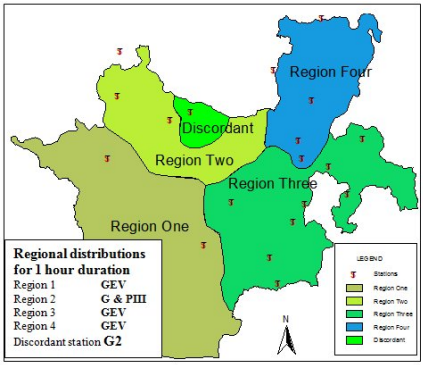

Figure 5.12: Established homogenous regions

5.5.2 Regional Quantiles

The quantiles for the classified regions are estimated based on the selected best fit distribution. The estimated quantiles are then pooled together to calculate the mean of those stations within the region for each return period and each duration. The pooled mean quantiles are used for the estimation of the regional IDF parameters for the specified region. Typical pooled regional quantiles for region one and durations of 30 minutes and one hour are shown in figure 5.13.

Return period in years(T)	Quantiles from regional distribution				Regional quantiles (mean of the stations)	
	Aman station		Jinka station			
	30 minutes	60 minutes	30 minutes	60 minutes	30 minutes	60 minutes
2	29.38	39.11	27.24	32.28	28.31	35.70
5	36.84	47.08	33.63	40.37	35.24	43.73
10	40.85	50.70	37.06	45.00	38.96	47.85
25	45.04	53.98	40.66	50.12	42.85	52.05
50	47.64	55.73	42.88	53.46	45.26	54.60
100	49.84	57.04	44.77	56.43	47.31	56.74

Figure 5.13: Station and regional quantiles for 30 and 60 minutes of region one

The IDF parameters for each classified regions have been derived from pooled quantiles for each regions and parameters derived on the basis of a minimum

SEE. The estimated regional IDF parameters are shown in figure 5.14.

Region	Parameters	Estimated parameters for the indicated frequency					
		T=2	T=5	T=10	T=25	T=50	T=100
	A	1885.08	2029.85	1877.43	1628.18	1394.11	1781.66
	B	14.25	12.81	10.10	6.62	3.20	7.47
	C	0.92	0.89	0.86	0.82	0.78	0.81
Region one	SEE	0.61	0.75	0.85	1.06	1.25	1.07
	A	1483.25	1777.78	2211.10	2811.00	3464.46	4262.60
	B	0.01	0.99	5.35	11.15	16.94	23.27
	C	0.91	0.90	0.91	0.93	0.95	0.96
Region two	SEE	2.24	1.61	1.10	0.59	0.52	0.72
	A	1551.18	2182.20	2537.83	2992.38	3315.94	3576.87
	B	7.47	10.10	11.15	12.67	13.76	14.45
	C	0.92	0.93	0.93	0.94	0.94	0.94
Region three	SEE	0.22	0.37	0.51	0.75	0.97	1.20
	A	1403.61	1852.58	2098.90	2471.82	2741.05	2791.64
	B	10.80	10.09	9.24	9.21	9.23	7.47
	C	0.90	0.91	0.92	0.93	0.93	0.93
Region four	SEE	0.55	0.71	0.91	1.25	1.58	1.95
	A	840.72	1768.13	2967.40	4978.40	7986.20	11664.43
	B	34.03	55.42	71.99	88.05	104.67	117.38
	C	0.82	0.92	0.99	1.06	1.12	1.17
Station Gojeb	SE	5.35	5.02	4.65	4.23	4.01	3.91

Figure 5.14: Estimated regional IDF parameters with the SEE

5.5.3 Validation of the Regional IDF Parameters

In order to verify whether the estimated parameters are adequately representing the classified regions, the intensity of rainfall obtained from the estimated parameters of the stations within the region is compared with the intensity values obtained from the estimated regional parameters. The R^2 value for all stations within the region obtained from graphs of the two intensity values it can be concluded that the regional parameters significantly represent the station parameters. Figure 5.15 indicates the graph of regional and at-station intensity values for region one.

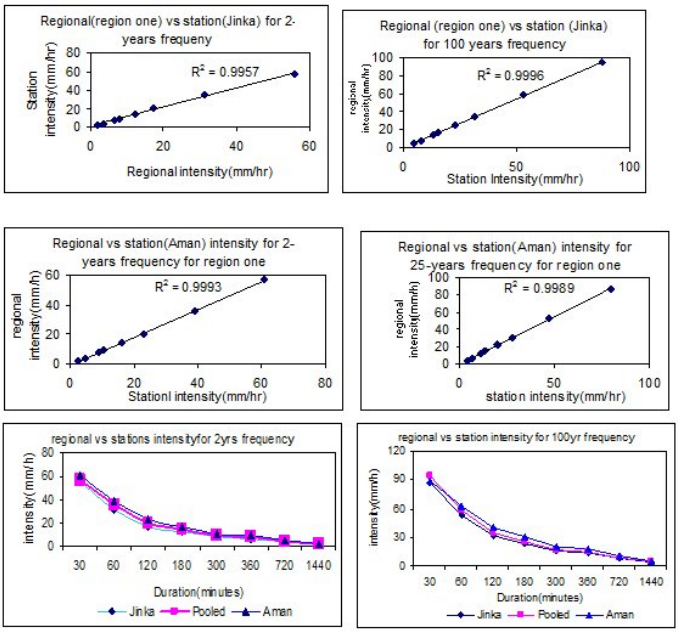

Figure 5.15: Evaluation of estimated regional IDF parameters for region one

5.5.4 Regional IDF Curves for Un-Gauged Catchments in SNNRP

IDF curves are constructed for the classified regions based on the regional intensity on a double logarithmic scale using the IDF curve fit tool as shown in figure 5.16. These curves can be used for intensity determinations for un-gauged areas within these regions except for the limitations described in the previous sections.

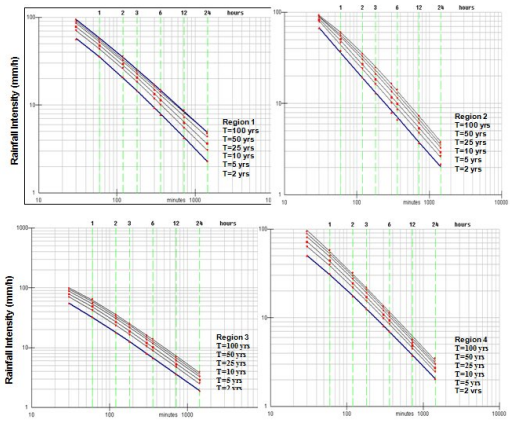

Figure 5.16: Derived Regional IDF curves in order to use in un-gauged catchments

5.6 Conclusion

Three different approaches have been implemented to derive rainfall intensity-Duration-Frequency relationships in the SNNRP State. The first method is the general IDF mathematical form that relates the intensity, duration and frequency of rainfall analytically. The second relationship is the IDF curve plotted on a double logarithmic scale with intensity as an abscissa and duration as ordinate. The third method is the IDF map and regional curve applicable for un-gauged areas of the regional state.

The mathematical form of the IDF is developed in the form of $I = A/(B+D)^C$ for each station in the region based on the estimated optimum IDF parameters. In general, the value of "A" coefficient increases with an increase in return period for most of the stations considered. However, there are some cases where this coefficient decreases with an increase in the return period. The "B" constant and the "C" exponent depend on the relative increase or decrease of the "A" coefficient. For most of the return periods these two parameters increase with an increase of "A" coefficient and vice versa.

The best-fit IDF curves are developed based on the optimum parameters for each station by making use of the IDF curve fit tool in which all the curves show a similar shape. An exception for the shape of these curves is for the case of the Gojeb station in which an elliptic shape is obtained. The reason for this deviation might be the short record length of the annual maximum rainfall used for this station.

At-station IDF curves and mathematical expressions can be used to estimate the rainfall intensity of a given return period and duration for areas within 25 km radius from the principal stations (as per WMO Guidelines). In order to extract the intensity of rainfall of any duration and frequency at areas farthest from the principal stations, the Regional IDF curve or maps can be used to derive such rainfall intensity quantities. Therefore, planners and designers in the country as well as in the Regional State can effectively utilize one or all of the procedures to derive the IDF value in any part of the region for planning and designing purpose. We also recommend that the projects operating in the State may revisit their planning and design guidelines on the basis of the new findings.

5.7 References

Cunnane, C. (1989) Statistical Distributions for Flood Frequency Analysis.

Dupont, B.S & Allen, D.L. (2000) Revision of the Rainfall Intensity Curves for the Common Wealth of Kentucky. Research Report. Kentucky.

Maidment, D.R., (1993) Hand Book of Hydrology, McGRAW-Hill. Inc. USA

Rao, K.H, & Hamed, A.R. (2000) Flood Frequency Analysis. CRC press LLC, Florida

Sine, A. (2004) Regional Flood Frequency Analysis for Blue Nile River Basin, Ethiopia, Msc Thesis. Arbaminch University, Arbaminch, Ethiopia.

www.Alanasmith.Com. (1996) IDF Curve fit Software version 2.07. Alan A. Smith Inc. Software Development Company. Canada.

www.ethiopar.net.(2002) The Federal Democratic Republic of Ethiopia, Basic Information. Southern Nations and Nationalities.htm

6 Regional Low Flow-Duration -Frequency (QDF) Analysis of Upstream Lake Victoria, Tanzania - Tadesse Taye Meskele, Patrick Willems

Tadesse Taye Meskele, *Patrick Willems*[1] [2]

[1] Arba Minch University
School of Graduate Studies
P.O.Box 21
Arba Minch, Ethiopia.
E-mail: tadesse_taye@yahoo.com
2 Katholieke Universiteit Leuven
Hydraulic Section
Kasteelpark Arenberg 40, BE-3001
[2] Katholieke Universiteit Leuven
Hydraulic Section
Kasteelpark Arenberg 40, BE-3001
Leuven,Belgium.
E-mail: Patrick.Willems@bwk.kuleuven.be

6.1 Abstract

This study aims at constructing regional low flow frequency curves for the upstream Lake Victoria basin, Tanzania. This is done based on at-site calibrations of low flow frequency distributions and low flow QDF relationships for some of the stations along the basin. The low flow data for six stations are considered and analysed for their distribution using the Q-Q plots method developed by Willems. The analysis of the results reveals that all of the stations show an exponential distribution. Furthermore, low flow-duration-frequency (QDF) curves are developed at these stations and model fitting is performed separately for each station. These curves relate to the low flow values as an integral function of return period and flow duration.

QDF models are often applied in regional studies, leading to regional QDF relations derived for hydrologically homogenous regions. This paper is the first experimental work on the attempt to regionalise a QDF plot for the upper Lake Victoria basin. The regional QDF plots developed can be used to estimate the availability of water during specific time intervals (aggregation periods) and for different return periods within this homogenous region.

6.2 Introduction

As a result of population growth, economic development and adverse effects of land use and climate change the pressure on water resources is constantly increasing. The impact on freshwater systems is most severe during periods of low groundwater and low stream flow, resulting in significant and widespread economic and environmental damage during extreme droughts. Thus, to design and manage water resource schemes, it is essential to estimate the spatial and temporal variability of droughts in order to mitigate the impact on surface and groundwater resources.
A drought is a natural disaster which develops very slowly without being noticed and which can be generally defined as a natural event resulting from an extreme decrease in precipitation during an extended period of time (Smakhtin, 2000). However, the focus of this paper is limited to hydrological drought characterised by a decrease in stream flow, which will result in low flows. The low flow charac-

teristics of a stream are a measure for the adequacy of the stream flow to provide requirements to municipal or industrial supplies, for supplemental irrigation, disposal of liquid wastes, and maintenance of suitable conditions for fish. Some of these low-flow characteristics are also useful as parameters in regional draft-storage studies, as the basis for forecasting seasonal low flows and as indicators of the amount of groundwater flow into the stream (Riggs, 1972).

During a period of hydrological drought, as flows decrease, the proportion of river flow arising from surface runoff becomes negligible. In the absence of rainfall, the magnitude of the base flow component also continues to decrease and minimum river flows occur when a prolonged dry period occurs. The analysis of these continuous low flows and their frequency of occurrence is one of the concerns in low flow hydrology (Smakhtin, 2000). Moreover, establishing the relation between low flow discharge, flow duration and frequency of occurrence in an integrated way enables to demonstrate the probabilistic picture of the low flow regime of a river in both flow and time dimensions.
In most cases the locations for which low flow estimates are required do not have stream flow data which could be directly used since it is impractical to gauge all the river reaches. Thus, regional low flow analyses have to be employed to provide estimates of low flow where no gauge exists. That is to say regional low flow frequency analyses are essential for low flow estimation on ungauged rivers.

6.3 Study Objectives

The main objective of this study is to analyse the low flow hydrology within the basin and to establish a relationship between the low flows, duration and their return period. This compasses the generation of the independent low flows at the gauging station and, later on, low flow frequency analyses to evaluate the ability of a stream to meet specified flow requirements at a particular location. Subsequently, fitting of the parameters with the calibrated distribution is performed to establish the low flow-duration-frequency (QDF) relation which is the basis for regionalisation to estimate the flows at ungauged sites.
This is done for a number of gauging stations having adequate observed stream records in the basin, with the main goals of developing low flow QDF curves to represent a probabilistic picture of the low flow regime of a river in both flow and

time dimensions, and to describe the relationship between the low flow Q, the time scale D and the return period or probabilistic frequency F.

Unlike the gauged catchments where there are adequate observed stream flow records, ungauged catchments pose a different problem. Thus, a regionalisation approach is used for the construction of regional curves for low flow frequency estimation, which enables the prediction of the low flows at ungauged sites.

6.4 Materials and Methods

6.4.1 Data Consideration

The hydrological data available for this study are discharge data recorded at six different gauging stations within the basin. The source of these data is the FRIEND Nile project. The selection of the stations is based on the time resolution of the available data. The daily time resolution is the most favourable as it contains more detailed information about the discharge of the stream and the low flow events. Figure 6.1 shows the description of the selected hydrodynamic stations within the basin.

No.	ID	Name	Country	Period of record	No. years	Area (km^2)	MAR (mm)
1	115022	Kagera at Kyaka Ferry	Tanzania	1971-1977	7	58370	1018
2	115182	Ngono at Kyaka/ Bukoba Road	Tanzania	1978-1989	12	2608	993
3	115172	Ruvumo at Mwendo Rerry	Tanzania	1970-1977	8	10970	962
4	115162	Kagera at Rusumo Falls	Tanzania	1971-1978	8	30200	1582
5	115152	Kagera at Nyakanyasi	Tanzania	1970-1978	9	48228	1873
6	115192	Ngono at Kalebe Bridge	Tanzania	1970-1978	9	1185	1035

Figure 6.1: Selected hydrometric stations of upstream Lake Victoria, Tanzania, for low flow analysis

6.4.2 At-Site Low Flow Analysis - Independent Low Flows Extraction

With regard to the analysis of the low flows, the first step is the extraction of the low flows from the time series. The independence of the low flows is an important condition underlying the extreme value theory. The WETSPRO tool developed by Willems (2004a), which uses the peaks-over threshold (POT) technique, can be used to select independent low flows while ascertaining high degrees of independency. The tool contains a series of Microsoft Excel macros for analysing extreme flow data (Willems, 2004a). This VBA code uses a procedure based on the 'recession constant' of subflow to ascertain independency between the successive low flows. The method independent of the subflows uses the recession constant of the overland flow. The recession constant can be defined as a time at which a flow component reaches a value lower than 37% of its peak after an exponential decrease in time during dry weather periods. This method considers two successive peaks as independent when the time p between these two peaks is longer than the recession constant k, and when the minimum discharge between these two peaks is smaller than a fraction f of the peak discharge (e.g. smaller than 37%). In addition, a criteria $q_{max} > q_{lim}$ is used to avoid the selection of small peaks.
The method based on the recession constant of the base flow can also be used for POT selection. According to this method, independency is reached when the smallest discharge between the two peaks reaches almost the base flow value.

6.4.3 Extreme Value Analysis

For a given stream having a discharge data record for a certain number of years, the same or larger number of low flows is possible. These low flows are the basis for determining the probability of occurrence of low flows of various magnitudes. This is done by arranging the low flows in descending order and assigning the cumulative probability to each value which will constitute the theoretical probability distribution for the low flows.
An empirical approach to determine the form of the theoretical probability distribution of low flows consists in fitting a number of theoretical distributions to observed data and deciding, by means of suitable criteria, which distribution fits the data best (use goodness-of-fit tests). This method is a subjective one and not

always conclusive. The choice of distribution is narrowed down by selecting one of the three distribution families of the generalised extreme value distribution or the generalised Pareto distribution.
The most efficient way to analyse the type of distribution is by means of the so-called 'quantile-quantile plots (Q-Q) plots') (Willems, 1998a, b; Willems 2000). In Q-Q plots the empirical quantiles are plotted versus the theoretical quantiles. The empirical quantiles match the observed extremes x_i , $i=1$,., m ($x_1 \leq .. \leq x_m$), with $p_i=i/(m+1)$ as their corresponding empirical probabilities of exceedance, while the theoretical quantile is defined as $F^{-1}(1-p_i)$. The function $F(x)$ is the cumulative distribution that will be tested in the Q-Q plot (exponential Q-Q plot, Pareto Q-Q plot). For instance, the distribution and inverse distribution for exponential Q-Q plots are as follows:

$$F(x) = 1 - \exp(-\frac{x - x_m}{\beta}) \quad [1]$$

$$F^{-1}(1-p) = x_m - \beta \ln(p) \quad [2]$$

The hydrological extreme value analysis tool (ECQ) developed by Willems (2004b) at the Hydraulics Laboratory of K. U. Leuven, simplifies the fitting of the extremes in a visual way without the knowledge of the parameter values through adopted Q-Q plots. As Willems (2000) explains, the so-called quantile function U(p) is plotted instead of the inverse distribution $F^{-1}(1-p)$. The function U(p) is defined as the most simple function of p that is linearly dependent on $F^{-1}(1-p)$ and independent of the parameter values of F(x). The quantile plots (exponential, Pareto) are plotted with U(p) or ln(U(p)) on the horizontal axis and x or ln(x) on the vertical axis. The exact expressions for each quantile are given in the following:

$$\text{Exponential quantile plot: } (-\ln(\frac{i}{m+1}); x_i)$$

$$\text{Pareto quantile plot: } (-\ln(\frac{i}{m+1}); \ln(x_i))$$

Thus, these adopted Q-Q plots are used to set the fitting of the tail's empirical distributions by determining where the observation distributions appear more or

less linear. In other words, if the observations agree with the considered distribution, the points in Q-Q plots approach linearity. The minimum threshold values can also be determined from the slope Q-Q plots where the mean square error is at a minimum. This is a statistically optimal way of minimising the mean squared error of the regression so that the distribution above it is maximised. This method is applicable only for high flow extreme value analyses. Thus, a transformation 1/Q of the low flows is a must in order to use this method.

6.4.4 Low Flow-Duration-Frequency (QDF) Relationship

Once the parameters of the extreme value distribution are determined for a range of aggregation levels created by moving average, the uncertainty due to limited length of available time series and POT values in the calibration of the extreme value distributions for individual distributions can be reduced by fitting relationships between the parameters of the extreme value distribution and the aggregation level. The plot of these parameters versus the aggregation level indeed needs to be aligned to have a balanced mathematical relationship. When the balanced relationships for the parameters of the distribution are used to calculate the QDF relationships, calibrated QDF relationships will be derived. The equations used for the calibrated QDF relationships for the low flow Q, the aggregated duration D and the return period T are:

for $\gamma=0$, based on linear regression in the exponential Q-Q plot

$$x = \hat{x}_t(D) + \hat{\beta}(D)(\ln(T) - \ln(\frac{n}{\hat{t}(D)})) \quad [3]$$

for $\gamma>0$, based on linear regression in the Pareto Q-Q plot

$$\ln(x) = \ln(\hat{x}_t(D)) + \hat{\gamma}(D)(\ln(T) - \ln(\frac{n}{\hat{t}(D)})) \quad [4]$$

6.4.5 Results of Extreme Value Analysis and QDF Plot

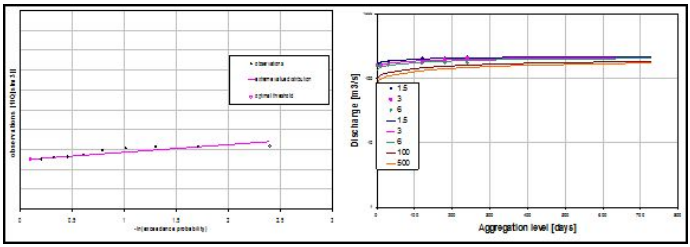

Figure 6.2: Exponential Q-Q plot showing normal tail for 1/Q and QDF plot at Kyaka Ferry

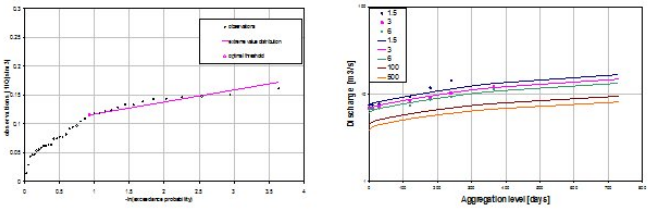

Figure 6.3: Exponential Q-Q plot showing normal tail for 1/Q and QDF plot at Kyaka/Bukoba Road

6.4.6 Regionalisation of QDF

In the Nile basin, marked hydrological differences are apparent among its sub-basins. As a result, single station low flow analyses are best applied to locations on the same stream. However, low flow characteristics are not available for all sub-basins of the Nile basin due to the absence of a gauging station or the poor quality of collected stream flow data. Therefore, regional relationships are developed to estimate low flow at sub-basins within homogenous low flow zones

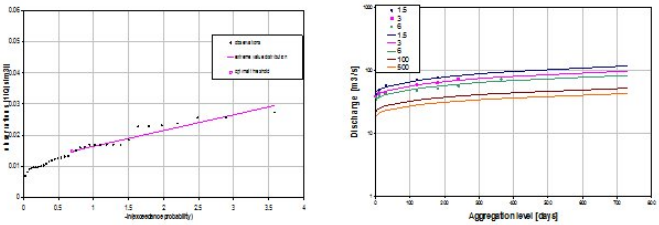

Figure 6.4: Exponential Q-Q plot showing normal tail for 1/Q and QDF plot at Mwendo Rerry

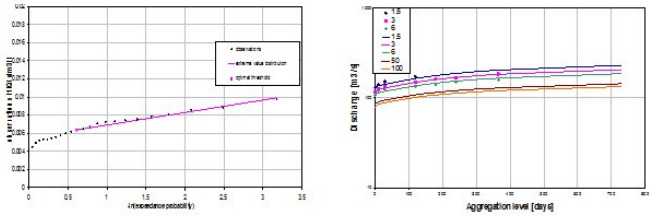

Figure 6.5: Exponential Q-Q plot showing normal tail for 1/Q and QDF plot at Rusumo Falls

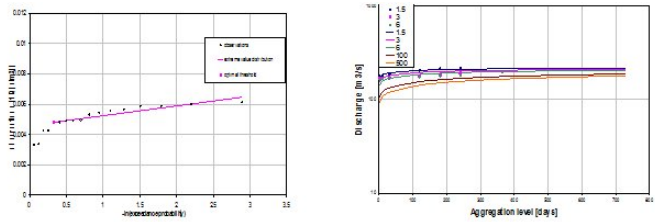

Figure 6.6: Exponential Q-Q plot showing normal tail for 1/Q and QDF plot at Nyakanyasi

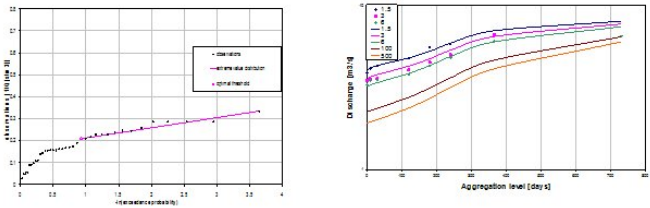

Figure 6.7: Exponential Q-Q plot showing normal tail for 1/Q and QDF plot at Kalebe Bridge

having similar catchment characteristics.

After an at-site analysis of the low flows and developing the QDF plots, the next step in the regionalisation of the QDF is to standardise the QDF plots at a site within this homogenous region by dividing discharges, with a product of discharge area (A) and mean annual rainfall (MAR) in this case, to convert the QDF plots to a similar scale. This technique relies on the basic assumption that the discharge is proportional to the product of the discharge area (A) and the mean annual rainfall (MAR). Thus, linear models are developed using regression analysis to investigate the proportionality. The regression analysis method is used to establish the relationship between the low flow, the product of area and the mean annual rainfall on a logarithmic scale. In the linear regression model, low flows (Q), drainage area (A) and mean annual rainfall (MAR) are included according to the following equation:

$$Log(Q) = a + blog(A * MAR)$$

The standardised curves in this homogenous region are then plotted together and a regional curve is fitted through the middle of the curves after choosing the representative curve from one of the curves and dividing by some factor which is dependent on the catchment area and the spatial variation in annual rainfall volumes. This means that all parts of the homogenous region contribute the same amount of discharge per AR. Thus, the low flows for ungauged sites can be easily determined by multiplying back the ordinates of the regional curve by the prod-

uct of catchment area and mean annual rainfall at that site.
Standardised and regional QDF plot results for the Tanzanian region of the upstream Lake Victoria are shown in figure 6.8 and 6.9. The linear models that show proportionality after a log transformation are presented in figure 6.10.

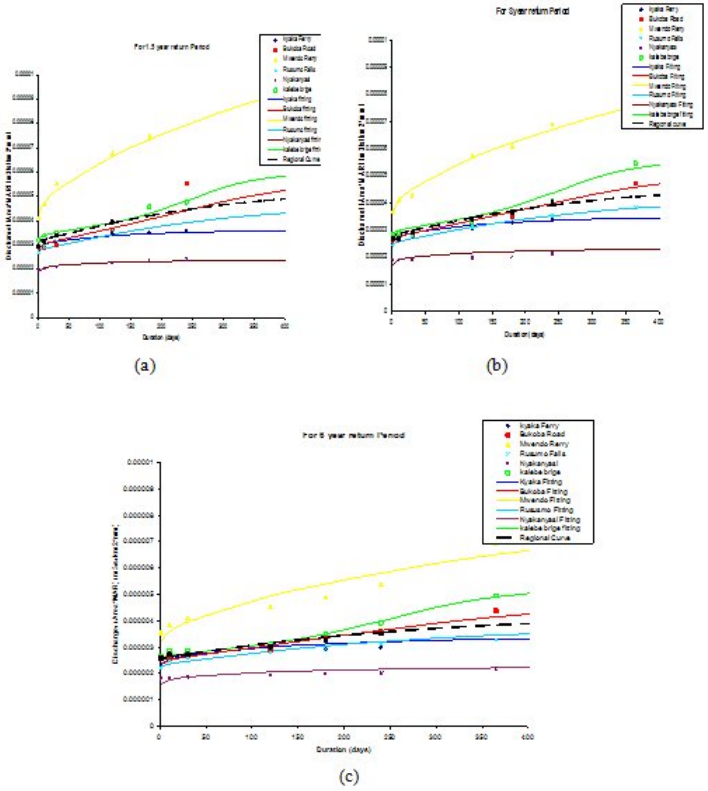

Figure 6.8: Standardised QDF plot for the stations at upstream Lake Victoria, Tanzania, for 1.5-year (a), 3-year (b) and 6-year (c) return periods

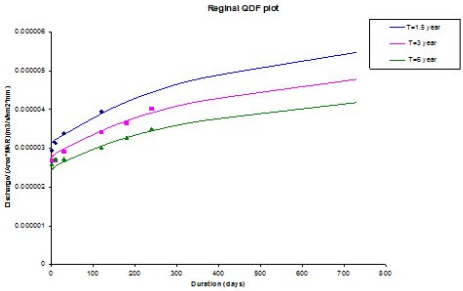

Figure 6.9: Regional QDF plot for upstream Lake Victoria, Tanzania

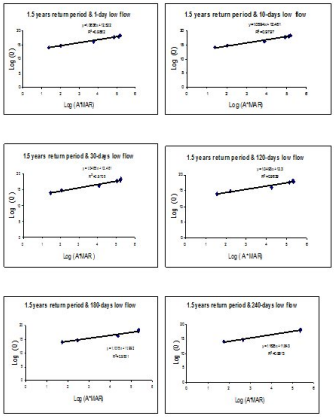

Figure 6.10: Linear regression models (Log (Low flows(Q)(m^3/s)) versus Log (drainage area (A) (km^2) mean annual rainfall(MAR)(mm)) for 1.5-years return period for 1, 10, 30,120,180 and 240-days low flow at upstream Lake Victoria, Tanzania

6.5 Discussion and Conclusion

For the purpose of estimating the probabilities of occurrence for low flows and for making tests of significance of such estimates, it is necessary to determine the

underlying probability distribution of the data. The low flow data for six stations in the upper Lake Victoria, Tanzania, were considered and analysed for their distribution using the Q-Q plots method developed by Willems. The analysis of the results revealed that all stations showed an exponential distribution. The knowledge of the probability distribution of minimum stream flow at these stations is useful for the water resources manager in the area.
Furthermore, low flow-duration-frequency (QDF) curves were developed at these stations and model fitting was performed separately for each station. The curves related to the low flow values as an integral function of return period and flow duration.

QDF models are often applied in regional studies, leading to regional QDF relations derived for hydrologically homogenous regions. This paper is the first experimental work on the attempt to regionalise a QDF plot for the upper Lake Victoria basin. The regional QDF plots developed can be used to estimate the availability of water during specific time intervals (aggregation periods) and for different return periods within this homogenous region.
In a regional QDF analysis it is assumed that the QDF from all gauged sites in a region can be combined in such a way as to produce a single regional QDF curve. This curve is applicable, after appropriate rescaling by some factor depending on the catchment area and the spatial variation in annual rainfall volumes, anywhere in that region.

The regional QDF can be used for different water use applications such as the design of water supply systems, the estimation of safe surface water withdrawals, and the classification of the potential of streams for waste dilution (assimilative capacity). It can be used to indicate the water shortages if the threshold level below which the water runs out is known for that typical use of water application.

6.6 Recommendation

This study was performed for some of the stations within the upper Lake Victoria basin. More research needs to be carried out in this field of regional low flow frequency analysis in order to be further extended to other stations and to develop regional QDF plots covering the entire units of hydrologically homogenous re-

gions in the Nile basin.
Another important research aspect to be considered in future consists in the analysis of the stationary series in the extreme value series, and in the investigation of cycles and trends. Current investigation indeed assumed that the series can be considered stationary. This assumption was not objected after visual check of the extreme value series but in fact requires a more detailed investigation on statistical trend tests.

The results obtained from this study are based on the data available for the analysis. The distribution of the stations used in the analysis varied from one region to another. In some regions only few stations were available for the analysis while for other regions a considerable number of stations were available. The reliability of the results obtained for the different regions are expected to vary depending on the amount of data included in the analysis. In this regard the results presented in this study need to be improved in the future when additional data are available.

6.7 Acknowledgments

This paper is part of a research work by Tadesse Taye under the supervision of Prof. P. Willems for the partial fulfilment of Master studies in Water Resources Engineering at the Katholieke Universiteit Leuven. The work was undertaken as part of the Drought and Low Flow Analysis within the FRIEND/Nile project sponsored by the Flemish government and UNESCO. The authors are greatly indebted to the FRIEND/Nile project organisers of Cairo Office UNESCO for their sincere help and support.

6.8 References

Abdo G., Sonbal M., & Willems P, 2005. Flood Frequency Analysis of the Eastern Nile Rivers. FRIEND Nile Conference paper, Sharm El-Sheikh, Nov. 2005.

Eyasu Y. H., 2005. Development and Management of Irrigated Lands in Tigray, Ethiopia. Ph.D Dissertation. Wageningen University, Netherlands.

Fleig A., 2004. Hydrological Drought - A comparative study using daily discharge series from around the world. Master thesis, Institut für Hydrologie.

Gustard A., Bullock A. and Dixon J. M. Low flow estimation in the United Kingdom. Institute of Hydrology, Report No. 108.

Gustard A.and Gwyneth A. C., 2002. FRIEND - a global perspective 1998-2002. FRIEND REPORT 2002. Centre for Ecology and Hydrology, Wallingford, UK.

Hassan A. Fahmi and Willems P., 2005. Analysis of the return periods of Low Flow hazards in Egypt and Sudan. FRIEND Nile Conference paper, Sharm El-Sheikh, Nov. 2005.

Hayes Donald C., 1991. Low-Flow Characteristics of Streams in Virginia. United States Geological Survey Water-Supply Paper 2374.

Hortness J. E., 2006. Estimating Low-Flow Frequency Statistics for Unregulated Streams in Idaho. Scientific Investigations Report 2006-5035Prepared. U.S. Geological Survey, Reston, Virginia.

Howe Y. Lim & Melvin L. Lye, 2003. Regional Flood Estimation For Ungauged Basins in Sarawak, Malaysia. Hydrological Sciences-Journal-des Sciences Hydrologiques, 8(1): 79- 94.

Juraj M. Cunderlika and Taha B.M.J. Ouardab, 2006. Regional flood-duration-frequency modeling in the changing environment. Journal of Hydrology 318 (2006) 276-291.

Kabubi J., Mutua F., Willems P., Mngondo R., 2005. Low Flow Frequency Analysis Based on Runoff Subflow Filtering and Independent Low Flow Periods Selection for the Lake Victoria Basin. FRIEND Nile Conference paper, Sharm El-Sheikh, Nov. 2005.

Karyabwite D.R, 2000. Water Sharing in the Nile River valley. Project GNV011. UNEP/DEWA/GRID-Geneva.

Kroll, C.N., & Vogel, R.M., 2002. Probability Distribution of Low Stream flow Series in the United States. Journal of Hydrologic Engineering,Vol. 7,No. 2:137-146.

Marco, Juan B., Flow regionalization a stochastic flow model for QDF analysis. Universidad Politecnica de Valencia - Departamento de Ingenieria Hidraulica y Medio Ambiente - APDO. 22012 - 46071 Valencia - Spain.

Matalas N.C., 1963. Probability distribution of Low lows. Professional paper 434-A. U.S. Geological Survey. Washington, D.C.

Maxine D. Z., Virginie K., Andrew R. Y., Daniel C., 2003. Flow-duration-frequency behaviour of British rivers based on annual minima data. Journal of Hydrology 277 (2003) 195-213.

Mirghani M., Willems P., Kabubi J., 2005. QDF Relationships for Low Flow Return Period Prediction. FRIEND Nile Conference paper, Sharm El-Sheikh, Nov. 2005.

Mkhandi S. and Kachroo R. Regional flood frequency analysis for Southern Africa.South Africa FRIEND: IHP IV Technical documents in Hydrology No.15: 130-150.

Murakami M., 1995. Managing Water for Peace in the Middle East: Alternative Strategies. The United Nations University , Tokyo, Japan.

Nicol A., The Nile: Moving Beyond Cooperation. UNESCO/ IHP/WWAP.IHP-VI/Technical Documents in Hydrology/PC?CP Series/No. 16.

Paul N. Ogiramoi, 2005. Delineation of flood homogeneous regions based on hierarchical method and regional growth curve mapping for the river Nile basin. Matser thesis,K.U Leuven University,Belgium.

Ramachandra A. Roa & Khaled H. Hamed, 2000. Flood Frequency analysis.CRC Press LLC, Florida.

Riggs H. C, 1972. Low-Flow Investigations. USGS publication book 4: Hydrologic Analysis and Interpretation. U.S. Geological Survey. Washington, D.C. I.

Smakhtin V.U., 2001. Low flow hydrology: a review. Journal of Hydrology 240 (2001) 147-186.

Thomas T, R K Jaiswal, R Galkate, 2004. Forecasting and Frequency Analysis of Low Flow for Beas at Pandoh - a Case Study. IE (I) Journal-CV, Vol 84: 297-302.

Vogel, R.M., & Kroll, C.N., 1989. Low-Flow Frequency Analysis Using Probability-Plot Correlation Coefficients. Journal of Water Resources Planning and Management, Vol. 115, No.3: 338-357.

Vogel, R.M., & Kroll, C.N., 1990. Generalized Low -Flow Frequency Relationship for ungaged sites in Massachusetts. Water Resources Bulletin vol. 26, No.2: 241- 253.

Willems P., 2000. Compound intensity/duration/frequency-relationships of extreme precipitation for two seasons and two storm types. Journal of Hydrology 233 (2000) 189-205.

Willems P., 2004. ECQ: Hydrological extreme value analysis tool reference manual. K.U.Leuven University.

Willems P., 2004. Extreme value analysis. Statistics for water Engineering .IUPWARE Lecture Note. K.U.Leuven University.

Willems P., 2004. IUPWARE course text, separate document "QDF formula" Note. K.U.Leuven University.

Willems P., 2004. WETSPRO: Water Engineering Time Series PROcessing tool reference manual. K.U.Leuven University

Willems P., 2004-2005. Statistics for water Engineering. IUPWARE Lecture notes. K.U Leuven University, Belgium.

Yue S. & Pilon P., 2005. Probability distribution type of Canadian annual minimum stream flow. Journal-des Sciences Hydrologiques, 50(3): 427-438.

7 Phytoplankton Biomass in Relation to Water Quality in the Lakes Abaya and Chamo, Ethiopia - Eyasu Shumbulo, Fikre Assefa

Eyasu Shumbulo, *Fikre Assefa*[1]

[1] Arba Minch University
P.O.B. 21.

7.1 Abstract

This report presents results of algal biomass and physicochemical parameters analysed during the last six months, which is part of the year-round project. The report reveals that the algal biomass of the two study lakes is related to nutrient availability and water transparency. The limiting nutrient was found to be NO_3-N. NO_3-N was varied from 0.18 to 1.00mgl^{-1} and from 0.15 to 1.10 mgl^{-1}, whereas the algal biomass varied from 0 to 10.2 mgChlm^{-3} and from 86 to 101 mgChlm^{-3} for the Lakes Abaya and Chamo, respectively. The average lake water transparency was 14.5cm for Lake Abaya and 27.8cm for Lake Chamo. This shows that, for Lake Abaya, the low water transparency is attributable to a low algal biomass. The project is running until the end of 2006 and more information is expected by then.

7.2 Introduction

The water quality of a water body affects the abundance, biomass, species composition, productivity and physiological condition of aquatic organisms. Therefore, a good quality of water is required if species are to flourish in an ecosystem. Three methods are in use for the assessment of water quality: physical, chemical and biological measures.
Biological methods have comparative advantages over the two other measures, not least because of their low costs and the ease with which they are conducted. According to APHA et al. (1999), the common biological methods used for assessing water quality include among others the collection, counting and identification of aquatic organisms; biomass measurement; and metabolic rate measurement. The information gathered may help to identify the nature, extent and biological effects of pollution, to document the short- and long-term variability of water quality and to correlate the biological mass or composition with water chemistry or condition.

In this study, algal biomass is used as a reference parameter. Most algae, particularly planktonic algae, have long been used as an indicator of water quality. Thus, the objective of the present study was to investigate the temporal variations in the biomass of phytoplankton in relation to some physicochemical variables in

the Lakes Abaya and Chamo and to predict their relation to aquatic productivity.

7.3 The Study Area

The two study lakes, Lake Abaya and Lake Chamo, are the most southern lakes found around Arba Minch town. The region around these lakes is characterised by a moist sub-humid climate with an annual rainfall of about 900mm (Tekle-Giorgis, 2002). The region experiences alternating dry and wet seasons, with the dry period between November and February and peak rainfalls occurring during April and May and again during October and November.
Lake Abaya (figure 7.1) is located between 6°02' to 6°35'N latitude and 37°40' to 37°5'E longitude in Southern Ethiopia, east of Arba Minch town. The lake has a surface area of 1.160 km^2, which means that Lake Abaya is the second largest lake (next to Lake Tana) in Ethiopia.

Figure 7.1: Map of the Lakes Chamo and Abaya

Lake Abaya is the largest of the Ethiopian rift valley lakes, with a maximum depth of 13m and a length of 60km at an elevation of 1169m a.s.l. Lake Abaya receives inflow from a number of large rivers (such as River Bilate) and it overflows to Lake Chamo during the high water periods.

Lake Chamo (figure 7.1) is a tectonic lake and the southernmost lake of the Ethiopian Rift Valley (5°45' N latitude and 37°30' E longitude). It is fed by a perennial river, Kulfo, that enters Lake Chamo from the north, and by a number

of small but non-perennial rivers including the Rivers Sile and Sego. The lake is characterised by a gently sloping shoreline covered by extensive emergent and submergent vegetation.

7.4 Materials and Methods

Surface water samples were regularly collected from the two lakes and occasionally from the feeder rivers. In-situ measurements were performed for some parameters: Lake water transparency was estimated using the Secchi disk. Surface water temperature and pH were measured with a portable digital pH meter. Alkalinity was determined by titration with standard HCl. Electrical conductivity was determined in lab. with a conductivity meter. Phytoplankton biomass was estimated as Chlorophyll concentration based on the monochromatic method (Lorenz, 1967, as outlined in Wetzel & Likens, 2000).
Various chemical parameters were analysed by using the Hack spectrophotometer 2000. Samples filtered through glass fibre filters (GF/C) were used for the analyses of chemical parameters except alkalinity, total phosphate and total solids.

7.5 Results and Discussion

7.5.1 Physicochemical features

Some physical characteristics of the two study lakes and the feeder rivers measured over the study period are given in figure 7.2. The mean surface water temperature is 32.8°C for Lake Abaya and 29.5°C for Lake Chamo. Lake transparency is very low for Lake Abaya (14.5cm), owing to its high turbidity that might be due to turbid feeder rivers. In the case of Lake Chamo, lake transparency has a relatively higher value (mean=28cm).

Figure 7.2 also presents the aggregate chemical features of the lakes measured over the study period. The Total Solids (TS) value varies from 751 to 850mg/L and from 1298 to 1429mg/L for the Lakes Abaya and Chamo, respectively. The high TS value for Lake Chamo may stem from plankton materials. Electrical conductivity (K_{25}) varies from 958 to 1200μS cm^{-1} and from 1876 to 1976μS cm^{-1} for the Lakes Abaya and Chamo, respectively, with higher values for Lake

Chamo. Total alkalinity (in mgl^{-1}) is also relatively higher for Lake Chamo, which is close to earlier studies (e.g. Kebede et al., 1994; Gebre-Mariam et al., 2002) with respect to Lake Chamo.

Sampling date	Station	Water T.	Z_{SD} (cm)	pH	Total alkalinity ($mg\ l^{-1}$)	K_{25} ($\mu S\ cm^{-1}$)	TS ($mg\ l^{-1}$)	Turbidity (NTU)
29-3-05	Abaya	34	14	8	506	1054	751	-
	Chamo	29	31	9	850	1950	1354	-
	Bedessa	30	-	8.1	-	-	-	-
	Bilate	31	-	8.4	-	-	-	-
	Hamesa	32.1	-	8.2	-	-	-	-
26-4-05	Abaya	30	12	8.7	480	958	850	-
	Chamo	30	25	9.4	821	1897	1298	-
24-5-05	Abaya	35	13.5	9.0	500	1200	820	-
	Chamo	32	23.8	9.3	912	1876	1386	
27-6-05	Abaya	32	15	8.57	467	1174	812	-
	Chamo	29.5	29	8.80	853	1962	1429	-
25-7-05	Abaya	33	17	8.5	490.7	1156	774.5	92.2
	Chamo	27	30	9.2	816	1976	1323.9	55
	Bedessa	31	-	9.1	194.7	63	42.2	1800
	Bilate	29	-	8.7	193.3	175	117.3	1500
	Hamesa	29.5		8.0	153.3	73	48.9	1200
22-9-05	Abaya	-	15.5	8.92	-	1159	776.5	99.5
	Chamo	-	-	9.25	-	1949	1305.8	67

Figure 7.2: Surface Water Temperature, ZSD, pH, Total Alkalinity, Conductivity (K_{25}), Total Solids and Turbidity measured over the study period

Figure 7.3 and 7.4 present the concentration of inorganic nutrients measured over the study period. Nitrate levels recorded in this study are much higher than those reported for Lake Chamo by the author of this paper and by others (e.g. Belay & Wood, 1982: 217-445 $\mu g\ l^{-1}$). Nitrite-nitrogen concentrations were usually found out to be zero, although a low concentration (< 10 $\mu g\ l^{-1}$) was reported last year. Similarly, low concentrations of nitrite (2 -18 $\mu g\ l^{-1}$) were recorded in 1979 for Lake Chamo by Belay and Wood (1982). The concentrations of nitrite-N were always much lower than those of nitrate-N and Ammonium-nitrogen as they usually are in African lakes (Talling & Talling, 1965; Tilahun, 1988). Ammonium-nitrogen ranges from about 0.13 to 0.5 $mg\ l^{-1}$ and from 0.05 to 0.8 $mg\ l^{-1}$ in the Lakes Abaya and Chamo, respectively. Surface concentrations of ammonium-nitrogen in the lakes are often temporarily raised a) following the collapse of algal blooms and b) during increased circulation (Kalff, 2002).

Sampling date	Station	NO_2–N (mg/L)	NO_3N (mg/L)	NH_3-N (mg/L)	PO_4-P (µg/L)	TP (µg/L)	Cl^- (mg/L)
29-3-05	Abava	0.01	0.18	0.5	0.3	3.5	-
	Chamo	0.03	0.29	0.8	0.5	6	-
	Bedessa	0.08	7	0.9	4.1	8.2	-
	Bilate	0.1	9.2	0.85	5	8.7	-
	Hamesa	0.07	6.5	0.6	4.0	6.5	-
26-4-05	Abava	0	0.3	0.3	0	4	-
	Chamo	0	1.1	0.6	0.9	5.9	-
24-5-05	Abava	0.02	0.2	0.2	0.8	5.1	-
	Chamo	0.01	0.15	0.75	0.8	5.4	-
27-6-05	Abava	0.071	0.4	0.23	-	-	-
	Chamo	0.058	0.4	-	-	-	-
25-7-05	Abava	0	0.6	0.16	?	4.2	97.8
	Chamo	0	0.75	0.56	5.3	5.6	135.1
	Bedessa	0.036	8.8	1.08	53.6	96	24
	Bilate	0.005	12.5	1	86	86.5	39
	Hamesa	0	7.0	1.1	73	99.5	42
22-9-05	Abava	0	1.0	0.13	0	2.7	
	Chamo	0	0.85	0.05	0	2.2	

Figure 7.3: Concentration of inorganic nutrients recorded over the study period

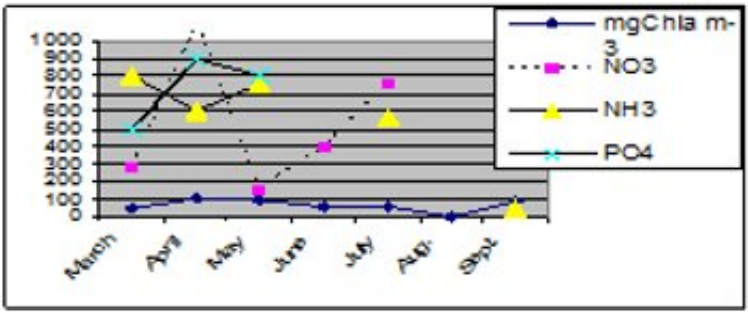

Figure 7.4: Inorganic nutrients in relation to algal biomass

7.5.2 Phytoplankton biomass

Phytoplankton biomass estimated as chlorophyll concentration exhibits temporal changes (see figure 7.5), with a larger value corresponding to high rainfall data. Phytoplankton biomass varies from 86 to 101 (mean=75.7) mg m^{-3} for Lake

Chamo and from 0 to 10.2 (mean=4.4) mg m^{-3} for Lake Abaya. The average standing crop recorded for Lake Chamo in this study is larger than that in the previous study by this author but still comparable to the values reported for the Lakes Abaya and Chamo (Belay & Wood, 1982), Lake Abijata (Wood et al., 1978) and Lake Ziway (Belay & Wood, 1984). The reason for the increased value could be the increased rainfall in this period.

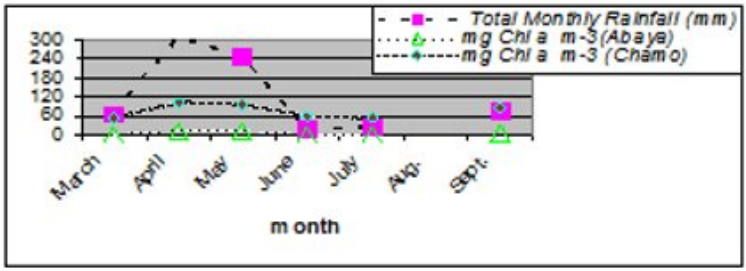

Figure 7.5: Algal biomass in relation to rainfall

7.6 Conclusions and Recommendations

The inorganic nutrient concentration of the lakes is increasing. This might be due to the inflow of flood-driven materials from the surroundings. Therefore, the disposal of untreated wastes and the application of fertilisers and other chemicals need to be checked. To establish the exact level of water quality, further repeated and extended studies are required This project is running until the end of 2006 and more information is expected by then.

7.7 Acknowledgements

This work is funded by the GTZ-Project financed to AMU. We gratefully acknowledge the AMU Research and Publication Office Coordinator, Dr. Mekennen Ayana, and the GTZ-Project Coordinator, Dr. Semu Ayalew, for the facili-

ties and encouragements rendered, without which the development of this paper would have been impossible.

7.8 References

APHA, AWWA, & WEF (1999). *Standard methods for the examination of water and wastewater*. 20^{th} ed. American Public Health Association, New York.

Belay, A., & Wood, R.B. (1982). Limnological aspect of algal bloom on lake Chamo in Gemu Gofa Adminstrative region of Ethiopia in 1978. *SINET: Ethiop. J. Sci*., 5: 1-19.

Gebre-Mariam, Z., Kebede-Westhead, E. & Desta, Z. (2002). Long term changes in chemical features of waters of seven Ethiopian rift valley lakes. *Hydrobiologia*, 477: 81-91.

Girma, Tilahun (1988). *A seasonal study on primary production in relation to light and nutrients in Lake Ziway, Ethiopia.* M.Sc. Thesis, Addis Ababa University, Addis Ababa.

Kalff, J. (2002). L*imnology: Inland Water Ecosystems*. Prentice-Hall, Inc, NJ.

Kebede, E. (1996). Phytoplankton in an alkalinity-salinity series of lakes in the Ethiopian Rift Valley. PhD Thesis, Uppsala University, Uppsala, Sweden.

Kebede, E., & Belay, A. (1994). Species composition and phytoplankton biomass in a tropical African lake (Lake Awassa, Ethiopia). *Hydrobiologia*, 288: 3-32.

Kebede, E., Gebre-Mariam, Z., & Ahlgreen, A. (1994). The Ethiopian rift valley lakes. Chemical characteristics along a salinity- alkalinity series. *Hydrobiologia*, 288: 1-12.

Kebede, E., & Willen, E. (1998), Phytoplankton in a salinity-alkalinity series of lakes in the Ethiopian Rift Valley. Arch. *Hydrobiol. Suppl. 4/Algological studies*, 89: 63-96.

Talling, J.F. and Talling, I.B. (1965) The chemical composition of African lake waters. *Int. Rev. ges. Hydrobiol*., 50: 421-463.

Tekle-Giorgis, Y. (2000). Comparative age and growth assessment of the African catfish, *Clarias gariepinus Burchell (Clariidae) and Nile Perch , Lates niloticus Linn (Centropomidae)* in the three southern Rift Valley lakes of Ethiopia, Lakes Awassa, Abaya and Chamo. Ph.D. Thesis, A. A. U, A.A.

Wetzel, R.G. and Likens, G.E. (2000). *Limnological analyses. 3rd ed. New York*, Inc., N.Y.

8 Application of a Semi-Distributed Conceptual Hydrological Model for Flow Forecasting on Upland Catchments of the Blue Nile River Basin: A Case Study of the Gilgel Abbay Catchment - Hayalsew Yilma, Semu Ayalew Moges

Hayalsew Yilma[1] *Semu Ayalew Moges*[2]

[1]Ministry of Water Resources
Addis Ababa, Ethiopia
Email: hayalsew@yahoo.com
[2]Arba Minch University
School of Graduate Studies
P.O.Box 21
Arba Minch, Ethiopia
Email: smoges@nilebasin.org

8.1 Abstract

This study focused mainly on the hydrological characterisation and application of a GIS-based semi-distributed watershed model (HEC-HMS) to establish rainfall-runoff relationships in the Gilgel Abbay Sub-basin, which is located in the uppermost part of the Abbay (Ethiopian Nile) River Basin.

The semi-distributed GIS-based model, HEC-HMS, was applied for both long-term and short-term simulations. In both cases, four combinations of basin models were used. According to the R^2 and IVF criteria, the model set containing the *Initial and Constant* method of excess runoff volume determination, the *Snyder Unit Hydrograph* and the *Recession* method of base flow estimation was found to be the best model combination for short-period flood forecasting. In accordance with the same criteria, the model combination containing *Deficit and constant loss*, the *Snyder Unit Hydrograph* and *Recession* as a flood forecasting model yielded satisfactory results for long-term simulation with regard to the study area.

8.2 Introduction

All water-related engineering activities require a proper estimation of the runoff magnitude. For efficiently designing, planning and managing river basin projects that deal with the conservation and utilisation of water for various purposes, the long-term water availability and extreme flows are of vital interest. In order to accurately determine the quantity of surface runoff that takes place in a river basin, an appropriate understanding of the complex relationships between rainfall and runoff processes, which depend upon many geomorphologic and climatic factors, is necessary. The simulation of time series of representative streamflow values requires a model that is simple enough to be understood as well as to be used, yet complex enough to be representative of the system.

Establishing a rainfall-runoff relationship is the central focus of hydrological modelling, from its simple form of unit hydrographs to rather complex models based on fully dynamic flow equations. As the computing capabilities are increasing, the use of these models to simulate a catchment has become a standard. Models are generally used as utility in various areas of water resources develop-

ment, among others in assessing the available resources, in studying the impacts of human interference in an area such as land use change, deforestation and other hydraulic structures as for instance dams and reservoirs (Moreda, 1999).

The current study focused mainly on the hydrological characterisation and application of a GIS-based semi-distributed watershed model, HEC-HMS, in the Gilgel Abbay Sub-basin to establish rainfall-runoff relationships and to perform a preliminary investigation of the hydrological dynamics of climate change.

8.3 The HEC-HMS Model

GIS-based hydrological model systems are increasingly becoming major hydrological modelling tools because of their capability to handle the spatial variation of hydrological and physiographic inputs of the watershed. Several models which are either embedded in the GIS environment or have the capability to import the GIS-derived spatial and temporal attributes have been developed, including ArcView GIS-based models such as HEC-HMS, SWAT GRASS GIS-based models as for instance AGNPS, ANSWERS, GLEAMS and TOPMODEL as well as several others which are locally developed and used for specific objectives (Semu, 2003).

HEC-HMS (the Hydrologic Engineering Center's Hydrologic Modeling System) is the United States Army Corps of Engineers' hydrologic system computer programme developed by the Hydrologic Engineering Center (HEC). The programme simulates precipitation-runoff and routing processes, both natural and controlled. HEC-HMS is the successor to and replacement for the HEC's HEC-1 programme and for various specialised versions of HEC-1. HEC-HMS was designed to improve the capabilities of HEC-1 and to provide additional capabilities for *distributed modelling and continuous simulation* (USACE, 2000).

HMS contains four main components: 1) an analytical model to calculate overland flow runoff as well as channel routing; 2) an advanced graphical user interface illustrating hydrologic system components with interactive features; 3) a system for storing and managing data, specifically for large, time-variable data sets; and 4) a means for displaying and reporting model outputs (Semu, 2003).

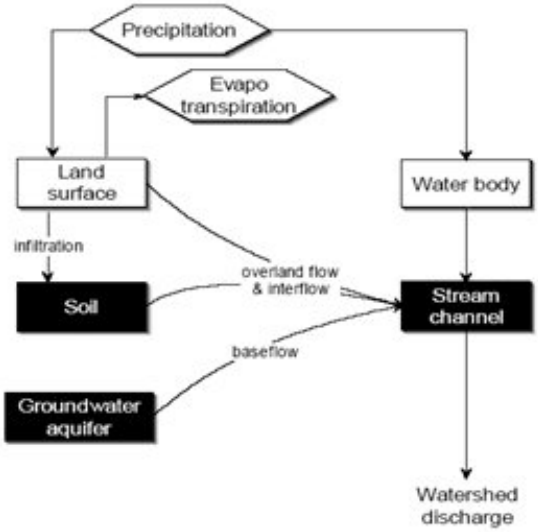

Figure 8.1: Typical HEC-HMS representation of watershed runoff (USACE, 2000)

8.4 Description of the Catchment

Ethiopia has about 12 major drainage basins, among which the Abbay (the Ethiopian Nile) River basin is by most criteria the most important one. It accounts for about 17.5% of Ethiopia's land area, 50% of its total average annual runoff, and 25% of its population. With Lake Tana it has the country's largest freshwater lake, covering about 3.000 km^2. The Abbay River itself has an average annual runoff of about 50 BCM. The rivers of the Abbay basin contribute about 62% on average to the mean Nile total at Aswan, a high dam in Egypt. Together with the contributions of the Rivers Baro-Akobo and Tekeze, Ethiopia accounts for more than 80% of the runoff at Aswan (BCEOM, October 1998).

The hydrography of the basin is dominated by the Abbay River, which rises in

the centre of the catchment and develops its course in the clockwise spiral. It collects tributaries all along its length of almost 1000 km before reaching the Sudan border.
The study area, the Gilgel Abbay Sub-basin, is located south of the famous Lake Tana. The Gilgel Abbay River, which in Amharic literally means "the small abbey", has its source in the mountainous Sekela area and flows northward receiving other tributaries on its way to Lake Tana, where it joins other big rivers like Megech, Ribb and Gumara and forms with these the great Abbay River (Blue Nile).

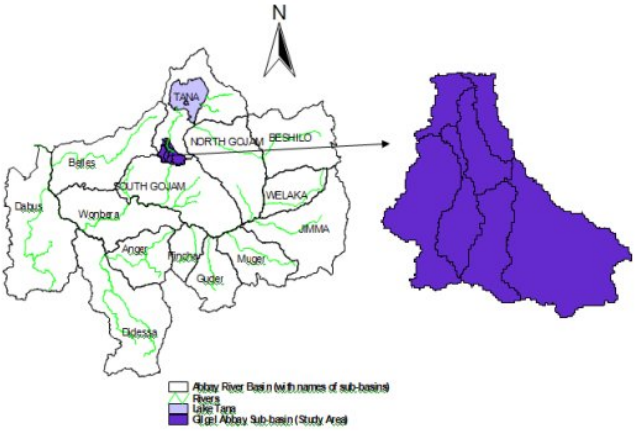

Figure 8.2: Study area (BCEOM, 1998)

8.5 Data Analysis

8.5.1 Hydrological and Climatic Data

The 10-year average seasonal rainfall, potential evapotranspiration and discharge in millimetres per day are plotted (figure 8.4) to characterise the hydrology and

Station name	Name of the river	Area (km^2)	Record		Missing data (%)	MAF		MAR (mm)	r.c.
			Period	Length (Years)		m^3/sec	mm		
Gilgel Abbay Nr. Merawi	Gilgel Abbay	1664	1993-2002	10	0	55.838	1058.24	2046.372	0.52

Figure 8.3: Summary information on the available flow and rainfall data used for the study

climate of the sub-basin. As can be seen from the table above and the mean seasonal diagram below, the Gilgel Abbay Sub-basin has in general a high rainfall runoff transformation coefficient (0.52), with more than 50% of the rainfall converted to runoff. Moreover, it exhibits mono-modal behaviour. The high annual runoff coefficient may be partly attributed to the lower evaporation values in the highland areas of the catchment. As figure 8.3 indicates, the annual rainfall over the basin is greater than the annual evaporation volume by 34.4%. This may also be partly due to a bias introduced to the areal rainfall as a result of the poor representation of the whole sub-basin with only two rainfall stations.

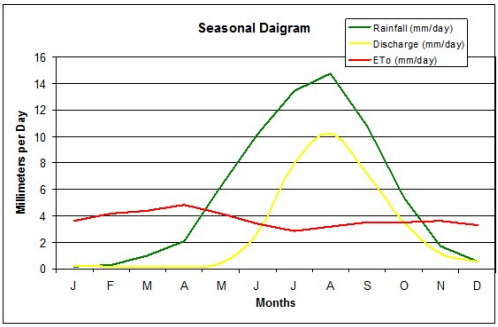

Figure 8.4: Seasonal mean variations of rainfall, discharge and evapotranspiration in the Gilgel Abbay Sub-basin

8.5.2 Topographic Data

Using terrain data with a resolution of 90m by 90m, the terrain pre-processing is carried out using HEC-GeoHMS in an ArcView GIS environment as a series of steps to derive the drainage networks. The steps consist in computing the flow direction, flow accumulation, stream definition, watershed delineation, watershed polygon processing, stream processing, and watershed aggregation. Prior to this, the sinks of the DEM have to be filled in order to avoid problems in calculating the flow direction. Then the resulting "depressionless" terrain model as shown in figure 8.5 (A) is used as input for the analysis. The *Terrain Processing* menu is used to modify the process and to analyse the terrain.

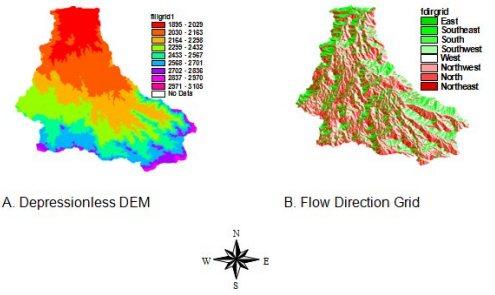

Figure 8.5: Spatial data development process and final HMS project for the Gilgel Abbay Sub-basin

After having finalised the stream and sub-catchment delineations, HEC-GeoHMS computes several topographic characteristics of streams and watersheds. The streams' physical characteristics (such as length, upstream and downstream elevations, and slope) are extracted from the terrain data and stored as attributes in the stream table. Similarly, the sub-catchments' physical characteristics (such as longest flow lengths, centroidal flow lengths, and slopes) are extracted from the terrain data and stored as attributes in the watershed table.

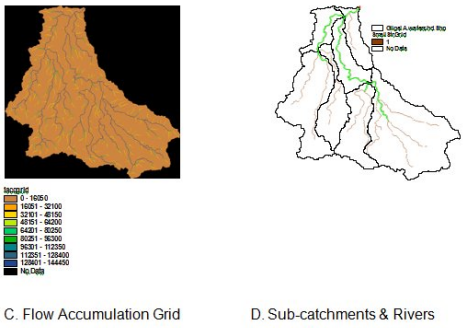

Figure 8.6: Spatial data development process and final HMS project for the Gilgel Abbay Sub-basin

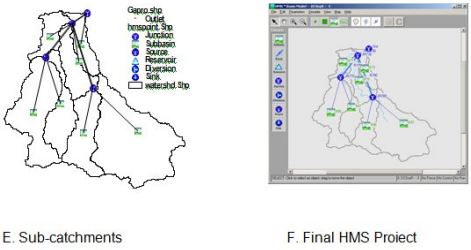

Figure 8.7: Spatial data development process and final HMS project for the Gilgel Abbay Sub-basin

8.6 Modelling Results and Discussion

As mentioned before, modelling is performed in the HEC-HMS environment. HEC-HMS is a highly graphical user interface model and involves the construction of three model components that are required for a run: the Basin Model, the Meteorological Model and the Control Specification Model.

On the basis of the available data and evaluation of the model components, the combinations of models shown below are chosen. The models are applied for both the short-period (seasonal) and long-term continuous mode.

The combinations of models used in the Basin Models are as follows:

- **Combination A**: Initial& Constant Loss Model, SCS UH Transformation Model, and Recession Base Flow Model (ICScsR)
- **Combination B**: Initial & Constant Loss Model, Snyder UH Transformation Model, and Recession Base Flow Model (ICSnyR)
- **Combination C:** Deficit-Constant Loss Model, SCS UH Model, and Recession Base Flow Model (DCScsR)
- **Combination D**: Deficit-Constant Loss Model, Snyder UH Model, and Recession Base Flow Model (DCSnyR)

Six years of data from 1993 to 1998 are used for the calibration of the Gilgel Abbay Sub-basin for long-term continuous modelling. For short-term (seasonal) continuous modelling, only 4 months of data (May - Sep. 2000, which cover the rainy season of the study area) are selected for the calibration of the sub-basin. Verification of the model is done using four years of data (1999-2002) for long-term continuous modelling, whereas for short-period (seasonal) continuous modelling five months of the rainy season of a different year (May - Sep. 2002) are used.

With regard to both the short-term (seasonal) and the long-term modelling processes the procedure of automated calibration (optimisation) fine-tuned by the manual calibration method is found to give better results.
The objective function used for the short-term (seasonal) model for measuring the goodness of fit between the computed and the observed hydrographs is the Sum of Squared Residuals. Two methods of search available in HEC-HMS are the Univariate Gradient Method and the Nelder-Mead Search Algorithm, with the Univariate Gradient Search Algorithm being used for this study. For the long-term model, the objective function used is the Peak-Weighted RMS Error, the search method is the Univariate Gradient Method.

In this study, the well-known Nash-Sutcliffe (1970) efficiency criterion (R^2) is used for the assessment of the performances of the selected models.

$$R^2 = 100\left(1 - \frac{\sum_{i=1}^{n}(f(Q_{obs}) - f(Q_{cal}))^2}{\sum_{i=1}^{n}\left(f(Q_{obs}) - \overline{f(Q_{obs})}\right)^2}\right)$$

where f(Q_{obs}) and f(Q_{cal}) are the observed and calculated streamflow (or transformed streamflow), $\overline{f(Q_{obs})}$ is the mean observed streamflow (or transformed streamflow) over the calibration period and n is the number of time steps.
The Index of Volumetric Fit (IVF) is another criterion used for performance assessment of the models in this study.

8.7 Results

The summary of the results for the model calibration and verification periods in both the short-period (seasonal) and the long-term continuous mode is shown in figure 8.8 below.

Modelling mode	Method			Calibration			Verification		
	Loss	Transformation (UH)	Base flow	R^2	IVF	% Change in volume	R^2	IVF	% Change in volume
Seasonal	I/C	SCS	Recession	51.3	1.01	-0.86	57.8	0.993	0.71
	I/C	**Snyder**	**Recession**	**62.4**	**1.02**	**-2.34**	**72.7**	**1.090**	**-9.18**
	C/D	SCS	Recession	64.0	1.03	-2.6	69.7	0.997	0.28
	C/D	Snyder	Recession	58.0	1.004	-0.38	65.7	0.988	1.21
Long-term	I/C	SCS	Recession	61.6	1.00	-0.005	68.9	1.16	-16.17
	I/C	Snyder	Recession	65.5	1.00	-0.004	68.6	1.16	-16.3
	C/D	SCS	Recession	67.1	1.00	-0.002	72.0	1.17	-16.82
	C/D	**Snyder**	**Recession**	**73.0**	**1.00**	**0.03**	**74.8**	**1.14**	**-13.98**

Figure 8.8: Application results of the various combinations of HEC-HMS models for the Gilgel Abbay Sub-basin

8.7.1 Short-Period Simulation

According to the R^2 and IVF criteria, the short-period (seasonal) forecasting mode generally performs well, particularly during the verification period. As can be seen from figure 8.8, the best model combination for the study area consists of the *Initial & Constant Loss Model, the Snyder Unit Hydrograph and the Recession Base Flow Model* (= combination B).
This model set produces an overall efficiency (R^2) of 62.4% in the calibration and 72.7% in the verification periods. The volumetric fit was also close to unity in both the calibration and the verification periods, showing higher model consistency. But the percent change in volume during verification is relatively higher in this model combination (-9.18%).
As figure 8.9 reveals, the model reproduces a good hydrograph fit in terms of shape during both the calibration and the verification periods. However, a tendency of overestimation can be observed between June and July in both periods. And as can be evidenced from the error diagram, there are no systematic errors in both the calibration and the verification periods, which indicates the model adequacy.
According to the R^2 criterion, the least performance (R^2 = 57.8%) in the verification period is exhibited by the following model combination: the *Initial & Constant Loss Model, the SCS UH Transformation Model and the Recession Base Flow Model* (= combination A).

8.7.2 Long-Term Simulation

The best model combination which gives the best performance for the sub-basin contains the *Deficit-Constant Loss, the Snyder Unit Hydrograph and the Recession models* (= combination D). The performance efficiency (R^2) in the calibration and verification periods is 73.0% and 74.8%, respectively. While the model reproduces a better hydrograph fit in terms of shape and volume during calibration, calibration results consistently underestimate the peak flow values, whereas the verification results do so to a lesser extent.
Another noticeable feature of the long-term simulation consists in the fact that while all model combinations give an excellent volumetric fit during the calibration process, the verification results consistently overestimate the volume; the

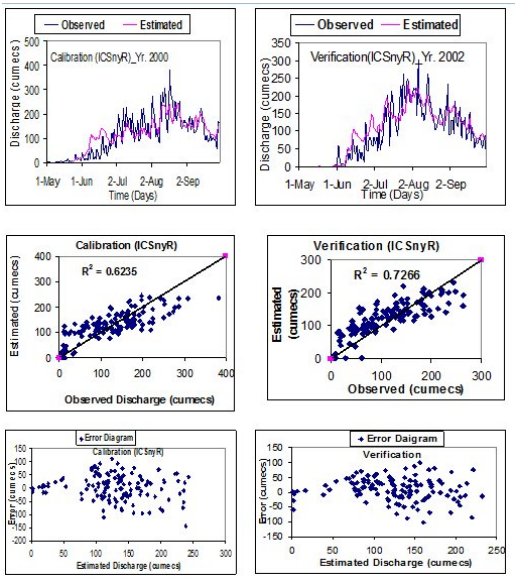

Figure 8.9: Short-period results for the Gilgel Abbay Sub-basin

percentage changes in volume range from 13% to 16.3%.
Further diagnosis of the error diagrams reveals little or no systematic errors.
According to the R^2 criterion, similar to the short-term simulation, the least performance (R^2 = 68.6%) in the verification period is exhibited by the following model combination: the *Initial & Constant Loss Model, the SCS UH Transformation Model and the Recession Base Flow Model* (= combination A).

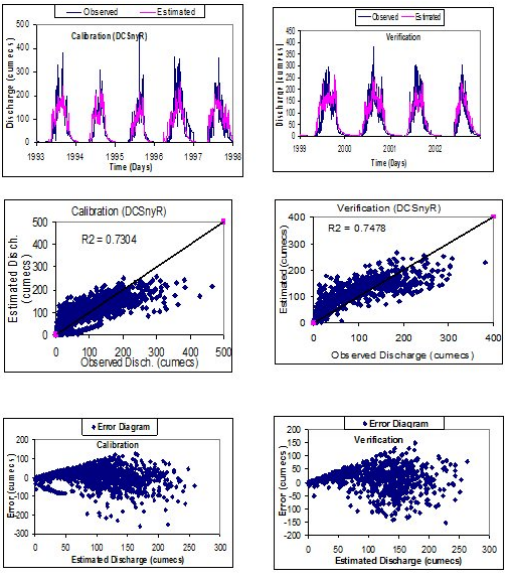

Figure 8.10: Long-term results for the Gilgel Abbay Sub-basin

8.7.3 Climate Change Analysis

After having the model calibrated and verified, attempts are made in order to asses the possible wet season climate (rainfall) change on the corresponding streamflow hydrograph and the volume at the model gauge station in the study area. The model combination used for this assessment is combination B (IC-SnyR: *Initial & Constant Loss Model, Snyder UH Transformation Model, and Recession Base Flow Model*).This combination gives the highest R^2 (72.7%) value in the verification period of the short-term (seasonal) model, 1 May 2002 to 30 Sep. 2002. The same period is used for the assessment of the rainfall change impact.

Values of 5%, 10% and 15% decrease and increase in the ordinates of the seasonal rainfall hyetograph are used to estimate the corresponding change in the

streamflow hydrograph and volume. The results of the response of the river discharge for 5%, 10% and 15% decreases in the rainfall amount are shown in figure 8.11. The estimated response of the Gilgel Abbay River at the model gauge station for 5%, 10% and 15% increases in the rainfall amount shows the same linear trend. This is due to the linearity assumption in the unit hydrograph used for the direct runoff transformation.

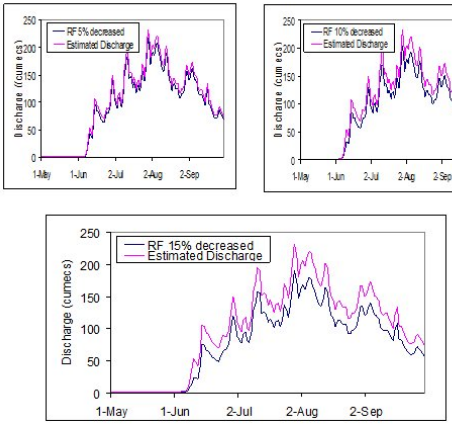

Figure 8.11: Estimated response of the Gilgel Abbay River at the model gauge station for 5%, 10% and 15% decrease in the rainfall amount of the catchment

8.8 Conclusion

Regarding the GIS-based semi-distributed HEC-HMS model, the following conclusions can be reached:

1. According to the R^2 and IVF criteria, the model set containing the Initial and Constant Method of excess runoff volume determination, the Snyder Unit Hydrograph and the Recession Method of base flow estimation is

found to be the best model combination for short-period flood forecasting in the Gilgel Abbay Sub-basin.

2. In accordance with the same criteria, the model combination containing the *Deficit and Constant Loss Model, the Snyder Unit Hydrograph and the Recession Model* as a flood forecasting model gives satisfactory results for long-term simulation in the study area.

3. For both the short-term and the long-term simulations, model combinations containing the *SCS Unit Hydrograph* do not give the best performances for the Gilgel Abbay Sub-basin.

4. As can be seen from the results of the climate change analysis, percentage changes in the ordinates of the rainfall hyetographs result in higher percentage changes in the streamflow volume.

8.9 References

BCEOM (1998). Abbay River Basin Integrated Development Master Plan Project, Phase 3, Master Plan, Volume 1, Appendixes to the Main Report Part 1, 1.Irrigation. The Federal Democratic Republic of Ethiopia, Ministry of Water Resources.

Moges, S.A. (2003). Development and Application of Hydrologic Design Support Tools for Pangani River Basin in Tanzania (PHD Thesis). University of Dar Es Salaam.

Moreda, F. (1999). Conceptual Rainfall-Runoff Models for Different Time Steps with Special Consideration for Semi-arid and Arid Catchments. Laboratory of Hydrology and Inter-University Program in Water Resources Engineering, Vrije Universiteit Brussels (V.U.B.).

Nash, J.E., & Sutcliffe, J.V. (1970). River flow forecasting through Conceptual models. Part I: A discussion of Principles. Journal of Hydrology, 27(3), 282-290.

USACE (2000). Hydrologic Modeling System HEC-HMS. Technical Reference Manual. US Army Corps of Engineers, Hydrologic Engineering Center.

USACE, (2001). Hydrologic Modeling System HEC-HMS, Users Manual. US

Army Corps of Engineers, Hydrologic Engineering Center.

USACE, (2003). Geospatial Hydrologic Modeling Extension HEC-GeoHMS. User's Manual. US Army Corps of Engineers, Hydrologic Engineering Center.

9 Low Flow Analysis and Regionalisation of the Blue Nile River Basin - Tegenu Zerfu, Semu Ayalew Moges

Tegenu Zerfu, Semu Ayalew Moges[1]

[1]Arba Minch University
School of Graduate Studies
P.O.B. 21.
Arba Minch, Ethiopia
Corresponding authors:
semu_moges_2000@yahoo.com
zerfutegenu@yahoo.com

9.1 Abstract

Low flow analysis and regionalisation were carried out for the Blue Nile River Basin (BNRB) using three approaches: low flow frequency analysis, the flow duration curve and the Base Flow Index. On the basis of low flow frequency analysis six homogeneous regions were identified. The GEV distribution provided a good fit to low flows in the regions one, two and three while the Wakeby distribution fitted well in the regions four, five and six. The method of probability-weighted moments was considered the best parameter estimation procedure compared with the method of moments and maximum likelihood. Moreover, the regression model of mean annual minimum flow (7 days) as a function of catchment characteristics was developed for the delineated six regions to predict the 7-day minimum flow quantile of the return period T for ungauged catchments in the basin.
On the basis of Flow Duration Curves (FDC) with a duration of 1, 7, 10 and 30 days, four homogeneous regions were identified. The right tail end of the flow duration curve beyond the 80% exceedence flows was used to group the characteristics of the curve and the BNRB was classified into four homogeneous regions. Similarly, the low flow characteristics of the basin were classified into five homogeneous regions on the basis of the Base Flow Index (BFI).

The use of one or the other established low flow region generally depends on the information requirement of planners and designers in the water sector. For instance, if low flow volume or discharge of a return period T is required by a certain ungauged catchment, the regionalisation based on low flow frequency can be used. In the case of BFI regions, one can generally estimate the mean subsurface flow contribution of each homogeneous region.

9.2 Background and Introduction

The beneficial use of stream flows requires a proper balance between agricultural, industrial and domestic demands on the one hand and in-stream conditions on the other hand to support wildlife aquatic and recreational uses. In general, during storm seasons, a sufficient amount of water is available for both off-stream and in-stream uses. Dry periods, however, are critical. There are many possible def-

initions of low flow. In this study, low flow is the simple lowest mean flow over durations ranging from 1 to D days in a year (FREND, 1989).
Low flow characteristics can be determined by frequency analysis and flow duration analysis. Frequency analysis relates the minimum average discharge for a given number of consecutive days to the recurrence interval in years. Flow duration curves show the flow characteristics of a stream throughout the range of discharge. Low flows of a stream vary randomly. Moreover, the durations of low flows are important. A prolonged period of low flows is the drought. Thus, any analysis of low flows must consider both magnitude and duration. The duration can be taken into account by averaging the flows over a period of time (1 day, 7 days, 10 days, 30 days, etc.).

The estimation of flow regimes at ungauged sites may be achieved by transfer of statistics derived from gauged catchments using regionalisation procedures. The term *regionalisation* in hydrology refers to the grouping of catchments into homogeneous regions. A homogeneous region is a region which has sites with similar low flow characteristics. Therefore it has the same standardised frequency distribution form and parameters.
Information on the magnitude and frequency of low river flow estimates is essential for planning water supplies, water quality management, issuing and renewing waste disposal permits as well as hydropower and the impact of prolonged droughts on aquatic ecosystems. The estimation of low flow is also important for small-scale irrigation projects that contribute significantly to poverty alleviation by means of an increased crop production and generation of rural employment (Abebe, 2003). Thus, the analysis of low flows could provide an accurate understanding of the demand that may safely be placed on a stream flow.

Little study has been carried out on the low flow characteristics of the Abbay River Basin so far. Furthermore, the volume and duration of dependable base flow is not quantified. Most of all, the availability and quality of information are not adequate. Hence, any further development of water resources projects within the region is difficult and unreliable, unless the low flow characteristics are well known. Therefore, this study tried to analyse and characterise the low flow of the Abbay River Basin and to provide the necessary low flow information for gauged and ungauged sites.

9.3 Location and Description of the Study Area

The study area, the Abbay Basin, is located in the north-west part of Ethiopia, between 7○45'-12○45'N latitude and 34○05'-39○45'E longitude (see figure 9.1). This river basin is by most criteria the most important river basin in Ethiopia and has a water availability index for water scarcity of 3602 m^3/capita (Engelmann & La Roy, 1993).

It covers about 17.58% of the Ethiopian land area, 43.11% of the country's total average annual runoff and 25% of the population of Ethiopia. The study area has an average annual runoff of about 52.6bcm. The annual rain fall varies between above 800 mm to 2220 mm, with a mean about 1420 mm. The basin collects tributaries all along its length of 992 km, before reaching the Sudan border above the Rosaries dam (BECOM & ISL Consulting Engineers, 1990).

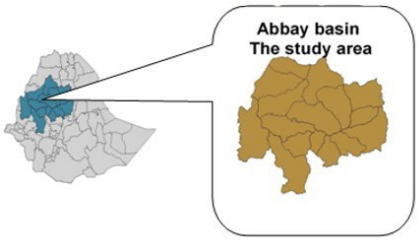

Figure 9.1: Location map of Blue Nile River Basin

9.4 Sources, Availability and Analysis of Data

In order achieve the goals of the research, various data from different agencies and individuals were collected, including time series data, topographical data and a digitised map of the study area.

9.4.1 Flow data

128 hydrological stations are available in the basin, with 68 stations offering data. 38 gauging stations with an average record length of 23 years were used for the analysis.
The stations consisted of daily flow series and were used to produce different durations of low flows, flow duration curves, base flow and base flow index. Moreover, they were used for low flow frequency analysis for the whole region.

Range of missing data in % from the record length

Range of missing data in %	Number of stations
0-5	18
5-10	19
10-20	17
20-30	8
30-50	3
>50	63

9.4.2 Digitised map

A digitised contour map of the basin with a scale of 1:5000 was collected from the Ministry of Water Resources of the GIS Department. These data were used as basic input for developing a digital elevation model (DEM), flow accumulation and flow direction. They were also employed in specifying the exact location of the gauging stations, all of which are necessary for regionalising the basin into a homogeneous region.

9.4.3 Data screening

The calendar year is used in defining an annual minimum value. Only stations without zero flow in their series were analysed. The 7-day annual minimum flow series were used in the frequency analysis as it is usually necessary to nullify the effects of minor river regulations.
In abstracting annual minimum series from daily data, missing data were filled by using the following procedure:

1. Missing periods of up to 15 days during the dry season were completed by interpolation.

2. Missing data of up to 30 consecutive days in the wet season were completed using daily seasonal mean values.

3. Any calendar year containing periods of missing data which did not fall into any of the above-mentioned categories was rejected for further analysis.

A typical filled station graph is displayed in figure 9.2 to show that the filled data points follow the same pattern as the measured ones.

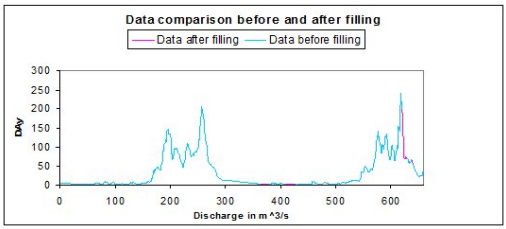

Figure 9.2: Graph showing filling of the missing data

9.4.4 Test for Independency and Stationarity

A basic assumption in the use of statistical distribution in hydrological frequency studies is that the sample data are random variables without any serial correlation. One of the means for measuring the extent to which a minimum in one year is dependent on the value of the previous year is the lag-1 serial correlation coefficient denoted by r1. It displays the strength of the relationship between a value in a series and another value preceding it by one time interval. For a strict random series the value of r1 must differ from zero only by sampling variation; for sequences showing strong persistence it is close to one.

Thus, the following tests were used to detect the randomness and the serial correlation of the data.

1. W-W test (Wald-Wolfowitz test)

2. Lag-1 serial correlation coefficient test

13 of the analysed stations were found to be dependent using the W-W test; 13 stations were correlated using the serial correlation test. 10 stations were common to both tests. Those stations which showed a serial auto correlation or dependency behaviour were discarded from further analysis.

In any time series, data outliers may or may not exist. These outliers may be due to personal errors during recording and to the inadequacy of measuring devices as well as to extreme conditions of natural phenomena. Unless the source of the outliers is clearly identified, it is difficult to completely remove outliers from the analysis. Outliers can be excluded from the estimation procedure only if it is certain that annual minimum flows can be adequately modelled by a single distribution form (Cunnane, 1989). Thus, an outliers test was not done in this study; but to avoid the effect of outliers an efficient method of parameter estimation like PWM was used. Even if outliers are retained in the analysis, they have only a small effect if an efficient method of parameter estimation such as ML or PWM is used (Cunnane, 1989).

9.5 Methodology and Procedure

In general, the study comprised the following methods and procedures:

- Collection of relevant data such as hydrological data, meteorological data, topographic and a digitised map of the basin

- Checking of adequacy, consistency and independency of the data

- Application of three different low flow analysis techniques:
  I. Low flow frequency analysis
  II. Flow duration curve of duration D
  III. Base flow index (BFL)

- Low flow frequency analysis:
  I. Computing of static parameters of selected stations within the basin

II. Regionalisation of the basin into homogeneous regions based on statistical values using GIS ArcView
III. Selection of frequency distribution for the delineated regions
IV. Derivation of frequency curves using the standardised flow data for all regions
V. Regional homogeneity test describing the delineated region
VI. Regression model analysis for estimating the annual minimum flow for each region

- Flow duration curve:
  I. Identification of pertinent duration in this case (1, 7, 10, 13)
  II. Grouping of the FDCs based upon the right-end tail portion of the curve

- Base flow index:
  I. Base flow separation using a standard method (Institute of Hydrology method)
  II. Computing the BFI
  III. Classification of homogeneous regions on the basis of the BFI range

9.6 Low Flow Analysis and Regionalisation

Before the low flow frequency procedure was applied, homogeneous regions had been identified using statistical moments. Thus, conventional moments, L-moments and L-moment ratios had to be computed. Final grouping of similar regions was validated using tests such as homogeneity and discordance tests.

9.6.1 Low Flow Frequency Analysis and Regionalisation

The LCs-LCk moment ratio of standardised flow of the stations was plotted with the L-moment ratio diagram (LMRD) of various distribution functions (see figure 9.3). Furthermore, stations which lie in the same distribution were preliminary grouped as a homogeneous region. This was done on the basis of the fact that stations from the same homogenous region will be distributed along the same distribution of LMRD (Dalrymple, 1990).

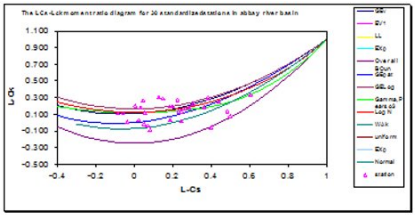

Figure 9.3: LCs-LCk moment ratio diagram for 30 standardised stations

Homogeneity Test: CV and LCv Homogeneity Test

A simple test based on the variability of at-site CV values was used. The main statistic device considered was the coefficient of variation of the individual sites' CV within the region (CC). In a region of m stations and n_j years of records at the j^{th} station having a standardised low flow discharge (q_{ii},i= 1,2,3,. n_j), the coefficient of variation is defined as follows:

$$cv_j = \frac{\left[\sum_{j=1}^{nj} \frac{(q_{ji} - \bar{q}_j)^2}{n_j - 1}\right]}{\bar{q}_j} .$$

The weighted regional coefficient of variation of all the Cv_j (CC) is defined as follows:

$$CC = \frac{1}{cv} \sum_{j=1}^{m} \frac{\left(cv - \bar{cv}\right)^2}{(m-1)} .$$

Sites which have approximately close Cv_j values and which lie within the same geographical proximity were first grouped together in one region and the internal homogeneity of the regions expressed numerically in terms of the flow statistics CC was determined. The criterion used to check for regional homogeneity was based on the value of CC. For homogeneous regions a value of 0.3 or less was

allowed.

With regard to the results obtained, all stations grouped preliminary as a homogeneous region satisfied the CV and LCv homogeneity test criteria.

Region name	CC value		Conclusion
	Conv. CV-based method	L-moment CV-based method	
Region one	0.109	0.082	Homogeneous
Region two	0.292	0.292	Homogeneous
Region three	0.196	0.186	Homogeneous
Region four	0.297	0.291	Homogeneous
Region five	0.296	0.287	Homogeneous
Region six	0.279	0.281	Homogeneous

Figure 9.4: Results of the CV-based homogeneity test for the Abbay River Basin

Discordance Measure Test

The discordance measure is intended to identify those sites that are grossly discordant with the group as a whole. The discordance measure D estimates in how far a given site (i) forms the centre of the group (Roa & Hamed, 2000).

If $U_i=[t^{(i)},t3^{(i)},t4^{(i)}]^r$ is the vector containing the t, t_3 and t_4 values for site (i), then the group average for NS sites within the region is given by

$$\overline{U} = \frac{1}{NS} \sum_{i=1}^{NS} U_i \quad .$$

The sample covariance matrix is given by

$$S = (NS-1)^{-1} \sum_{i=1}^{NS} (U_i - \overline{U})(U_i - \overline{U})^T \quad .$$

The discordance measure is defined by

$$D_i = \frac{1}{3} (U_i - \bar{U})^T S^{-1} (U_i - \bar{U}) .$$

A site (i) is declared to be unusual if D_i is large. A suitable criterion for classifying a station as discordant is that D_i should be greater than or equal to 3.
All of the stations grouped preliminary as a homogeneous region in each region satisfied the discordance test criteria.

REGION ONE			
S.No	Station Number	Discordant Measure	Remark
1	111018	0.44	Homogeneous
2	112028	0.44	Homogeneous
3	112031	0.44	Homogeneous
REGION TWO			
S.No	Station Number	Discordant Measure	Remark
1	115006	0.87	Homogeneous
2	114008	0.62	Homogeneous
3	112012	1.02	Homogeneous
4	114009	0.18	Homogeneous
REGION THREE			
S.No	Station Number	Discordant Measure	Remark
1	112017	0.41	Homogeneous
2	114012	0.12	Homogeneous
3	113028	0.73	Homogeneous
4	113018	0.75	Homogeneous
REGION FOUR			
S.No	Station Number	Discordant Measure	Remark
1	115008	0.53	Homogeneous
2	114007	0.37	Homogeneous
3	113001	0.07	Homogeneous
4	114001	0.86	Homogeneous

Figure 9.5: Results of the discordant measure test for the Abbay River Basin

According to the results obtained in the section above the basin was regionalised into six homogeneous regions (see figure 9.7).

REGION FIVE			
S.No	Station Number	Discordant Measure	Remark
1	112027	1.04	Homogeneous
2	113013	0.12	Homogeneous
3	111010	0.41	Homogeneous
4	114013	0.78	Homogeneous
5	113036	0.75	Homogeneous
6	114014	0.33	Homogeneous
REGION SIX			
S.No	Station Number	Discordant Measure	Remark
1	115005	0.41	Homogeneous
2	112029	1.14	Homogeneous
3	112002	0.32	Homogeneous
4	115007	2.06	Homogeneous
5	113002	0.53	Homogeneous
6	113019	0.53	Homogeneous
7	113012	0.77	Homogeneous
8	113023	0.17	Homogeneous
9	112014	1.12	Homogeneous

Figure 9.6: Results of the discordant measure test for the Abbay River Basin

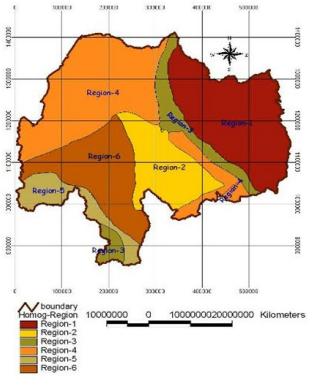

Figure 9.7: Map of the established homogeneous regions of the Abbay River Basin

Selection of Statistical Distribution by LMRD

According to Hosking (1990) the L-moment ratio diagrams are based on the relationship between the L-moment ratios. A diagram based on LCs vs. LCk can

be used to identify appropriate distributions. The best parent distribution is that one for which the average value of the point (LCs, LCk) of all stations within the region gets close to one of the drawn LMRD of the parent distribution. The result obtained in the study is shown in figure 9.8.

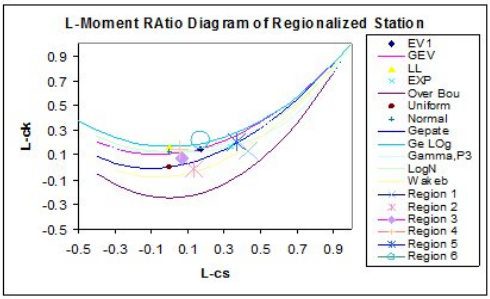

Figure 9.8: Regional average of LMRD for the regions of the Abbay River Basin

Accordingly, the most possible underlying candidate distributions are summarised in figure 9.9.

Region Name	Average regional L-moments (t,t_3,t_4)	Selected candidate distribution
Region one	(0.664,0.429,0.132)	Wake by
Region two	(0.36,0.135,-0.012)	Gepat/ Wake by
Region three	(0.344,0.067,0.020)	Gepat/ Wake by
Region four	(0.364,0.052,0.142)	Gev/LL
Region five	(0.446,0.365,0.142)	Gev
Region six	(0.331,0.148,0.218)	Gev/Glog

Figure 9.9: Selected candidate distributions for the regions of the Abbay River Basin

In the following section, a test for the acceptability of the candidate distribution is presented.

Selection of Frequency Distribution

Several statistical distributions are available for use to date, but a problem arises when having to choose the right one which fits the observed annual minimum flow data. The result of fitting a distribution also depends on the method of parameter estimation. There is no distribution that is universally accepted to fit low flows (Cunnane, 1986). The three parameter estimation methods used for evaluation are the *Method of moment* (MOM), the *Method of maximum likelihood* (ML) and the *Method of probability weighted-moments* (PWM).

For the candidate distributions which were chosen in the previous section the following method of estimation procedure was applied: i) GEV (MOM, ML, PWM); ii) LL (MOM, ML, PWM); iii) Gepat (MOM, ML, PWM); iv) Wakeby (WAK4, WAK5, PWM); and v) Glog (MOM, ML, PWM).
For the Wakeby distribution, the MOM and ML methods were not used because moment estimates of parameters of the Wakeby distribution could not be obtained easily.

Results for the Selection of Parameter Estimation Method

Goodness-of Fit-Measure

For the already identified regions, the goodness-of-fit measure (Z) helps to test whether or not a given distribution fits the data acceptably. This measure is based on L-moments of the at-site data. If the observed sites form a homogenous region (a) L- moments of the sites are well summarised by regional average, indicating that the scatter of the individual sites' moments above regional average represents nothing else than sampling variability and (b) it can be assumed that the region's population L-moments are likely to be close to the average of the sample L-moments of the observed data.
For a chosen distribution, the goodness-of-fit measure Z^{dist} is defined as follows:

$$Z^{dist} = \left(\frac{\tau_4^{dist} - \bar{t}_4 + \beta_4}{\sigma_4} \right) ,$$

where $\bar{t}_4$ is the average L-kurtosis value computed from the data of a given region, σ_4 denotes the standard deviation of $\bar{t}_4$ which can be obtained by repeated simulation of a homogeneous region with the distribution under test and of sites having low flow record lengths similar to those of the observed data.

β_4 is the bias of $\bar{t}_4$ and τ_4^{dist} the average L-kurtosis value computed from simulation for a fitted distribution.

For short record lengths ($n \leq 20$) and a large population L-skewness ($T_3 \geq 0.4$), a bias correction factor for t_4 is required. Hence, in a goodness-of-fit test the fitted L-kurtosis value τ_4^{dist} is not compared with the regional average $\bar{t}_4$ itself, but with the bias-corrected version $\bar{t}_4$ - β_4.

Small values of Z^{dist} imply that the considered distribution can be accepted as the true underlying frequency distribution for the region. According to Hosking and Wallis (1993), if I Z^{dist} I ≤ 1.64, the distribution is acceptable. The results obtained for goodness-of-fit were as follows:

Region name	Candidate distribution	Goodness of fit measure (Z^{dist})	Remark
Region one	Wakeby	0.234	Desirable
Region two	Wakeby	0.030	Desirable
Region three	Gepat	0.157	Desirable
	Wakeby	0.157	Desirable
Region four	GEV	0.019	Desirable
	LL	0.037	Desirable
Region five	GEV	0.026	Desirable
Region six	GEV	0.060	Desirable
	Glog	0.870	Desirable

Figure 9.10: Goodness-of-fit measure for the candidate distributions for each region

Similar tests were carried out using standard error of estimates. Based upon the goodness-of-fit and minimum standard error of estimates the following distribution and parameter estimation methods were selected for the different regions in the Blue Nile River Basin:

Region name	Distribution and parameter estimation methods
One	Wakeby/PWM
Two	Wakeby/PWM
Three	Wakeby/PWM
Four	GEV/PWM
Five	GEV/PWM
Six	GEV/PWM

Figure 9.11: Selected distribution and parameter estimation methods for the different regions

Derivation of the Regional Frequency Curve for the Homogeneous Region

Based on the results obtained in the section above the following distributions were found to be the best procedures for describing the annual minimum low flow and for predicting acceptable low flow estimates for the delineated regions:

Region name	Distribution and parameter estimation methods
One	Wakeby/PWM
Two	Wakeby/PWM
Three	Wakeby/PWM
Four	GEV/PWM
Five	GEV/PWM
Six	GEV/PWM

Figure 9.12: Recommended method and procedure method for the different regions

For developing the frequency curves of the six regions, a computer programme which could calculate the standardised flow, the non-standardised flow as well as the parameter of the selected distribution was used. This programme was compiled by Sine (2004). The established low flow frequency curves are shown in figure 9.13.

9.6.2 Prediction of Low Flow for Ungauged Catchments

A number of physical characteristics exist for a catchment and a number of numerical measures or indices have also been described in explaining and developing models that relate low flow to catchment characteristics. There are a number of measurable physical characteristics of catchments that might have an impor-

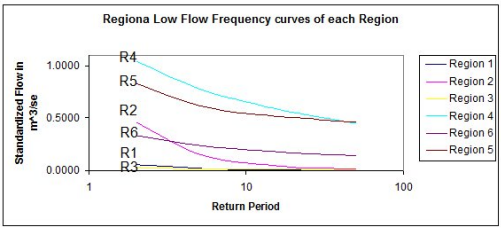

Figure 9.13: Low flow frequency curves of the different regions

tant relationship with low flow. The availability of data representing them is very important in developing a model that relates index low flow and catchment characteristics, which is given by

$\bar{O} = C\ A^a\ S^s\ R^r\ F^t$,

where
$\bar{O}$ = index low flow (= the mean annual minimum flow)
A = the catchment area in km^2
S = the slope expressed in percentage
R = the mean annual rain fall in mm
S = the shape factor (L^2/A)
BFI = the base flow index

with c, a, r, s and t as regression parameters.

To make the analysis simpler, the aforementioned equation was transformed into a linear form using logarithmic transformation:

$\text{Log}\ \bar{O} = \log C + a \log A + S \log S + r \log R + t \log F.$

Then, the estimation was performed on the parameters, namely, a, r, s, t and log c using the multiple linear regression technique. An important consideration in multiple regression analysis is to check whether the data are adequately described or not. In this study, the multiple coefficient of determination (R^2) was used as a measure of the ability of the regression model to describe variations in the dependent variable. The closer R^2 is to 1, the better the regression model fits the data.

For all regions the mean annual minimum flows were computed by the regression equation and compared with the actual annual minimum flows in the form of a graph for each station of all regions.
With regard to the regression equation, the one which was developed for region five was poorly correlated for some unknown reason .The others well modelled the regions with the available data. To obtain a better result for region five, the input data were collected, processed and predicted correctly. This involved the collection of additional data and further analysis.

Region name	Regression Equation	R^2
One	$Q = 1.417 A^{0.808} BFI^{7.943}$	0.957
Two	$Q = 0.007 A^{0.617} BFI^{-0.304}$	0.399
Three	$Q = 0.246 A^{0.457} BFI^{2.488} F^{-5.244}$	0.943
Four	$Q = 34.199 A^{5.378} BFI^{1.456}$	0.996
Five	$Q = 11.478 F^{-0.058} BFI^{5.631} S^{-1.31}$	0.822
Six	$Q = 0.020 A^{0.640} BFI^{2.843}$	0.908

Figure 9.14: Derived regression equation for the prediction of mean annual minimum flow (MALF) for the different regions of the BNRB

where A=area in km^2, BFI =base flow index, F= shape factor, S=slope in %.

9.6.3 Flow Duration Curves

Characteristics of Flow Duration Curves in the Low Flow Regimes

The cumulative frequency distribution of daily mean flows shows the percentage of time during which specified discharge is equalled or exceeded during the period of record. The relationship is normally referred to as the *flow duration curve* and although it does not convey any information about the sequencing properties of flows it is one of the most informative methods of displaying the complete

range of river discharges from low to flood flows. The curve is most conveniently derived from daily discharge data by assigning daily flow values to class intervals and by counting the number of days within each class interval. The proportion of the total number of days above the lower limit of any class interval is then calculated and plotted against the lower limit of the interval.

FDCs may also be obtained by applying a D day moving average to the original hydrograph. This enables the portion of D day periods when the average discharge over D days is greater than a given value to be estimated.
The low flow indices derived from the flow duration curve would be Q 95(1), Q95 (10) Q70 (1), Q70 (10) etc. This is determined on the basis of countries' adoptions and the purpose of the indices.
In this study, flow duration curves of 1, 7, 10 and 30 days were derived for 30 stations. As for the flow duration curves starting from the 80th percentile one-day discharge, Q80 (1) was used to generalise catchments. None of the stations had a Q80 (1) value equal to zero. Based on the characteristics shown in the right-tailed end portion of flow duration curves the basin flow duration curves were categorised into four homogeneous classes. This was done by means of visual inspection.

Five stations were grouped into group one FDCs. The stations 114007, 114008 and 114009 were located in the Didessa Catchment and the other two stations (station 115005 and 115007) were situated in the Dabus Catchment. The stations did not lie in the same regions categorised upon their low flow statistics.
Two stations, namely 115005 and 155007, lay in region six, the stations 114007 and 114008 in region four and station 114009 in region two.

In group two FDCs five stations were available: station 111010 from the Tana Catchment, the stations 112027, 112028 and 112029 from the Jema Catchment and station 113028 from the South Gojjam Catchment. Based on the regions formed on their low flow statistics the stations 111010 and 112027 lay in region five, station 112029 was located in region six, station 113028 in region three and station 112028 in region one.

Nine stations were grouped in group three FDCs. The stations 114001, 114012 and 1140013 were from the Didessa Catchment, the stations 113018 and 113036 from the South Gojjam Catchment, the stations 115006 and 115008 were located

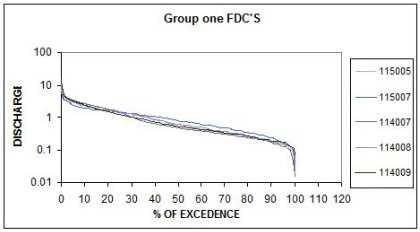

Figure 9.15: Group one FDCs

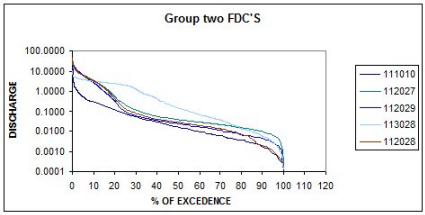

Figure 9.16: Group two FDCs

in the Dabus Catchment and the other two stations (11018 and 112031) were situated in the Tana Catchment and the North Gojjam Catchment, respectively. Similar to group one FDCs and group two FDCs, stations grouped in group three FDCs lay in different regions categorised upon their low flow statistics. The stations 111018 and 112031 lay in region one, the stations 114012 and 113018 in region three, the stations 115008 and 114001 in region four, the stations 114013 and 113036 lay in region five and station 115006 was located in region two.

In group four FDCs eleven stations were available: the stations 112002, 112012 and 112014 from the Muger Catchment, the stations 113012, 113013, 113019 and 113023 from the South Gojjam Catchment, the stations 113001 and 113002 from the Guder Catchment and the other two stations (112017 and 114014) from the North Gojjam Catchment and the North Diddesa Catchment, respectively. Based on the regions formed on their low flow statistics, the stations 112002, 112014, 113002, 113023, 113012 and 113019 lay in region six, the stations

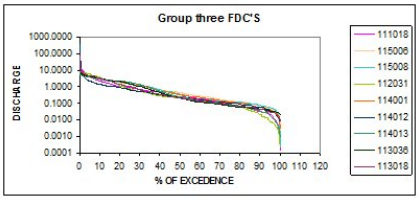

Figure 9.17: Group three FDCs

113013 and 114014 in region five, the other three stations (112012, 112027 and 113001) were situated in region two, three and four, respectively.

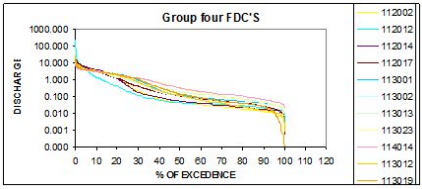

Figure 9.18: Group four FDCs

9.6.4 Base Flow Separation and BFI

Base Flow Separation

In order to determine the contribution of overland flow in a watershed to the streams in the watershed or the contribution of flow of the stored sources, it is necessary to separate out the base flow from stream gage data. The standard method (*Institute of Hydrology method*) is used for separation of base flow from main hydrograph.

The Institute of Hydrology method starts by partitioning the year into N-day periods and by determining the minimum flow within each period. These minimum flows are the potential turning points on the base flow hydrograph. (If the year is

not evenly divisible by N, any remaining days will be included in the last period of the year). The default value for N is 5 days. When several days within one period are tied for the lowest flow, the earliest day will consider the minimum, except during the last N-day period of each year, when the minimum will be considered to occur on the latest day.
To determine the turning points on the base flow hydrograph, the collection of N-day minimum flows is processed using a turning point test.

Institute of Hydrology (Standard Method) turning-point test:

Given three adjacent N-day minimum flows, Q_0, Q_1, and Q_2:

Q_1 is a turning point IF: $Q_1 * f <= Q_0$ and $Q_1 * f <= Q_2$

where f is a turning point test factor that must be greater than zero and should be less than 1.

If Q_1 is zero, it will always be a turning point. If either Q_0 or Q_2 are equal to zero, then the test is only performed against the non-zero value. If both Q_0 and Q_2 are zero, Q_1 cannot be a turning point unless it is zero. Adopting the prescribed method makes the base flow separation process less tedious and more consistent. For all 30 stations the base flow hydrograph was separated. Typical separated base flow hydrographs for station 113012 are presented in figures 9.19 - 9.21.

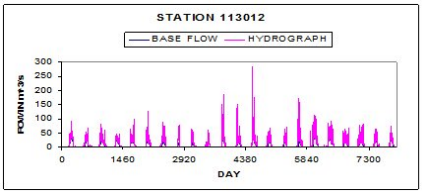

Figure 9.19: Typical hydrograph and base flow hydrograph

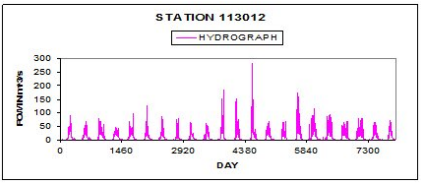

Figure 9.20: Typical hydrograph

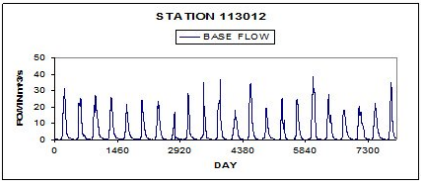

Figure 9.21: Separated base flow hydrograph

Base Flow Index

The base flow index is the total volume of base flow divided by the total volume of runoff for a period (Wahl, 1995). The base flow component of river flow is commonly expressed as a proportion of the total river flow, termed the Base Flow Index (BFI). A catchment with a BFI approaching 1 is highly dominated by base flow, while a catchment with a BFI approaching zero receives little base flow contribution.

From the main hydrograph, the base flow hydrograph and base flow index was calculated. The result obtained (the BFI) was used as one of the input parameters for the regression analysis. The grouping of stations according to their range of BFI is shown in figure 9.22.
Those stations categorized into group one FDCs had a BFI of 0.63-0.842 which means that 63%- 84.2% of the flow contribution stem from delayed storage and that the flow is mostly dominated by base flow. FDCs grouped into group two had a BFI of 0-0.4 which means that the flow is mostly dominated by surface

runoff.

33% of the stations grouped into group four FDCs had a BFI of 0.4 -0.5 and the remaining 67% had a BFI of 0.54-0.725. Moreover, 45% of those station grouped in group four FDCs had a BFI of 0.41-0.5, another 45% of the stations had a BFI of 0.6-0.7 and the other 10% had a BFI of 0.25-0.27.

Range of BFI	Station number	Base flow index
0-0.3	112029	0.22
	112012	0.263
	112028	0.274
0.3-0.5	112027	0.335
	111010	0.364
	112031	0.401
	112017	0.413
	111018	0.443
	112002	0.467
	113013	0.482
	112014	0.495
	113018	0.497
	113012	0.498
0.5-0.7	115008	0.537
	113036	0.56
	113002	0.604
	115006	0.623
	114008	0.628
	114009	0.629
	113019	0.647
	113028	0.664
	113001	0.671
	114014	0.674
	114012	0.682
	113023	0.692
0.7-0.8	114013	0.715
	114001	0.721
	114007	0.731
	115005	0.759
>0.8	115007	0.842

Figure 9.22: Grouping of stations based on the ranges of their BFI

9.7 Conclusion and Recommendation

The main objective of the study was to delineate the Abbay River Basin into hydrologically homogeneous regions on the basis of their low flow characteristics. Three approaches were utilised: the low flow frequency analysis, flow duration curves (FDC) and the base flow index (BFI).
On the basis of a 7-day annual minimum low flow frequency analysis, six homogeneous regions were delineated. Homogeneity was tested using the Hosking and Wallis test. Suitable distribution was fitted on the basis of the goodness-of-fit measure statistic (z) and the minimum standard error of estimate. Accordingly, the Wakeby distribution provided a good fit to low flows in the regions one, two and three while the GEV distribution fitted well in the regions four, five and six. The method of probability weighted moments was considered as the best parameter estimation procedure in comparison with the method of moments and maximum likelihood. Regression analysis was also applied to develop regression models for the prediction of mean annual minimum flow from ungauged catchments using catchment characteristics. The regression model adequately expressed all the regions except region two where R2 was less than 0.4.

The L-Moment ratio diagram provided a practical means to group stations into different regions and also identified the underlying distribution for a given region. Thus, the L-moment ratio diagram was used to group stations into same regions and to identify the underlying statistical distribution.
Flow duration curves of different durations were established. The flow duration curve represents a measure of hydrological response which embraces the full regime from flood flows to low flows. The flow regime of the Abbay River Basin was thus described by studying flow duration characteristics and base flow contribution. Accordingly, four groups of FDCs were established based on their pattern shown from the 80th percentile and the value greater than it.

According to the results obtained from the three approaches used for low flow regionalisation the author of this paper recommends that analysis and characterisation of homogeneous regions have to be done independently for each approach.

- Delineation of hydrologically homogeneous regions based on statistical parameters of gauged sites could be one of the possible alternative methods

of regionalisation.

- Most of the stations exhibit constant data in the low flow season, so the rating curve which is used to convert the measured stage in each station with regard to the low flow season has to be checked in terms of its accuracy and validity in the course of time. Otherwise, the rating curve constants have to be readjusted accordingly with the channel transformation.

- Different topographic and climatic parameters like slope, elevation, soil type, geology and hydrogeology indexes of each region should be determined so that a better regression model can be developed and the estimates of the mean annual minimum flow will be accurately estimated.

- Low flow frequency analyses of stations with zero flows have to be studied independently.

9.8 References

Abebe, A. (2003). Ethiopian Journal of water Science and Technology.

Admas, J.C., Brainerd, W.S., & Goldberg, C.H. (1992). Programmer's Guide to Fortran 90. McGraw Hill, Singapore.

Gustard, A., et al. (1989). Flow Regimes from Experimental and Network Data, Volume 1: Hydrological Studies, Institute of Hydrology ,Wallingford.

Baipai, A.C., Calus, I.M., & Fairley, J.A. (1978). Statistical Method for Engineers and Scientists.

Chow, V.T., Maidment, D.R., & Mays, L.W. (1988). Applied Hydrology. McGraw Hill Book Company, USA.

Cunnane, C. (1989). Statistical Distribution for Flood Frequency Analysis. World Metrological Organization Operational Hydrology Report, No.33.

French Engineering Consultants and ISL Consulting Engineers (1990). Abbay River Integrated Development Master Plan Project, Main Report Volume 1.

Gebeyehu , A. (1989). Regional Flood Frequency Analysis. PHD thesis report.

Giese, G.L., & Franklin, M.A. (1996). Water-Resources Investigations Report 96-4308. Magnitude and Frequency of Low Flows in the Suwannee River Water Management District, Florida.

Hamed, K.H., & Rao, A.R. (2000). Flood Frequency Analysis. CRC Press LLC, Florida.

Hosking, J.R.M., & Wallis, J.R. (1993). Some Statistics Useful in Regional Frequency Analysis. Water Resource Research, Volume 29, No.2. New York.

Loganathan, G.V., et al. (1985). Methods of Analyzing Instream Flows. Department of Civil Engineering, Virginia Polytechnic Institute and State University Bulletin 148.

Melesew, G.D. (1996). Regional Flood Frequency for Namibia and Zimbabwe. MSc thesis report, Dar es Salaam.

Raymond, J. (2001). Development of Low Flow Prediction Models for Southern Africa. PHD thesis report, Dar es Salaam.

Mkhandi, S.H., Mngodo, R., & Kachroo, R.K. (1997). Analysis of Flow Regimes in Tanzania.

Sine, A. (2004). Regional Flood Frequency Analysis. M.Sc. thesis report, Arba Minch University.

Swan, D. R., & Condie, R. (1983). Computation of the Base Flow Index, Water Resources Branch Inland Water Directorate, Environment Canada.

USWRC, United States Water Resources Council. (1976). Guidelines for Determining Flood Frequency, Bulletin No. 17 of the Hydrology Committee, Washington D.C.

10 Environmental Impact Assessment of Irrigation Development with Regard to the Amibara Irrigation Project in Ethiopia - Moltot Zewdie

Moltot Zewdie (MSc)[1]

[1](Tel 022-1112900)
<tambek72@yahoo.com>
Semu Ayalew (PhD), Eline Boelee (PhD) and Fentaw Abegaz(PhD)

10.1 Abstract

The study was conducted in the Amibara Irrigation Project area within the Middle Awash Valley of Ethiopia. The study was intended to assess the environmental impact of irrigation development and its severity in threatening the sustainability of the irrigated farm land. Moreover, it was meant to suggest possible intervention mechanisms to be devised in order to mitigate these problems.
The assessment was based a) on the description and analysis of long-time data at groundwater level and of soil salinity from 120 randomly sampled surface soil samples and 25 groundwater samples; b) on literature; and c) on an informal survey based on observations and interviews of 52 people using a checklist for the ecological data.
The study area was severely affected by soil salinity from secondary salinisation with high ECe levels that reached 154dS/m at some spots, by a shallow groundwater level of less than 1m below surface soil, by complete deforestation, and devastation of the range land. Such situations cause drastic changes in the overall environment and natural ecology. The causes of such impacts were the direct consequence of the irrigated agriculture and related activities.
In order to take measures in accordance with the problems which alleviate further degradation of the irrigated field and which sustain the production and productivity of the irrigation development, government intervention through the introduction of agro-pastoral production systems, double cropping and improved water management systems were taken into account as possibilities of a solution.

10.2 Introduction

Environmental impacts of water resources development have increasingly become an important aspect of interest since the 1960s. The overall interest in environmental issues in general culminated in the 1980s (Wooldridge, 1991). But environmental conservation was still given a lip service in many countries. The techniques for environmental impact assessment (EIA) were developed only during the post-1965 era, and in fact the term "EIA" itself gained widespread use only during this period. In early times, once man started crop production along the riverbanks and lakes, irrigation practice became common in many parts of the

world, including Ethiopia. In the late 1960s, the investment in irrigated farming systems covered a wide area in the Awash Valley. In the Middle Awash Valley, the Amibara-Melka Sadi farm was established by the Amibara Irrigation Project II (AIP II) in 1971, based on the survey report by Halcrow in 1965. The net area proposed for irrigation was 14,600 ha; 2100ha were under cultivation at that time, the rest of the area was covered by natural pasture. At first, it was proposed to extend to the entire potential irrigable area of the locality, which was a failure. Let alone to expand it could not able to maintain what was already developed. In the 1990s it faced a substantial decrease in cultivated land size. The major reasons consisted in the environmental degradation and loss of cultivated land through salinisation and even disruptive to human habitation though there were some social factors that may not be ignored like political changes and resource conflicts.

This irrigation development was established in an area where the life system of the original dwellers was completely different from the newly introduced one. The people's livelihood was completely supported by livestock rearing and the people had no know-how of irrigated farming. The development pushed and restricted then to the wet season grazing for all over the years. This situation developed a negative attitude among the pastorals for the development that extend from occasional damage on the farm to claim for the return of the cultivated land. Moreover, devegetation at the time of establishment, mismanagement of irrigation water and mono-cropping have played a major role in reducing the cultivated land size until today.

Since the irrigation development was established under such social and natural conditions, it was of paramount importance to assess the impacts it had brought to the environment so as to devise intervention measures to sustain the existing development and to learn a lesson for the future. The impact of such a wide development programme could not yet been seen with respect to the environment of the area, which has a great potential both land and water resources for future developments, if conditions are improved. In order to assess and indicate the environmental impacts of the irrigation development in the AIP II area, to mitigate the problems through suggesting intervention measures and to improve the positive impacts of the irrigation development, this study was conducted with

the objective of a) assessing the environmental impact of irrigation development and the problems with respect to the living conditions of the community, to land productivity and to the change of the natural system; and b) suggesting possible intervention methods to avert the problems and to preserve the sustainability of the farm.

10.3 Methodology

10.3.1 Data Collection

The environmental data like flood hazard, groundwater level and salinity, soil salinity, and ecological changes were collected by means of direct sampling, interviews and secondary data from MAADE and the Awash Basin Water Resources Authority. In addition to the survey data, secondary data on surface and groundwater hydrology as well as primary data on soil chemical properties were collected. The long-term records on surface water and groundwater were collected from WARC and the Awash Basin Water Resources Agency. The information collected focused on environmental changes as a result of the irrigation development. In this context, when environment was mentioned, it included the water, soil and vegetation resources in the pre- and post-irrigation development periods. Since the irrigation development was based on a diversion structure and a single cropping system (practised in the high flow regime), it did not affect the low flow characteristics of the river with respect to downstream users and aquatic life. Moreover, the farm did not use chemicals like fertilisers and herbicides that might have affected the environment. Since the insecticides and pesticides (agro-chemicals) used on the farm change over the years due to the occurrence of different types of diseases, pests and insects, it is difficult to analyse the effect, so that a long-time study is needed to show the cumulative effect. Hence, such types of environmental impacts were not included in this study.

10.3.2 Data Analysis

With regard to the assessment of the overall impacts of irrigation development on the natural environment, soil, vegetation, groundwater and surface water level as well as flow nature were analysed using descriptive statistics based on pre- and

post-irrigation development conditions. The natural conditions with and without the irrigation developments were assessed using literature, long-term data, direct sampling and laboratory analyses.

The spatial and temporal fluctuation of the groundwater level in the study area was determined on the basis of a brief analysis of an informal survey on the subsurface drainage manholes in the irrigated fields.
The contribution of the high groundwater table to the fast secondary salinisation was also assessed in detail:

1. The groundwater was analysed for its salt content from 25 piezometer well water samples in gm/lit. The conversion factor, 0.64ECw = gm/lit, was used (Majumdar, 2002).

2. Using the potential evaporation demand of the area over 7 months of off-season (no irrigation period) and assuming that it was fulfilled by the capillary rise of the groundwater, the salt precipitate in the soil profile was calculated in gm/m^2.

A brief assessment on the ecology was done on the basis of an interview using a checklist and a sample, addressing 52 people from the Afar region.

10.4 Results and Discussion

The results and discussion part incorporates the impact of irrigation development on the environment with regard to flood disasters as well as to degradation of natural resources like soil salinity, water logging and deforestation.

10.4.1 Flood Hazards

As to the information on the area from the elders addressed during the informal survey, the flood as such was not harmful during the pre-irrigation development period. They reasoned out that the river flooded the area from many overtopping (takeoff) sites that could possibly reduce its power and make it harmless. A report by FAO (1965) indicated that the Awash River flow rose up to 700m^3/sec, which was almost the double value of the 1999 flood (398m^3/sec) which at that time

resulted in a great disaster all over the area. This implies that the river training work following the irrigation development contributes to the change of the flow characteristics of the river, which confirms the suggestion of the people.
Despite the construction of the flood control structure, the river burst its banks and/or breached the dykes, which resulted in great disasters on properties. In 1999, for instance, 98% of the WARC compound (houses, stores and offices) were flooded, while 91% were highly damaged. In the MAADE, 90% of the Melka Sadi and more than 70% of the Melka Werer cotton farms were completely flooded, which led to a total loss of production in the flooded area (report on flood disaster by WARC and MAADE, 1999/2000).

The unpredicted (unexpected) occurrences of such high floods rendered the disaster very severe since the victims were not forewarned to take precautions, that is to say to evacuate their property from the area. Beyond the immediate disaster on properties, it also aggravated the salinisation process through a rapid and abrupt groundwater rise (less than 2m to 1m depth from surface) due to long-time stagnation all over the flooded area. Moreover, the psychological impact on the people who are in fear of floods every year in the summer season (especially in August) was taken into consideration.

10.4.2 Groundwater Fluctuation

The study area was located on fluvisols flanking the Awash River. It was in proximity to river way (on the flood plains of the river) and has level (flat land feature). The soil survey during the study for the irrigation development revealed that the depths to groundwater level in most of the irrigated farms of the Middle Awash and local areas were reported to be deeper than 10m (AIP II, 1982; Swales Haider, 1974; Fekadu et al. 1999). The repeated flooding on the flood plain in the pre-irrigation development period was balanced by the uptake of the reverian forest, which were present on the area that possibly keeps the water table to such deeper depth.

Since the establishment of irrigation development there was a rise of the groundwater level in the irrigated fields. The survey on manholes on the Melka Sadi Amibara irrigation farm in 2004 revealed that there was a significant rise of the groundwater level that might have affected plant growth, which was shallower

than 1m. The rise was continuous and rapid since the beginning of the irrigation development until the installation of the drainage system in 1992. Though in the latter periods the drainage system helped to restrict the groundwater level deeper than 2 m, the salinisation problem was still there. This could be most possibly due to the long duration off-season in association with the high evaporation demand (1700mm per 7 months of off-season) of the atmosphere. Such a high evaporation potential of the area could possibly tap the saline groundwater from a deeper level (2.0m-4.0m) (Garg 2001; FAO, 1984; Todd 1959) that was below the range of the subsurface drainage system which highly contributed to secondary salinisation. Hence, the single cropping system of the irrigation development facilitated the salinisation process through allowing a net upward flow of capillary water from the saline groundwater to the evaporation zone during 7 months of idle time.

Temporal water logging was an additional problem of the farm. In adequate land levelling (earthwork) in the scheme, associated with vertic soil of the area cause localised water logging following excess irrigation, wild flooding and intense rainfall. This was also reported by Halcrow (1985) and Haider (1985) who found out that 72% of the Melka Sedi cotton farms were estimated to suffer from water logging due to the above-mentioned causes.

10.4.3 Soil and Water Salinity

The laboratory analysis of the ECe for 120 soil samples from the AIP II area indicated that the ECe values amounted to 49dS/m and seldom to 154 dS/m in some areas. Based on this sample analysis, 20% of the sampled area had a salinity (ECe) greater than 4 dS/m, while 15% of the sampled area had a soil salinity higher than 8.0dS/m. According to the yield potential analysis (Ayers and Westcot, 1985) such salinity levels of the farm can reduce the yield potential of most crops which grow in the area to a significant level (cotton to 98%, sugarcane to 80%, maize to 40%, banana to 10%).

On the other hand the salinity level analysis of soil water and groundwater samples revealed that the ECe level decreased the soil profile, which showed capillary rise as the major source of soil salinity. This upward flow of groundwater (capillary rise) contained a significant amount of salt (2.448g/lit on average). Such

an upward salt influx deposited 3.515 kg/m^2 of salt in the soil profile and on the surface after evaporation during the 7 months of off-season, assuming that the evaporation potential of the area was totally fulfilled by means of the capillary rise. Most possibly such an amount of salt lifted to the soil profile and surface accounts to the net salt accumulation because there was no downward flow of water to leach it back to the groundwater during this season.

Field code	Location	Soil sampling depth		
		30-60	60-90	90-120
F1/1/11	MS	48.8	28.42	19.2
F10/5/4	MW	4.82	4.13	3.77
4C2	MS	14.12	19.27	16.54
4C10	MS	36.00	19.27	15.00
F9/3/2	MW	16.1	17.76	16.12
D2/20	MW	26.10	12.60	11.30
B7/8	MW	0.9	2.22	5.58

Figure 10.1: ECe (dS/m) values of soil samples from salt-affected fields of Melka Sedi and Melka Werer farms (AIP II area, 2004), Source: WARC, 2004

Hence, the major reason for salinisation of the soil in this particular area shifted to secondary salinisation. It was stated that the soil of the area was categorised to class A and that its ECe did not exceed 4dS/m except for some spots (Tadele, 1993; Halcrow, 1989; FAO, 1965). Moreover, the irrigation water source (Awash River water) had no restriction to irrigation as long-time monitoring confirmed (0.28- 0.98dS/m). So it is possible to state that the irrigated agriculture was the cause of the soil salinity.

Figure 10.2: Salt-affected field in the Melka Sadi unit farm (photograph by Moltot Zewdie, 2004)

10.4.4 Ecology

With the help of a brief assessment of the informal survey as well as by means of interviews and reference literature on ecology, the pre- and post-irrigation development period situations were outlined with respect to the ecological change. As stated by Halcrow (1989), livestock and the pastoralists form a very important and fundamental part of the environment before the development. They were reasonably in balance with the environment before the irrigation development. From this study it became clear that, formerly this area, supporting a far lesser population of livestock and corresponding human population, would have been more productive of shrubs, grass and trees than today. Taking substantial areas of traditional dry season grazing land for irrigation development exacerbated the ecological degradation, creating more pressure on the remaining land.
There was no alternative grazing option to rest the wet season grazing so as to give enough regeneration time. This situation resulted in further devastation of the productivity of the range through overgrazing and continuous depletion of the seed bank, which can ultimately, brings total degradation of the ecosystem.

The survey revealed that the area was highly productive of consumable dry matter by virtue of its location on the flood plain of the Awash River. As a result, it served for over 9 months of the dry season grazing, beyond supporting the pastoral livestock for such a long dry season, can also gave enough time for the

wet season grazing land regeneration, which can avoid the devastation of the wet season grazing.
The major causes for the degradation of the ecosystem consisted in land clearing for irrigation development, in the concentration of the pastoral livestock on the wet season grazing throughout the year and in the immigrants that engaged in clearing the remaining surrounding forests for charcoal production. As a result of such human actions there were tree and grass species whose populations severely declined (figure 10.3). These plant species were rich fodder sources of the Afar livestock. Hence, the devastation of these had negative repercussions on the life system of the pastoralists and highly increased their exposure to frequent droughts.

Si. No.	Grass species		Tree and bush species	
	Scientific name	Local name	Scientific name	Local name
1	Vossia cuspidate	Sitabu	Dobera glabra	Gerssa*
2	Chrysopogon lumulsus	Durfu	Acacia nilotica	Keselto
3	Cynodon dactylon	Rarieta	Gerewa ferruginea	Hedayito
4	Setaria acromelanea	Musa	Salvadora percica	Adayto
5	Sporobolus pellucidus	Hamilto	Acacia oerfota	Geriento

*No regeneration

Figure 10.3: Highly declined (devastated) vegetation species in the range land and cleared from the irrigated land, Source: WARC Lowland Forages and Forestry Research Section and Survey 2005

10.5 Conclusion and Recommendation

The irrigation development brought with it a change in the flow characteristics of the River Awash, namely by means of a flood protection structure that internally resulted in the flooding of the area as well as in property losses. In order to mitigate such frequent and sever flooding problems in addition to frequent monitoring and maintenance of the dyke, a flood early warning system must be

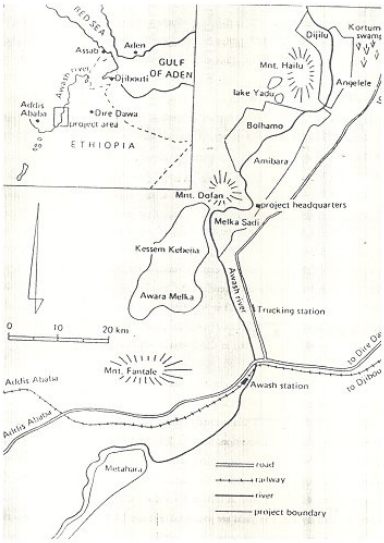

Figure 10.4: Location map of the Amibara Irrigation Project area in the Middle Awash Valley of Ethiopia

established in the river basin.
The irrigation development with its poor irrigation water management practices caused a shallow water table and high soil salinisation problems. The salinisation and water logging of cultivated land through the groundwater table rise treated the productivity of the area to the extent possibly led to abandon of a considerable land size every year. The single cropping system with its long off-season months was also the underlying reason for facilitating secondary salinisation. Thus, an improved irrigation system was of urgent need to sustain the irrigated farming in the area. Furthermore, double cropping needs to be introduced as well as the reduction of the directional flow of groundwater (capillary rise) in order to balance the upward influx of salt through leaching.

The reduction of natural flood plain dry season grazing due to irrigation devel-

opment resulted in reducing the livestock holdings per household as well as the productivity. The few unproductive livestock per household which was not supported by any other activity had a negative impact on the communities' lives and more or less forced the people to develop a negative attitude towards the irrigated farm so that they blamed the latter for the problems caused. Hence, governmental intervention through the introduction of agro-pastoral production structures and irrigated pasture programmes is essential in order to assist the subsistence system of the people and to avoid the negative attitudes of the community so as to guarantee the sustainability of the irrigated farming and the future expansion of similar developments in the area.

10.6 References

Ali Said (1994) Resource use conflict between pastoralists and irrigation development in the Middle Awash Valley of Ethiopia.

Ayers S. (1985), Water quality for Agriculture. Irrigation and drainage paper 29, FAO, 67 Rome Italy

Dougherty T.C and Hall A.W (1995) Environmental impact assessment of Irrigation and drainage project, FAO irrigation and drainage paper 53, HR Wallingford, United Kingdom

FAO (1985) Water quality for Agriculture, FAO Irrigation and Drainage Paper No. 29, Rome Italy

FAO (1965) Report on the Awash River Basin, Imperial Government of Ethiopia United Nation Special Fund FAO/SF: 10/ETH, 1995 Vol. IV, Addis Ababa, Ethiopia

FAO (1999) Modern water control and management practice in irrigation, impact on performance. Water reports No.16.

Fekadu Gedamu et.al, (1999) The arid land and resource management network in Eastern Africa, Pastoralism in the Afar Region of Ethiopia, Alarm publication, Addis Ababa, Ethiopia Technology, Pantnagar 263145, (U.S. Nagar), UTTARA Nachal, India

Fentaw A (1994) Studies on a pilot surface drainage system in the Amibara Drainage Projectarea of Middle Awash Valley, Ethiopia. MSc thesis at Wageningen University, Netherland

Garg A.K (2001) Land and Water Management in Irrigated areas, India

Gregorio Lopez Sanz (1999) Irrigated agriculture in the Gudina River high basin (Caslilla La Manch, Spain) economical and environmental impact. Journal of agricultural water management, Vol.40 Nos. 2-3, Spain

Haider G (1988) Irrigation Water Management Manual, Institute of Agricultural research, Addis Ababa, Ethiopia

Haider G and Kadiah A. (1987) Irrigation water management manual. IAR, Ethiopia

Halcrow (1988), Master Plan for the development of Surface water Resources in the Awash Basin. Ethiopian Valley Development Studies authority (EVDSA),Interim Report, Addis Ababa, Ethiopia.

Halcrow (1989) Master Plan for the developments of surface water resource in the Awash Valley. Draft final report Volume VII, Addis Ababa, Ethiopia

Halcrow (1969) Awash Valley Authority Melka Sedi Amibara Proposed Irrigation Project feasibility study Part I, general Report, Rome, Italy

Michael A.M (2001) Principle of Irrigation Engineering theory and practices, India

Majumdar W.K 2002, Irrigation water management principles and practice. New Dilhi, India

Wooldridge R (1991) Techniques for Environmentally Sound Water Resources Development, Vol. II, 41 HR Wallingford UK

Complete List of Volumes

Vol. 1

LARS 2007 Proceedings

Vol. 2

Alumni Summer School - Well Drilling and Rural Water Supply

Vol. 3

Summary of Master Theses from Arba Minch University

Vol. 4

Results from Expert Seminar - Topics of Integrated Water Ressources Management

Vol. 5

Adane Abebe - Hydrological Drought Analysis - Occurence, Severity, Risks: The Case of Wabi Shebele River Basin, Ethiopia

Vol. 6

Bogale Gebremariam - Basin Scale Sedimentary and Water Quality Responses to External Forcing in Lake Abaya, Southern Ethiopian Rift Valley

Vol. 7

Stefan Thiemann et al. Integrated Watershed Management - Financial Aspects of Watershed Management